THE GEOMICROBIOLOGY OF SUBGLACIAL SEDIMENTS

The University Of Sheffield.

A thesis submitted for the degree of Doctor of Philosophy in the Faculty of Social Science at the University of Sheffield

by

ANDREW GRAY

Department of Geography

University of Sheffield

July 2016

Abstract

Glaciers are intrinsic to life on our planet, enriching the marine waters into which they drain, and harbouring their own microbial ecosystems. Of these, the till-layers underneath glaciers and ice sheets, have been recently shown to support active microbial communities. Research that characterises this ecosystem is limited by poor access to sample, and so most of what is known of subglacial microbes: their function, and role within biogeochemical cycles, comes from point source sediment samples, or is inferred from meltwater geochemistry. This thesis details the work carried out to make direct assessment of several key geomicrobiological functions within subglacial sediments.

Very few direct measurements of microbial processes have been made within subglacial sediments, and so fundamental information about the subglacial ecosystems is lacking. This means, that despite bacterial species being reasonably well studied within subglacial sediments, there is limited understanding of their role within the subglacial carbon cycle, and few direct observations in support of hydrogeochemical evidence of a microbial role within sediment redox processes. This study utilised microcosm experiments, in which subglacial sediments from a range of glaciers were incubated at near *in situ* conditions, to directly assess the processes of microbial carbon cycling and geochemistry within them. Sediments were sampled from underneath the frontal margins, or within meltwater channels of nine glaciers, from Svalbard, Greenland, South Georgia and Livingston Island, giving a broad perspective of subglacial geomicrobiology.

These sediments, all of which had live microbial populations, were found to contain active chemoautotrophic species, active aerobic heterotrophs and anaerobic heterotrophs capable of denitrification and iron reduction. Under aerobic conditions, these sediments were net heterotrophic, with NEP values ranging from -0.0014 $\mu gCg^{-1}h^{-1}$ ($\pm$0.004) to -0.080 $\mu gCg^{-1}h^{-1}$ ($\pm$ 0.004). Strong evidence of microbial pyrite oxidation was observed within all sediments, with microbial processes accounting for between 48 and 93% of the sulphate ions produced during incubation. Investigation into the kinetics of microbial pyrite oxidation within these sediments, led to the conclusion that indirect oxidation of pyrite was occurring, with microbes most likely mediating pyrite oxidation through the reoxidation of ferrous to ferric iron at the mineral surface.

These results provide direct insight into key microbial processes within the subglacial environment. Carbon cycling was found to be complex, with some organisms most likely depending upon autochthonous organic matter derived

from chemoautotrophic activity, as well as allochthonous inputs of dead cellular matter as a source of carbon. The subglacial sediments analysed here, were found to be net producers of CO_2, which, if widespread, may have implications within the global carbon budget. Microbial populations were, in all cases, found to be active in mediating pyrite oxidation and, in so doing, indirectly enhancing carbonate weathering. Through these processes, microbes are involved within two of the main mineral weathering reactions which typically define meltwater chemistry in glacial outflow.

Acknowledgements

First acknowledgement must go to my supervisor, Andy Hodson, for guiding this project, and facilitating my field seasons. Without time out of the lab and on a glacier, I'm not sure I would have had the tenacity to finish. Also thanks to him and Aga Nowak, for collecting some of my most interesting samples from down south.

For supporting me throughout my field and labwork, and providing me with a floor to sleep in in Svalbard, my utmost thanks goes to Krystyna Kozioł. Other people who have been of great assistance and guidance in the field are: Emma Brown, Haz Lovell, Jacob Yde and Simon De Villiers.

This has been something of a low budget PhD, and many of my analyses would have not been possible without the generosity of other researchers. Thanks goes to Dave Pearce, for lending me his microscope and for inspiring me to use it. The radio isotope work would not have been possible without the guidance and support of Irene Johnson, Birgit Sattler and Marie Šabacká, who has also kept me going through this write up. I would also like to thank Harry Langford for answering my numerous questions throughout my lab work and analysis. For orientating me within a lab and facilitating my work I would like to thank Kathleen Taylor, Alan Smalley, Rob Ashurst and Emma Wharfe.

Finally I would like to thank my parents Michael and Linda Gray, for the support they have given me throughout my time at University and especially whilst writing up. A tiež sa chcem pod'akovat' Monike Mendelovej a jej rodine za ich lásku a podporu počas tohto najstresovejšieho obdobia môjho života. Bez vás, vašej pohostinnosti a domácich miláčikov by to nebolo možné. Ďakujem.

Contents

List of Figures

List of Tables

Less common abbreviations.

AG Argentina Glacier

BB Brucebreen

BP Bacterial production

BR Bacterial respiration

DAPI 4',6-diamidino-2-phenylindole nucleic acid stain

DOC Dissolved organic carbon

EDTA Ethylenediaminetetraacetic acid

FISH Fluorescence in situ hybridisation

FTIR Fourier transform infra red

HB Hørbyebreen Glacier

HN Heaney Glacier

IRGA Infra red gas analyser

LOI Loss on ignition

MK Mittivakkat Gletscher

OM Organic matter

PBS Phosphate buffered saline

PI Propidium iodide

PP Primary production

SOC Sediment organic carbon

ST Scott Turnerbreen

TB Tellbreen

TEAP Terminal electron accepting process

TCA Trichloroacetic acid

TDIC Total dissolved inorganic carbon

UHQ Ultra-high quality (deionised water)

VG Vestre Grønfjordbreen

VP Von Postbreen

XRF X-Ray Fluorescence

Chapter 1

Introduction

1.1 Background

The identification of abundant and active microbial communities underneath glaciers (Sharp et al., 1999; Skidmore et al., 2000; Foght et al., 2004; Cheng and Foght, 2007; Boyd et al., 2011) and ice sheets (Lanoil et al., 2009; Yde et al., 2010b; Pearce et al., 2013; Christner et al., 2014), has extended our appreciation of the cryosphere as a habitat. Little is known about the organisms occupying the basal sections of glaciers, and due to their inaccessibility, researchers are faced with the challenge of characterising an ecosystem with limited use of *in situ* experimentation or monitoring. Due to this limitation, and despite a large effort to investigate life under the Earth's ice masses, important and fundamental questions remain only partially answered. These principally relate to microbial function, with our knowledge of different and dominant metabolisms, and sources and transformations of energy, largely inferred from community analysis of sediments, and geochemical analyses of glacial waters. Without fully understanding the function of microbial communities underneath glaciers, it is difficult to interpret their place within key biogeochemical cycles, such as glacial carbon budgets and nutrient export, or their interaction with mineral phases within subglacial sediments. The subglacial environment is dynamic, with conditions dependent upon the overlying glacier's hydrology, movement and morphology (Cuffey and Paterson, 2010). Understanding microbiology underneath glaciers, therefore, becomes part of a wider understanding of subglacial processes, with linkages between hydrology, physics and chemistry of a glacier,

all influencing conditions for life there.

Where liquid water is present under glaciers, the microbes that inhabit subglacial sediments have been shown to be active in a range of metabolic and geochemical processes. Foremost in understanding this ecosystem's role within its environment, is understanding from where it derives energy and nutrients - it is easy to conceive a subglacial system comprised of allochthonous, dormant cells. Microbial carbon dynamics are globally important, and carbon cycling by supraglacial ecosystems contribute significantly to cryospheric carbon budgets (Anesio et al., 2010; Hodson et al., 2010a). Less is known about the subglacial carbon cycle, however, with uncertainty relating to the importance of different metabolisms, as well as the origin and type of organic carbon metabolised by subglacial heterotrophs.

A combination of genetic and geochemical evidence suggests that microorganisms within subglacial systems may be deriving energy through mediating the oxidation or reduction of inorganic mineral species there. Direct observations of these processes are limited, however, due to the inaccessible nature of subglacial till. Consequently, understanding of the mechanisms behind these processes, the species implicit in geochemical reactions here, and the energetic benefit to subglacial microbes, is also limited. Genetic analysis provides, perhaps, the biggest clues as to microbial function with respect to geochemistry, though it does not provide evidence as to the *in situ* extent and relative importance of different cell-mineral interactions. Geochemical analyses on the other hand, are limited by difficulty in delineating biotic processes within outflow analysis, or by the replication and representation of a full range of *in situ* conditions within laboratory experiments.

Glaciers and ice sheets cover an area of approximately 17000000 km^2 (Boetius et al., 2014), roughly 10% of the Earth's surface. The more research is directed at the study of subglacial life, the wider the limits of identified habitable conditions become, with active microbial ecosystems within subglacial lakes under Antarctica (Pearce et al., 2013; Christner et al., 2014), and with active microbial metabolisms measured at temperatures below the freezing point of water (Panikov et al., 2006). The volume of potentially inhabitable sediment under glaciers, thereby, implies its importance through size alone, with its inclusion as a glacial habitat significantly increasing the volume of the cryo-biosphere. Investigating microbial processes within subglacial ecosystems can shed new light into the limitations and adaptations of life on our planet. Moreover, though extreme by our standards, glaciers have offered refugia for microbial life through geological

time scales, and as such, contemporary microbial processes may provide insight into strategies through which life has survived and evolved on our planet.

Glaciers are important biogeochemical engines, producing conditions favourable for rock weathering, as well as providing a transport mechanism for redistributing weathered chemical species within the environment. The processes that occur underneath ice masses, may have implications outside of the subglacial environment, therefore, being important to connecting ecosystems. Several studies have demonstrated the importance of glaciers in supplying bioavailable iron (Raiswell et al., 2008a; Hawkings et al., 2014; Death et al., 2014), organic carbon (Hood et al., 2009; Fellman et al., 2014; Lawson et al., 2014; Hood et al., 2015), nitrogen and phosphate (Slemmons et al., 2013; Hawkings et al., 2015) to river, lake, fjord or marine ecosystems. Microbial processes have the potential to be invoked within any of these, with specific linkages being discussed in the following literature review. In polar regions, where nutrient supply is often tightly coupled to nutrient uptake (Siegfried et al., 2013), and in context of a warming Arctic, where ice masses are decreasing (Hagen et al., 2003; Gardner et al., 2011; Velicogna et al., 2014), it is now crucially important to fully understand the processes that underpin these biogeochemical cycles.

With subglacial microbes seemingly implicit in a range of carbon and mineral weathering processes, it is important to consider their role within glacial biogeochemical cycles. Despite multiple lines of genetic and geochemical evidence, there are surprisingly few direct measurements of these processes in sediment. Direct measurement within controlled experiments will enable better characterisation of the relative importance of different microbial processes, and will also provide a method whereby microbial mineral interactions can be separated from bulk chemistry. The central research problem here relates to a poor understanding of the key geomicrobial processes within subglacial environments; what are the factors that constrain physiological activity, and to what extent are mineral constituents being utilised for energy? This project utilises a novel sampling strategy along with microcosm experiments to investigate subglacial geomicrobiology in an attempt to further characterise this poorly quantified environment. Through direct observation of microbial function within key geochemical cycles, it is hoped that our general understanding of subglacial environments is improved, and its importance within context of the whole glacial ecosystem better understood.

1.2 Roadmap

This thesis is composed of three central research chapters, each investigating a different aspect of subglacial geomicrobiology. These follow a review of the literature (Section 1.3), in which concepts broached within the preceding background section are expanded upon; a statement of the project's aims and objectives (Section 1.5); and a chapter detailing the fieldwork through which subglacial sediment was collected for experimentation (Chapter 2). The topic of each research chapter is derived from each one of this project's aims. The first, details an ecological study of the collected sediments (Chapter 3); The second, investigates metabolism and carbon cycling within the collect sediments (4); and the third, studies the role and mechanisms through which microorganisms mediate subglacial mineral weathering processes. Overarching conclusions and ideas for future research are detailed in a final summary chapter (Chapter 6).

1.3 Literature Review

1.3.1 The Subglacial Environment

Direct observation of the subglacial environment is difficult, yet hydrology and geology at the glacier bed play an important role in defining conditions for life under the ice. The concepts that form our understanding of subglacial hydrology are derived from bore-hole data, as well as from dye-traces, geochemistry and hydrograph data from glacial outflow (Nienow et al., 1998; Swift et al., 2005; Wadham et al., 2010a). During the ablation season, supraglacial snow and ice meltwater make up the majority of subglacial flow, as percolation and direct flow through moulins and crevasse convey surface water to the glacier bed (Cuffey and Paterson, 2010). Basal melt contributes significantly less to the total volume of subglacial water. It may be present throughout winter, however, as it occurs through the combined heating influences of pressure from overlying ice, friction at the ice-rock interface, and geothermal heating, rather then being driven by seasonal radiation budgets (Alley et al., 1997).

Determining the dynamics of water under the ice offers further difficulties. Temperate glaciers are thought to be characterised by a distributed drainage system throughout winter, or early in the melt season. Here, flow is tortuous, due to low winter water volumes and the closure of developing channels by ice flow (Cuffey and Paterson, 2010). The distributed system then evolves into a

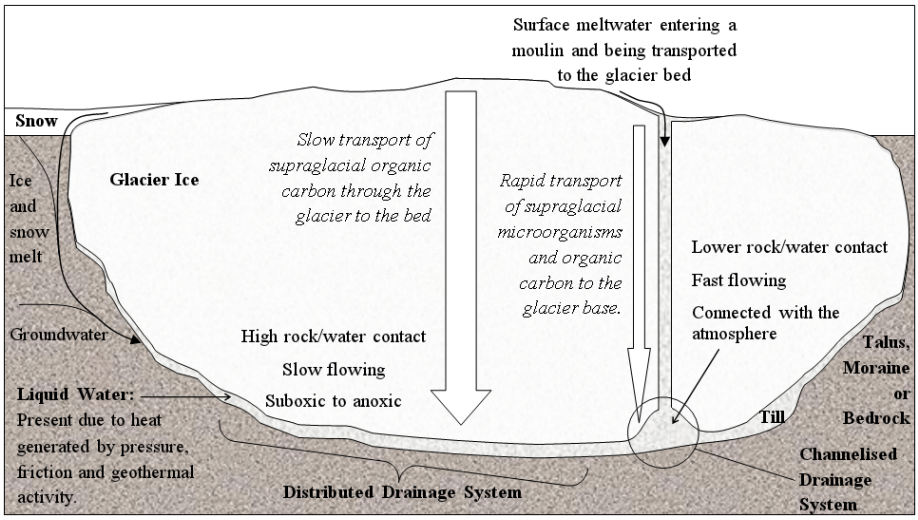

Figure 1.3.1: Cross-section of a glacier showing major water and cell transport pathways.

faster flowing system as surface ablation conveys larger volumes of water to the glacier bed. This melts larger channels into the ice, or incises into the underlying till, thereby forming a more efficient conduit for outflow (Fountain and Walder, 1998; Nienow et al., 1998; Tranter et al., 2002; Cuffey and Paterson, 2010). These two flow pathways are depicted in Fig. 1.3.1. A similar system of subglacial drainage development has been suggested for smaller Arctic polythermal glaciers (Bingham et al., 2005; Bartholomew et al., 2011). Larger ice sheets, however, are thought to be characterised by distributed hydrology across the majority of their bed. Flow is restricted at the cold-based ice sheet margins, until high volumes of summer melt force a channelised drainage system to develop through the ice or bedrock (Skidmore and Sharp, 1999; Rippin et al., 2003; Cuffey and Paterson, 2010).

Differences in, and seasonal development of, subglacial drainage channels have important implications for subglacial ecosystems and biogeochemistry. A slow flowing distributed system is likely to head towards anaerobic conditions, as the biogeochemical oxygen demand utilises the dissolved oxygen in the meltwater (Tranter et al., 2002; Wadham et al., 2008). Conversely, large, open flow channels that form a connection with the atmosphere allow gaseous exchange and are oxygenated (Tranter and Skidmore, 2005; Wynn et al., 2006). Water residence time as it flows under a glacier, may also influence the dominant

weathering processes. For example, a switch from carbonate dissolution to silica weathering as calcium weathering sites are depleted (Tranter et al., 2002), or waters become saturated with calcium ions (Wadham et al., 2010a).

With flow pathways playing a defining role in rock-water contact times, and oxygen conditions under a glacier, the analysis of bulk water chemistry in glacial outflow has long been used as a method for describing subglacial hydrological processes (e.g. Tranter et al. (1996)). However, without factoring biotic weathering kinetics into the chemistries used to define subglacial conditions, there is the potential for misinterpretation, for example, where low oxygen could be a result of high biological oxygen demand rather than longer water residence time. It is important, therefore, that subglacial biotic processes are well defined, for outflow chemistry to be accurately interpreted.

1.3.2 Life under ice: Subglacial Biology

Since the discovery of viable cells underneath glaciers by Sharp et al. (1999) and Skidmore et al. (2000), there has been a race to collect subglacial samples and analyse them for the signs of life. At the time of writing, ecosystems have been characterised from under Alpine glaciers (Sharp et al., 1999; Foght et al., 2004), Arctic Glaciers (Skidmore et al., 2000; Kaštovská et al., 2006; Bhatia et al., 2006), Antarctic glaciers (Stibal et al., 2012b) and the Greenlandic (Yde et al., 2010b) and Antarctic (Lanoil et al., 2009; Pearce et al., 2013; Christner et al., 2014) Ice Sheets. Table 1.1 summarises some key data from these studies, and others in which subglacial microorganisms have been identified.

The studies in Table 1.1 hint at the type of ecosystem which occupy the basal ice and sediments under the glaciers sampled. All samples contained bacterial communities, with the presence of dividing and recently divided cells also evident in some cases (Sharp et al., 1999; Skidmore et al., 2000). The cell counts reported were significant, ranging from 5 x 10^4 cells g^{-1} of sediment in former subglacial lake Hodgson in Antarctica (Pearce et al., 2013), to 1.8 x 10^9 cells g^{-1} of sediment under an alpine glacier in Switzerland (Sharp et al., 1999). Though it is hard to make a direct comparison as absolute cell counts were reported in a variety of units, the range shown in Table 1.1 falls between that of supraglacial ecosystems, such as cryoconite granules (Stibal et al., 2006; Langford et al., 2010; Anesio et al., 2010) and concentrations found in englacial ice (Priscu et al., 1999).

With meltwater from the glacier surface transporting supraglacial cells into

the subglacial system (see Fig. 1.3.1), understanding the subsequent survival of those cells, and whether this flux forms the basis of the subglacial ecosystem, would enable a better understanding of the scope of subglacial ecology. The presence of active, autochthonous communities of microbes is likely, with Bhatia et al. (2006) observing that the subglacial microbial community was distinct from the same glacier's englacial and supraglacial microbes. Kaštovská et al. (2006), whilst finding viable phototrophs in subglacial sediments, also recorded a distinct lipid signature from the subglacial community and Boyd et al. (2014) determined *in situ* activity from metabolic by-products, measured within early season meltwaters.

The culturing and phylogenetic approaches that form the basis of most of the studies in Table 1.1, also indicate cell viability, though give less direct evidence as to cell origin. A limitation of all of these studies, however, is that they are unable to assess the size of the active microbial community. Enumerating viable subglacial cells in combination with phylogenetic study would provide a better estimation as to the origin of cells and of *in situ* metabolic and geochemical potential from sediment microbiota.

Of the organisms reported in these studies, a diverse range of groups with implied, similarly diverse, metabolic and geochemical roles were identified by molecular and culturing techniques. Bacteria were the most abundant observed microorganisms within sediment, though their observation has also received more attention than that of other domains or viruses. Heterotrophs, chemolithotrophs and methanogenic archaea are common metabolic types that have been present under a range of glaciers and ice sheets (see Table 1.1). The presence of chemolithic and methanogenic communities, along with fungi, that have also been reported in subglacial samples (Sonjak et al., 2006; Kaštovská et al., 2006) supports the hypothesis of a geochemically active ecosystem, with an implied microbial role in iron, nitrogen, sulphur and carbon cycling. The relative activity and importance of different communities, however, is still an unknown, with controls on diversity likely a result of carbon limitation (Stibal et al., 2012b), oxygen conditions (Tranter and Skidmore, 2005), and mineralogy (Mitchell et al., 2013).

Restricted access to sample is a major limitation of subglacial microbial studies. Whereas geochemical processes can be inferred from meltwater outflow, genetic analysis requires material sample, and access to the glacier bed prevents the collection of sediment from a broad, or representative range of subglacial till features. Therefore, whilst informative, the analysis offered by the studies

in Table 1.1, is limited in scope when seeking to infer microbial diversity at a glacier scale, let alone the role of subglacial sediment ecosystems with in global methane and nitrogen cycles.

1.3.3 Activity and Microbial Carbon Cycling in Subglacial Sediment

The most fundamental processes within any microbial ecosystem, relate to the where and how of nutrient provision and synthesis. Almost all known forms of life are carbon-based, deriving cellular mass and energy from transformations of inorganic, organic, or a combination of forms of carbon. The diverse range of trophic strategies identified in the studies summarised by Table 1.1, suggests that subglacial microorganisms are involved in the synthesis of inorganic carbon into biomass, as well as the incorporation and mineralisation of organic carbon forms. Understanding the subglacial carbon cycle is fundamental to describing the limitations and adaptations of subglacial microbes, including the relative importance of different metabolisms. Through this, the subglacial ecosystem can be considered relative to cryospheric, or global carbon cycles.

1.3.3.1 Subglacial Metabolism and Carbon Cycling

Primary producers have been identified in a number of subglacial studies in the form of chemoautotrophic species (Gaidos et al., 2004; Mikucki and Priscu, 2007; Lanoil et al., 2009; Boyd et al., 2014). Chemoautotrophic energy demands can be met through the oxidation of reduced mineral species (Ehrlich and Newman, 2009), and so freshly comminuted subglacial sediment may provide them with a potentially rich source of electron donors. Also, as they utilise inorganic forms of carbon to meet cellular carbon demands (Mehrotra and Sumbali, 2009), they are not limited by the supply of organic compounds, which may be transient, or depend upon local geology in subglacial environments. Indeed in some ecosystems, where organic carbon is limiting organotrophic growth, chemoautotrophic carbon fixation can be a crucial supply of organic material for heterotrophic bacteria or higher organisms (Dattagupta et al., 2009; Boschker et al., 2014). Phototrophic cells have also been identified within the subglacial environment (Kastovská et al., 2005; Bhatia et al., 2006; Cheng and Foght, 2007), though they are almost certainly present as a result of transport from supraglacial ecosystems, and little is known about their adaptation, if any, to subglacial

Table 1.1: Summary of studies that have identified subglacial microbes.

Area	Cell Count	Organisms Present	Study
Tsanfleuron, Haut d'Arolla, Switzerland	0.3 x 10^6 - 1.8 x 10^9 1.5 x 10^7 - 2.1 x 10^8 (g^{-1} dry mass)	Sulphide oxidisers	Sharp et al. (1999)
John Evans Glacier, Ellesmere Island	N/A	Aerobic chemoheterotrophs; Anaerobic nitrate reducers; Sulphate reducers; Methanogens.	Skidmore et al. (2000, 2005)
Fox Glacier, Franz Josef Glacier, New Zealand	2.3 ± 0.1 x 10^6 7.4 ± 3.9x 10^6 (g^{-1} dry mass)	Aerobic and microaerophillic heterotrophs; N^2 Fixing bacteria; Nitrate and Fe(III) reducing bacteria.	Foght et al. (2004)
Subglacial Lake Grímsvötn, Iceland	4 x 10^7 (g^{-1} dry mass)	Autotrophs, psycrophilic bacteria	Gaidos et al. (2004)
John Evans Glacier, Ellesmere Island	N/A	58% of subglacial DNA not present in supraglacial or proglacial sample	Bhatia et al. (2006)
Werenskioldbreen and Torellbreen, Svalbard	2.1 x 10^5 - 5.3 x 10^5 (g^{-1} dry mass)	Autochthonous chemoheterotrophs; Allochthonous cyanobacteria and microalgae.	Kaštovská et al. (2006)
Conwaybreen, Kongsvegen, and A. Lovenbreen, Svalbard	9000 CFU L^{-1}	Penicillium Mycobiota	Sonjak et al. (2006)
Kamb Ice Stream, West Antarctic Ice Sheet	2-4 x 10^5 (g^{-1} dry mass) Corrected based on storage period growth rates.	Heterotrophs; Neutrophilic and acidophilic chemolithotrophic iron or sulphur oxidisers.	Lanoil et al. (2009)
SW Greenland Ice Sheet (sediment core)	2.3 x 10^8 - 7.6 x 10^7 (cm^{-3})	Heterotrophs; aerobic iron and nitrate reducers	Yde et al. (2010b)
Robertson Glacier, Alberta, Canada	N/A	Nitrifying bacteria; Nitrifying archea.	Boyd et al. (2011)
Wright Glacier, Antarctica Russell Glacier, Greenland	8 x 10^6 (g^{-1} wet mass) 9 x 10^5 (g^{-1} wet mass)	Chemoorganotrophs, Chemolithotrophs, Heterotrophs, Methanogenic Archaea	Stibal et al. (2012b,c)
Subglacial Lake Hodgson, Antarctica	5 × 10^4 (g^{-1} wet mass)	Sulphur and nitrogen cycling bacteria	Pearce et al. (2013)
Subglacial Lake Whillans, Antarctica	N/A	Chemoautotrophic and heterotrophic bacteria, archaea.	Christner et al. (2014)

conditions.

Heterotrophic bacteria were ubiquitous within the samples referred to in Table 1.1, and together, these studies imply a range of heterotrophic metabolisms. These include a wide range of specialisms, though can be broadly categorised into aerobic and anaerobic respiration, both deriving energy and biomass through the breakdown of organic carbon compounds. The end member of anaerobic metabolism involves the reduction of hydrogen, and/or organic acids into methane to meet the energy demands of methanogenic archaea (Chapelle, 2001). Methane has been found within subglacial pore waters (Skidmore et al., 2000; Boyd et al., 2010; Stibal et al., 2012c), alongside which methanogenic phylotypes were identified (Boyd et al., 2010; Stibal et al., 2012c). Thus methanogenesis has been suggested as a potentially important subglacial carbon cycling pathway in anaerobic sediments and is perhaps the best studied subglacial metabolism.

Less research has been conducted relating to other anaerobic metabolisms in subglacial environments, despite their greater efficiency relative to methanogenesis. Observations from groundwater systems inform us that sediment microbes may utilise redox reactions as a means of respiration. In the absence of oxygen, anaerobic metabolisms can use NO_3^-, Fe^{3+}, SO_4^{2-} or CH_4 as electron acceptors in the oxidation of organic matter or hydrogen (Lovley and Chapelle, 1995). Utilisation of one, or another, of these electron acceptors is partially defined by the energetic efficiency of each terminal electron accepting process (TEAP), with NO_3^- being the most efficient, followed by Fe^{3+}, SO_4^{2-} and then CH_4 (Lovley and Chapelle, 1995). However, anaerobic metabolisms can typically only utilise simple organic compounds as electron donors (Lovley and Chapelle, 1995), and so competition for electron donors may also regulate the occurrence of different TEAPs in an environment. This is especially the case in oligotrophic environments, where activity by microbes capable of utilising more efficient TEAPs, are able to maintain electron donor concentrations at levels lower than bacteria that utilise less efficient TEAPs are able to exploit (Lovley and Chapelle, 1995; Chapelle, 2001).

There is evidence supporting the occurrence of each of these TEAPs within the subglacial environment, though their wider importance, as well as our understanding of their relative distribution within subglacial sediments, is severely limited by the need to infer processes from point samples of sediment or water. Sulphate removal in incubations, stable isotope evidence and genetic evidence, have suggested the presence of sulphate reducing bacteria within some subglacial environments (Skidmore et al., 2000; Wadham et al., 2004; Mikucki and

Priscu, 2007). Sulphate reduction was not found to be common to all subglacial sediments (Foght et al., 2004; Yde et al., 2010b), however, perhaps because of the availability of more energetically favourable electron acceptors (Wadham et al., 2004). Genetic and culture evidence, also suggests a role for iron reducing microbes within several studies (Foght et al., 2004; Mikucki and Priscu, 2007; Yde et al., 2010b; Thór Marteinsson et al., 2012), though there are no direct measurements of its occurrence within subglacial sediments. There has also been evidence to suggest active denitrification within some subglacial samples, primarily through genetic analysis of sediment (Gaidos et al., 2004; Boyd et al., 2011), but also from isotopic evidence, coupled with the removal of snowpack nitrate during subglacial transport (Wynn et al., 2007; Yde et al., 2010b).

Finally, though under-represented within microbial studies of the subglacial environment, fungi also seem likely to be active as heterotrophs within the subglacial carbon cycle, with strains identified in two studies of Svalbard sediments (Kaštovská et al., 2006; Sonjak et al., 2006). Sonjak et al. (2006), not only makes high counts of *Penicillium* spp. within sediments from two Svalbard glaciers, but the presence of low molecular weight secondary metabolites suggests that they are active *in situ*. As with bacterial heterotrophs, fungi such as *Penicillium* spp., would utilise organic carbon sources to meet their nutrition demands and respire carbon dioxide as a by-product (Dix, 2012).

These studies provide a clear picture as to the types of metabolic potential associated with a range of subglacial samples and are simplified by the interactions shown in Fig. 1.3.2. A more detailed assessment of metabolic processes under *in situ* conditions is lacking, however, as even with the identification of phylotypes relating to specific metabolisms, metagenomic or culture techniques do little to assess the relative size or activity of specific communities. Addressing subglacial microbiology within the scope of carbon biogeochemistry, several studies have measured microbial activity using ex situ incubations. Chemoautotrophic activity measurements are only available from one glacial sample (Boyd et al., 2014), and from Subglacial Lake Whillans sediment (Christner et al., 2014). Whereas more has been published on heterotrophic activity, with rates of respiration or bacterial production available from six studies, encompassing glaciers and sub-ice sheet sediments (Mikucki et al., 2004; Gaidos et al., 2004; Kastovská et al., 2005; Mikucki and Priscu, 2007; Lawson, 2012; Christner et al., 2014; Doyle, 2015). Rates of methane production have been characterised within sediments from three glaciers (Boyd et al., 2010; Stibal et al., 2012c). Though, as yet, there are no assessments of fungal activity within subglacial sediments.

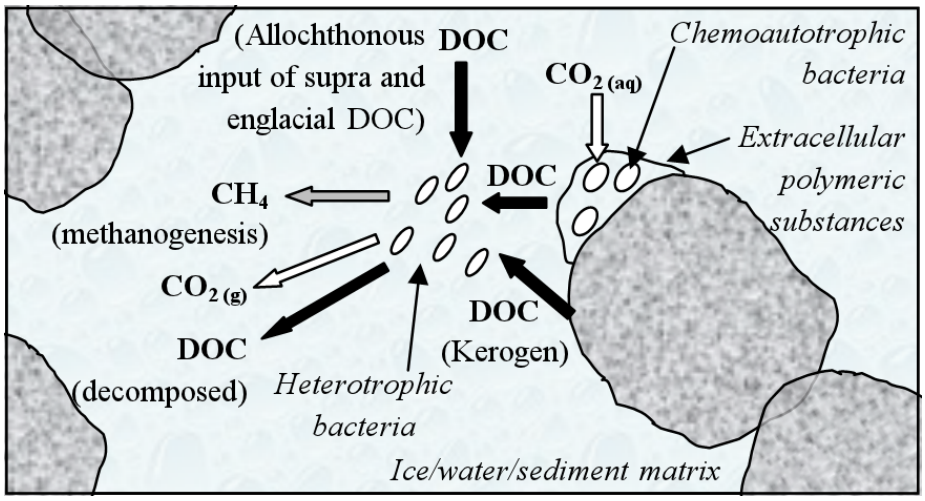

Figure 1.3.2: A simplified schematic showing the possible fluxes of dissolved organic carbon (DOC) (black arrows), methane (grey arrows) and inorganic carbon (CO_2) (white arrows) within subglacial sedimentary environments. Not to scale.

Comparing these studies is difficult, due to a wide range of glacier types and locations, as well as differences relating to *in situ* and/or experimental conditions, not to mention differing standards for normalising carbon transformations. Despite this, the general trend in these studies suggests that rates of carbon fluxes as a result of heterotrophic respiration exceed those of chemoautotrophic carbon fixation. Measured rates of methanogenesis proceeded at a rate far lower (carbon equivalent) than either heterotrophic or autotrophic metabolisms. Moreover, increases in methane evolution concomitant to H_2/CO_2, or acetate amendment (Stibal et al., 2012c), suggests that subglacial methanogens are capable of operating either autotrophically or heterotrophically.

The subglacial till environment is one in which spatial and temporal variations in oxygen conditions can be expected to coincide with melt season dynamics (Wynn et al., 2006; Irvine-Fynn and Hodson, 2010). With both obligate aerobic and anaerobic species evident within subglacial sediments, it is probable that community shifts will occur as a result of oxygen supply to sediments from meltwater or meltwater channels. It is a major limitation of these studies, and indeed most subglacial studies, that they are often based upon point samples, only representing the subglacial community corresponding to conditions at that point. More should to be done to address the relationship between physico-

chemical controls and metabolism under glaciers in order to assess how the microbial carbon cycle might respond spatially under a glacier, or temporally through a melt season.

A good example of this problem can be found within the research conducted upon methanogenesis. Long lag periods were observed before methane production was measurable during ex situ experimentation (Boyd et al., 2010; Stibal et al., 2012c; Lawson, 2012). This perhaps suggests that a relatively stable environment, such as found in sub-ice sheet sediments, may be necessary to allow conditions to develop so that methanogenesis becomes energetically favourable with respect to H_2 competition from other anaerobic metabolisms. Alternatively the methanogenic communities could have been dormant upon sampling, with no energetic constraints, or, perhaps they were inhibited by oxygen within the microcosms themselves. Research into methane within the subglacial environment is further inhibited by a lack of study into methanotrophs, though methane uptake in proglacial soils suggests that there is potential for it to be coupled with methanogenesis (Yde et al., 2010a).

Though the balance of metabolisms is, perhaps, not well enough understood to draw conclusions as to community carbon transformations within subglacial sediments, it is evident that a supply of organic matter is necessary to support heterotrophic respiration and growth. Indeed, the diversity of subglacial prokaryotes has been shown to be somewhat dependant upon sediment organic matter content (Barker et al., 2010; Stibal et al., 2012b,c). The next section (1.3.3.2) examines organic carbon within the subglacial environment, as well as the current state of knowledge with respect to the role that microorganisms play in utilising or creating these compounds.

1.3.3.2 Organic Carbon in the Subglacial System

Glacial sediments can contain organic compounds from surprisingly diverse origins, though these vary considerably in quality. The sediment itself can be rich in fossilised organic carbon if the geology underlying a glacier is sedimentary in nature. Rock-based organic compounds such as kerogen, have been suggested as a possible carbon source for subglacial heterotrophs (e.g. Wadham et al. (2004); Lafrenière and Sharp (2005) and Mitchell and Brown (2008)). Wadham et al. (2004) utilised isotope ratios of respired carbon in sediments from Finsterwalderbreen, Svalbard, to inconclusively suggest that the metabolised organic carbon fraction was kerogenous. Later work on the same sediments, however, instead

determined that the subglacial community had a preference for lower molecular weight carbon forms, only utilising rock-derived organic carbon once more labile substrates had been exhausted (Lis et al., 2010; Lawson, 2012; Lawson et al., 2015). Even then it was uncertain whether the carbon utilised was kerogen, as younger sedimentary organic matter was also present (Lawson, 2012). Kerogen, and other lithogenic organic matter tends to be complex and recalcitrant, being difficult to break down, even in warmer temperatures (Petsch et al., 2001). Further, whereas it is abundant within Svalbard geology, for example, it would be absent within the granitic sediments common to Greenlandic or Alpine glaciers. An alternative source of organic carbon would, therefore, be required to fuel heterotrophic growth.

Overridden terrestrial, lacustrine or marine organic material is another potential source of organic carbon for subglacial microbes; one that will vary in quality depending upon source. The incorporation of higher vascular plants such as found in tundra environments would provide less labile lignin-based material (Barker et al., 2006). Marine or lake sediments, on the other hand, would contain higher concentrations of proteinaceous particulate organic matter (Meyers and Ishiwatari, 1993; Parlanti, 2000; Yamashita et al., 2010; Lawson et al., 2015). It is possible, therefore, that the material present prior to glaciation has ongoing impacts upon contemporary subglacial ecosystems. And indeed this was observed by Stibal et al. (2012b) and Stibal et al. (2012c), when greater abundance, diversity and rates of methanogenesis were apparent in subglacial sediments of lacustrine history, compared with overridden Holocene-aged soils..

With pathways shown in Fig. 1.3.1, organic carbon may also enter the subglacial environment from basal ice melt, or from snow and supraglacial meltwater. This may originate from the supraglacial microorganisms that occupy glacial snow and ice (Hodson et al., 2008), and wash into subglacial sediment, a significant organic carbon flux, during the melt season (Koziol et al., *in review*). Anthropogenic aerosols, products of combustion, have also been found in high concentrations on glacier surfaces in Alaska (Hood et al., 2009; Stubbins et al., 2012). Moreover, spectral analysis indicated that they were proteinaceous compounds, with high bioavailability (Hood et al., 2009; Stubbins et al., 2012). These forms of supraglacial organic carbon may be transported to subglacial sediments through ablation, conveyed by crevasse systems, moulins, or through inter-granule percolation (Brown, 2002; Kaštovská et al., 2006; Bhatia et al., 2006). Cells or aerosol that remain in the accumulation zone are eventually incorporated into glacial ice (Priscu et al., 2007; Stubbins et al., 2012), and so

when basal ice reaches the pressure melting point, englacially transported cells and organic material become available for degradation by subglacial microbes.

Autochthonous primary production within subglacial sediments provides, perhaps, a final organic carbon source for subglacial heterotrophs (Stibal et al., 2012c; Boyd et al., 2014; Christner et al., 2014; Lawson et al., 2015). Activity from autotrophic methanogens, and chemoautotrophic communities can incorporate inorganic carbon into biomass, thereby making it available for other metabolisms. Furthermore, experiments in Lawson (2012) show a preference for subglacial microbes to utilise lower molecular weight carbon sources. It is likely, therefore, that autochthonous cellular organic carbon and extracellular exudes, as well as cellular material supplied by glacial meltwater, represent an important source of bioavailable organic carbon to subglacial communities. A further benefit that comes from utilising organic matter supplied by glacial melt water, and autochthonous products, is that they can be re-supplied, and so respiration is not reliant upon finite geological organic matter, or serendipitously overridden lake sediments.

There is a growing body of evidence which suggests that glaciers are important as exporters of proteinaceous organic carbon to fjord and marine ecosystems (Lafrenière and Sharp, 2005; Barker et al., 2006; Hood et al., 2009; Dubnick et al., 2010; Stubbins et al., 2012; Fellman et al., 2014; Hawkings et al., 2015; Hood et al., 2015). It so follows, that fluxes of labile organic carbon are available to subglacial ecosystems also. Some of the above mentioned organic carbon dynamics are fairly well quantified, especially with respect to glacial runoff. However, quantification of englacial cell concentrations, or primary production by subglacial autotrophs, remain the product of a small number of studies (e.g. Priscu et al. (1999) or Boyd et al. (2014)). Though there are several studies which identify potential sources of organic carbon for use by subglacial microbes, experiments performed by Lawson (2012) are, currently, the only to assess microbial usage of these fractions. More needs to be done to assess how the quality and quantity of carbon supply affects productivity in subglacial sediments, what repercussions this may have for labile carbon and nutrient export by glaciers, and how carbon metabolism may be linked other microbial processes in the sediment.

1.3.4 Subglacial Hydrogeochemistry: An Old Paradigm

Prior to evidence of active microbial life within subglacial sediments, glacial meltwater chemistry was considered to simply relate to inorganic mineral weathering reactions. With solute predominantly being derived from carbonate dissolution and the oxidation of sulphides (Thomas and Raiswell, 1984; Tranter et al., 1993, 1994; Chillrud et al., 1994; Tranter et al., 1996; Brown, 2002). The identification of microbes with subglacial sediments precipitated a steady realisation that many of the observations within glacial outflow could be best explained through microbial processes, such as the removal of snowpack nitrates (Tranter et al., 1994), or the magnitude of observed metal sulphide oxidation (Bottrell and Tranter, 2002). The subglacial environment with the inclusion of microbial processes, is a much more complex place. Now, mineral weathering may also be subject to factors that affect microbial populations rather than being governed by abiotic redox reactions and solute equilibria. Hence, variations in microbial activity, competition for resources, and physical controls upon community structure may also affect outflow chemistry. To understand subglacial hydrogeochemical processes, one must now, therefore, consider the role of microbes, and their influence upon the bulk chemistry of subglacial outflow.

1.3.5 Subglacial Geomicrobiology: A Thesis

The shift in understanding of subglacial environments, from being functionally abiotic to containing geochemically active and metabolising microorganisms, has introduced the need to reassess its former model of rock-water geochemistry. In the new geomicrobial model, microbes are introduced as key mediators of mineral weathering processes, carbon and nutrient cycles under glaciers. This topic, however, is still very much in its infancy. In general terms, microbes may directly influence mineral weathering through active oxidation of reduced mineral phases for the generation of energy (Chapelle, 2001), or through the preferential scavenging of nutrients or organic compounds within mineral latices (Ehrlich and Newman, 2009). Indirect weathering from microbes may also occur, through the introduction of organic acids, carbonic acids and protons into the environment from metabolic by-products, and from the generation of acid through the oxidation of metal sulphides (Welch and Ullman, 1993; Uroz et al., 2009; Madsen, 2011). The following sections describe research conducted in order to ascertain the microbial role in some key subglacial chemical cycles.

1.3.5.1 The Weathering of Metal Sulphides

Sulphur is a common constituent of igneous and sedimentary geology, often appearing in its reduced form as a metal sulphide mineral (Ehrlich and Newman, 2009). It is an important element to microbial life as a constituent of cells, but its role to microbes in geological environments mostly relates to its involvement in oxidation reduction reactions. Reduced forms of sulphur such as pyrite, may be microbially oxidised and serve as a source of energy, whereas oxidised forms such as sulphate, may be reduced when used as an electron acceptor by anaerobic metabolisms (Ehrlich and Newman, 2009; Chapelle, 2001).

With sulphate frequently observed in high concentrations in subglacial outflow, this suggests sulphur cycling as a dominant redox reaction in the sediment rich waters underneath glaciers (Lamb et al., 1995; Tranter et al., 1996, 2002; Bottrell and Tranter, 2002; Irvine-Fynn and Hodson, 2010; Skidmore et al., 2010). Moreover, it suggests that the oxidation reduction reactions involved in its state change may be a key source of energy for subglacial microbes (Boyd et al., 2014). In other environmental systems, the oxidation reduction reactions of sulphur species are often controlled by microbial processes (Hurtgen et al., 2002; Kehoe et al., 2004; Mazumdar et al., 2008; Geelhoed et al., 2009; Luther et al., 2011; Stam et al., 2011). It became apparent that this was a likely scenario for subglacial sediments also, with Bottrell and Tranter (2002) observing sulphate concentrations in subglacial outflow, far in excess of that which could be supplied through abiotic oxidation of pyrite alone. The importance of pyrite to subglacial microbes also has support from genetic evidence (Skidmore et al., 2005; Lanoil et al., 2009; Stibal et al., 2012b; Boyd et al., 2014) and from a study by Mitchell et al. (2009), which incubated sterile mineral phases in a subglacial channel and found that the pyrite phase became colonised with bacteria that was genetically most similar to the native consortia. Direct measurements of microbial pyrite oxidation have also been made in laboratory experiments by Sharp et al. (1999); Montross et al. (2012) and Boyd et al. (2014), all of which observed enhanced rates of sulphate production from microbial processes. Under reducing conditions, Wadham et al. (2004) has also identified active sulphate reduction within sediments at Finsterwalderbreen, Svalbard.

The oxidation reactions that govern pyrite weathering remain poorly understood in natural systems despite significant research into sulphide oxidation and its relation to acid mine drainage. Metal sulphide can be oxidised by molecular O_2, or through an electron exchange process that most commonly occurs with

Fe^{3+}; these reactions are summarised by Equations 1.3.1 and 1.3.2 respectively (Singer and Stumm, 1970). Bacterial oxidation of pyrite can occur through two processes: indirect oxidation, in which the microbial role relates to the reoxidation of Fe^{2+} within solution, or, direct oxidation, in which bacteria directly oxidise the Fe^{2+} and S^{-} in pyrite, through a poorly understood enzymatic oxidase process, which utilises molecular O_2 as an electron acceptor (Nordstrom et al., 2008; Smith et al., 2012). Direct and indirect bacterial oxidation of pyrite are also described in terms of Equations 1.3.1 and 1.3.2 respectively, however, the rate at which the reactions occur via bacterial catalysis, is significantly faster than through abiotic processes (Nordstrom et al., 2008).

$$FeS_2 + 3.5O_2 + H_2O \leftrightarrow 2SO_4^{2-} + 2Fe^{2+} + 2H^+ \tag{1.3.1}$$

$$FeS_2 + Fe^{3+} + 8H_2O \leftrightarrow 2SO_4^{2-} + 2Fe^{2+} + 16H^+ \tag{1.3.2}$$

For researchers, the difficulty of investigating these reactions comes when trying to separate the mechanism by which sulphide is oxidised. Analysis of the stable O-isotope composition within sulphate is frequently used to separate between the oxidation reaction pathways described by Equations 1.3.1 and 1.3.2, and to identify sulphate that is present from the dissolution of reactive sulphur minerals such as gypsum or anhydrite. The rationale behind this methodology relates to large differences between the $\delta^{18}O$ of air (+23.5‰) and water (-50 to +10‰) (Nordstrom et al., 2008), thereby allowing differentiation between oxygen sources that become incorporated into sulphate during either Equation 1.3.1 or 1.3.2. However, as the reactions expressed by Equations 1.3.1 and 1.3.2 involve several oxidation-reduction reactions, intermediate sulphur species may react with additional solvent molecules before being incorporated into the sulphate, thereby altering its $\delta^{18}O$ (Pisapia et al., 2007; Tichomirowa and Junghans, 2009; Smith et al., 2012). Further complications arise from the sorption of molecular O_2 onto pyrite surfaces, which may then be incorporated into sulphate, even though oxidation may be though Equation 1.3.2 (Nordstrom et al., 2008; Heidel and Tichomirowa, 2011). As well, oxidation through Equation 1.3.2 may occur, where the reactant water molecule is derived from the oxidation of ferrous iron (Equation 1.3.3), and thereby has the $\delta^{18}O$ of molecular O_2 (Pisapia et al., 2007).

$$Fe^{2+} + 0.25O_2 + H^+ \rightarrow 0.5H_2O + Fe^{3+} \quad (1.3.3)$$

Analysis of δ^{34}S within sulphate has also been investigated as a method whereby oxidation mechanisms can be explored (Balci et al., 2007; Nordstrom et al., 2008; Heidel and Tichomirowa, 2011; Smith et al., 2012). However, there has been no consistent trend in S-isotopic fractionation between pyrite and sulphate in laboratory oxidation experiments. Suggesting that our understanding of the oxidation process is limited when attempting to infer reaction pathways from S-isotope information. This is particularly relevant when considering that fractionation of S and O isotopes may also vary under differing environmental conditions, such as temperature, pH, redox and bacterial interactions (Nordstrom et al., 2008).

Despite these uncertainties, several glacial studies have utilised a stable isotope approach to prospect for bacterial pyrite oxidation, or to investigate subglacial hydrology by making distinctions between anaerobic and aerobic waters using the inferred pyrite reaction mechanism (Bottrell and Tranter, 2002; Wynn et al., 2006; Hodson et al., 2009; Wadham et al., 2010a). Without fully understanding this reaction mechanism, however, the confidence in this approach is low. For example, bacterial oxidation under aerobic conditions could be mistakenly interpreted to represent anaerobic conditions, should the majority of sulphate be produced through bacterial reoxidation of iron (Equations 1.3.3 and 1.3.2). Considering its implied importance in subglacial systems, a greater understanding of this process may be crucial for to our interpretation of life under glaciers, as well as strengthening the methods used to investigate it.

1.3.5.2 Iron

Iron is the fourth most abundant element in the Earth's crust and an important constituent of enzymatic electron transport mechanisms for most microorganisms (Ehrlich and Newman, 2009). In nature, iron is commonly present in three oxidation states (0, +2 and +3), the distribution of which is primarily controlled by local pH and oxygen conditions. Oxygenated systems with a pH greater than 5 tend towards ferric iron (Fe^{3+}) in the form of solid oxides, hydroxides and oxyhydroxides. Ferrous iron (Fe^{2+}) may be produced by the oxidation of metallic iron (Fe^0) under acidic conditions or, in the absence of oxygen, through the bacterial reduction of ferric solid phases (Ehrlich and Newman, 2009). Hence in many natural systems, iron is present in the solid phase, thereby reducing

its availability for assimilation by organisms (Raiswell and Canfield, 2012). In terrestrial systems where iron is plentiful, this is overcome by a multitude of adaptations, collectively referred to as siderophores, that utilise chelators to solubilise ferric iron for assimilation (Neilands, 1995; Dhungana and Crumbliss, 2005). In marine systems where there is little input of terrestrial waters or sediments, however, ecosystems may become restricted by iron limitation to phytoplankton photosynthesis (Behrenfeld et al., 1996; Geider and La Roche, 1994).

The Southern Ocean, a current object of interest to geoengineers looking for carbon sinks (Assmy et al., 2006), appears to be iron limited with respect to photosynthesis in stretches of open water (Coale et al., 2004), though not in areas closer to land masses (eg. the Weddell and Scotia Seas (de Baar et al., 1990)). This is interesting from a glacial perspective as it suggests that glaciers and ice sheets and, moreover, the iron cycling beneath them, is a potential delivery mechanism of terrestrial iron into the Southern Ocean.

Several studies have investigated the importance of glaciers in providing a source of bioavailable iron in the form of ferrihydrite, an amorphous, readily soluble iron oxyhydroxide, to Antarctic (Raiswell et al., 2008b; Hawkings et al., 2014) and Greenlandic (Hawkings et al., 2014; Statham et al., 2008; Bhatia et al., 2013) marine ecosystems. Whereas Death et al. (2014) utilised the MIT Global Ocean Model (Parekh, 2004) to attempt to quantify the impact of glacial derived iron export upon Southern Ocean productivity, suggesting a 40% increase in primary productivity as a result of sub-icesheet iron inputs. Little has been done, however, to physically measure ecosystem response to glacial inputs of iron. Moreover, the prospect of bioavailable iron reaching stretches of open, iron-limited waters through diffusive fluxes remains unlikely (Hopwood et al., 2015), though ice-rafted debris offers a potential delivery mechanism (Raiswell et al., 2008b).

Within the scope of this PhD project, the role of microbes in the subglacial iron cycle, driving these iron fluxes, becomes important. And whatever the eventual fate of bioavailable iron within subglacial outflow, its potential warrants further investigation. Again, it is iron sulphides such as pyrite that provide a plentiful supply of base material from which reactive iron nanoparticles may be produced (see Equations 1.3.1 and 1.3.2) (Raiswell et al., 2009, 2008b, 2006, 2008a). It follows, that as mediators of these reactions, microorganisms may be implicit in the subglacial iron cycle also, and hence in the formation of bioavailable iron oxy(hyd)oxides. Aside from the uncertainty relating to iron

transport into fjord and marine systems, and its uptake by organisms there, there are no current publications which investigate the role of microbiology in the formation of bioavailable iron under glaciers.

1.3.5.3 Nitrogen

Nitrogen is an essential nutrient for microbial life, making up cellular material like proteins and nucleic acids (Bothe et al., 2007). In nature, important inorganic forms of nitrogen for microorganisms include the dissolved compounds: ammonia, ammonium, nitrate and nitrite, as well as gaseous nitrogen (Ehrlich and Newman, 2009). The former, dissolved inorganic compounds of nitrogen are forms of nitrogen that microbes may assimilate, oxidise or reduce according to the processes outlined in the simplified nitrogen cycle shown in Fig. 1.3.3.

The presence of these compounds in an environment, however, is ultimately a function of the fixation of atmospheric nitrogen gas to ammonia. In glacial systems, this process may occur nonsymbiotically, by nitrogen fixing bacteria. However, the only evidence of direct fixation of nitrogen gas by a supraglacial ecosystem suggests that rates of fixation are exceeded by allochthonous inorganic nitrogen inputs (e.g. precipitation) (Telling et al., 2011). Furthermore, though the nitrogenase enzyme responsible for catalysing nitrogen fixation have been observed in subglacial sediments, no active fixation has, as yet, been detected (Foght et al., 2004; Boyd et al., 2011). Accessible forms of nitrogen must, therefore, be supplied to the glacier bed, from the melting of glacial ice or snow, in order for the processes in Fig. 1.3.3 to occur.

Boyd et al. (2011) offers perhaps the best available insight into subglacial nitrogen cycling processes, using gene biomaker analysis to show genetic potential for actively nitrifying, nitrate reducing and diazotroph microbes in sediments under Robertson Glacier, Canada. Microcosm experiments were also used to observe these traits. These findings agree with microcosm experiments used by Skidmore et al. (2000), Foght et al. (2004) and Montross et al. (2012), all observing a reduction of nitrate within anaerobic subglacial sediment, perhaps indicating assimilatory nitrate reduction, or denitrification. These studies, along with isotopic evidence from glacial waters (Wynn et al., 2007; Hodson et al., 2010b; Yde et al., 2010a), all suggest the potential for active subglacial nitrogen cycling at a variety of glaciers and, moreover, that production in sediments may be N-limited (Boyd et al., 2011). Ammonium and nitrate within snowmelt appears to be utilised subglacially, with isotopic evidence supporting

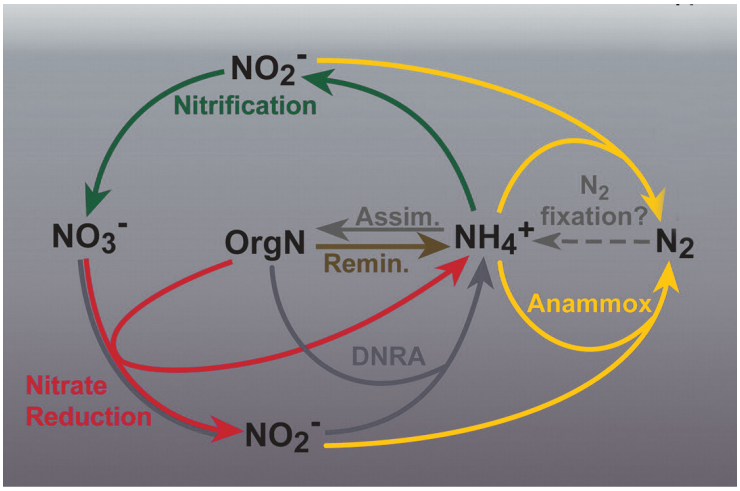

Figure 1.3.3: A simplified schematic of the nitrogen cycle. Adapted from Lam et al. (2009) DNRA is dissimilatory nitrate reduction and Anammox is anaerobic ammonia oxidation.

nitrification of ammonia inputs (Wynn et al., 2007; Ansari et al., 2013), and a reduction of nitrate (Tranter et al., 1994, 2002; Hodson et al., 2010b) during transport through glaciers. Whether the majority of sediments in distributed systems receive enough input to support nutrient demand or denitrification is unknown, however.

1.4 Summary

Subglacial sediments are an ecosystem shown to contain a wide range of microbial life. Within this diversity, are species that reflect the nutrient poor conditions, and abundant reactive mineral phases that are typical of subglacial conditions. Genetic analysis of sediment points to species typically involved in sulphur, iron and nitrogen cycling processes, as well as a range of metabolisms: aerobic and anaerobic heterotrophs, chemoautotrophs and methanogenic archaea. The linkage between microbial processes and geochemistry has also been observed within the geochemical analysis of glacial sediments or waters, which show evidence of pyrite oxidation, denitrification and carbonation as a result of biological energy and carbon transformations.

At the time of writing, there are a fairly large amount of studies documenting the diversity of subglacial microbial communities, as well as those which infer

microbial processes from chemical analysis of glacial waters. What is lacking within the literature, are studies that make direct measurements of the processes in which subglacial microbial communities are involved. This omission is in part due to difficulty of access, which has limited studies to either analysing point samples, or the use of proxies. Direct measurements of biological processes are necessary to assess the importance of microbes within subglacial biogeochemical cycles. Further, for these measurements to provide insight into processes at a whole-glacier scale, they must be made with respect to the complexity of ecological niches present within the subglacial sediment environment.

1.5 Aims and Objectives

Building upon the studies discussed within the literature review, the research undertaken for this PhD aims to directly characterise geomicrobial processes within the subglacial sediment ecosystem. By combining a novel sampling strategy with the use of direct biological measurements under experimental conditions, this work's aim is further set to investigate the importance of different physico-chemical conditions to subglacial life. Through a greater understanding of the complexity and variability of ecological niches underneath glaciers, whole-glacier biological processes may be better constrained. The aims of this research will be approached through the following three objectives:

1. The first objective will investigate how the microbial ecology of subglacial sediment is influenced by factors such as geology, organic matter content, glacier hydrology and geographic location. A combination of enumerative fluorescent staining techniques will be used to quantify live prokaryotic cells at a domain level within different subglacial sediments, as well as enumerating dead cells, and surface-derived autofluorescing material. This Objective is addressed in Chapter 3, and will form the basis from which further analysis of microbe-mineral interactions will be made.

2. The second objective will investigate subglacial carbon cycling by measuring the relative importance of heterotrophic and chemoautotrophic metabolisms within subglacial sediments of contrasting geology, organic matter content, glacier hydrology and geographic location. Factors which may influence microbial activity, such as sediment organic matter composition, oxygen conditions, and alternative electron acceptor availability will be explored using microcosm experiments. Through this Objective, insight

into the importance of subglacial metabolisms to overall glacial carbon cycling will be gained. This Objective is addressed in Chapter 4.

3. The third objective will investigate the role and importance of subglacial microbes in mediating pyrite, carbonate and silicate weathering reactions within glacial tills of contrasting geology and ecology. Microbial enhancement of weathering processes will be directly measured using microcosm experiments, and the mechanisms through which weathering occurs will be explored. This Objective is addressed in Chapter 5.

1.6 Experimental Design and Project Scope.

The majority of studies discussed in the literature review were limited in scope by sample availability, or restricted to the use of proxy studies. This study, therefore, made use of a relatively large number of sediment samples, taken from several glaciers, and utilised a microcosm approach to directly measure sediment microbial processes in parallel, and under controlled experimental conditions. This approach allowed investigation of ecology and geochemistry in context of natural variations in sediment and glacial properties, as well as providing the opportunity for controlled manipulation of conditions. Moreover, a microcosm approach allowed separation of biological processes from abiotic geochemistry, and hence precise measurement of microbial biogeochemical cycles.

Through this approach, Objective 1 sought to further the understanding of limitations imposed upon glacial ecosystems by differing geographical, physical and chemical conditions. Conversely, Objectives 2 and 3 sought to investigate this relationship by determining how microbes within glacial sediments influenced their ecosystem, through their involvement in the cycling of energy and matter. By adopting an experimental approach to address Objectives 2 and 3, this study provided empirical evidence for carbon cycling and geochemistry within subglacial sediment environments. This takes a different approach to the majority of culturing and genetic studies discussed within the Literature Review, in that it considers sediment processes above ecosystem potential. Moreover, it differs from the majority of biogeochemical studies, in that it focuses upon sediment-scale processes rather than seeking to quantify biogeochemical fluxes at a glacial scale. In taking a process led approach, much needed verification of the activity of microbes within subglacial sediments could be made, whilst their limitation and involvement in geochemistry could be considered in context

of their environment. The scale of study adopted here provided greater detail of some of the important microbial processes which may occur underneath glaciers. From this basis, it is hoped that more informed studies of subglacial biogeochemistry can be made, and the role of subglacial microbes within glacier biogeochemical cycles be more fully understood.

Chapter 2

Field Sites and Sampling

Accessing the subglacial environment is difficult. Whereas it is sometimes possible to find recently exposed till in front of retreating glacier margins, or to sample from melt water channels in winter and spring months, the resulting point samples may be limited in their representation of whole-glacier conditions. Moreover, single point samples can easily introduce bias and, if contaminated, mislead, when drawing conclusions about subglacial microbial ecosystems. To address the sampling limitations imposed by access to the subglacial environment, this study adopted a multi-glacier approach. Here, sediments taken from several different glaciers were used to increase the overall sample size, but to also assess commonality between different glaciers, different subglacial conditions, and different sediment geologies.

The sediments used in this project were collected from nine glaciers, located in Svalbard, Greenland, South Georgia and Livingston Island. With access to subglacial sediment always uncertain when first visiting a glacier, the samples described in this Chapter are the fruits from opportunistic sampling carried out over five field seasons. Though sampling was opportunistic, the resultant sample pool comprises of sediments from a range of locations, with different geologies, and taken from different bedform features. This chapter gives an overview of the glaciers investigated in this project, explains the sampling strategy adopted at each site and describes the sediment as it was found *in situ* before being gathered for further study in Sheffield. At the end of this Chapter, Table 2.1 summarises the key features and properties of each sediment.

With the sampling for this study being opportunistic, several glaciers were visited where no access to subglacial sediment was possible. These were: Flein-

isen, Foxbreen, Foxfonna, Larsbreen, Longyearbreen, Reiperbreen and Austre Grønfjordbreen in Svalbard, and Storglaciären, Sweden. Though sampling was not possible at these sites at the times visited (2012 for the glaciers in Svalbard, and 2013 for Storglaciären), the dynamic nature of glacial morphology leaves open the opportunity for sampling at these sites in the future.

2.1 Svalbard

Sediment was sampled from six glaciers in the Isfjorden area of Spitsbergen, part of the Svalbard archipelago, northern Norway. Four of these: Vestre Grønfjordbreen, Scott Turnerbreen, Tellbreen and Hørbyebreen, were sampled for the purpose of microbiological and geochemical microcosm experiments, whilst Von Postbreen and Brucebreen were opportunistic samples, taken for microbiological study only. Fig. 2.1.1 gives an overview of the glaciers sampled, with specific site coordinates listed in Table 2.1. Sampling in Svalbard was conducted in the late spring, and summer season of 2012, for all glaciers except Tellbreen, which was sampled in February 2013.

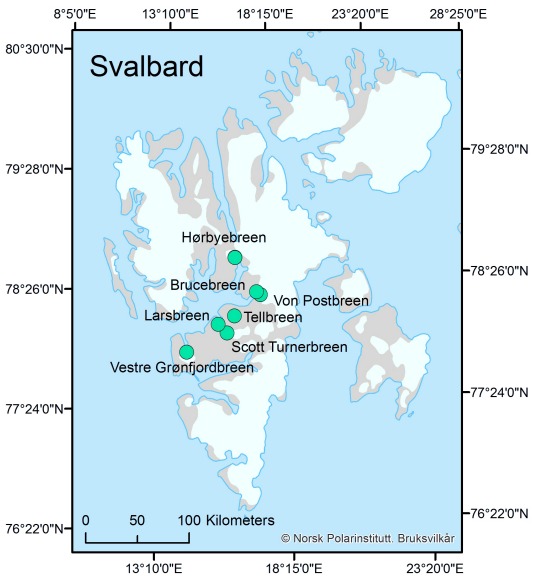

Figure 2.1.1: Svalbard glaciers from which sediment samples were taken during a 2012 field campaign.

2.1.1 Vestre Grønfjordbreen

Vestre Grønfjordbreen (N 77.94°, E 14.26°), hereafter VG, was the largest of a group of glaciers at the head of Grønfjord, in central-west Spitsbergen (Fig. 2.1.2). Local geology consists of argillites, siltstones and calcareous sandstones (Semevskij and Škatov, 1965). The forefield was dominated by the proglacial lake, Bretjørna, which was dammed from Grønfjord by push moraine complexes. Internal reflecting horizons observed by radio-echo sounding (Jania and Navarro, 2010) along with the the formation of a winter naled, indicate that VG was polythermal. Proglacial rivers from VG, and the adjacent Austre Grønfjordbreen, all feed into Bretjørna, which then breaches the push moraine and flows into Grønfjord itself. At the time of sampling, the VG ice margin was approximately 2 km from the push moraine complex, and though the timing of its most recent advance was unknown, the moraine gives evidence of two separate advances (H. Lovell, unpublished data).

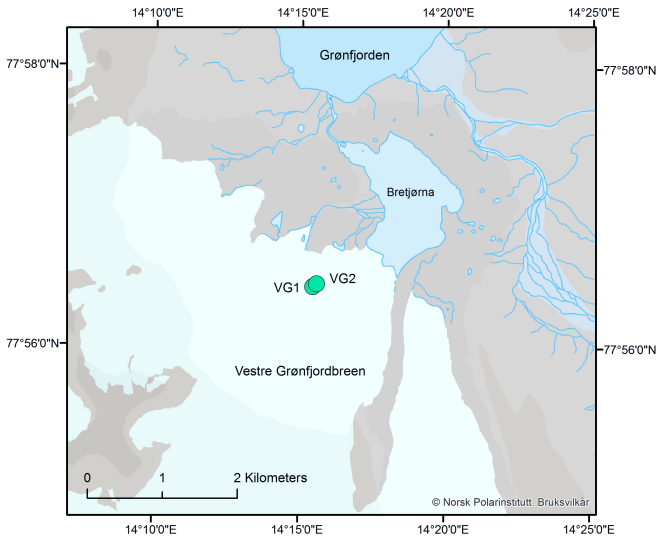

Figure 2.1.2: Grønfjordbreen, Svalbard. The green circles indicate the location of sampling sites at the 2012 glacial margin.

Several studies have been carried out in the area investigating: mass balance(Hagen et al., 2003), naled chemistry (Yde et al., 2012), geomorphology (H. Lovell, unpublished data) and glacial thermal regime (Jania and Navarro, 2010). In this context, VG was an excellent glacier at which to study subgla-

cial biogeochemistry, as experimental data can be put into context of outflow hydrology and chemistry. VG was visited on 6th August 2012. The retreating margin was used as an opportunity to sample freshly exposed glacial till from just underneath the ice. Sediment (shown in Fig. 2.1.6a) was poorly sorted, largely made up of fine grain silts, but with pebbles, cobbles and boulders also present, suggesting that it has not been reworked by a channelised flow.

Sediment was removed at two locations *c.* 200 m and 300 m west of the subglacial outflow channel (see Fig. 2.1.2 for an overview, and Table 2.1 for site coordinates). The sample sites were accessed from voids under the ice margin. Surface sediment was removed, allowing sediment from *c.* 20 cm depth to be collected using a flame-sterilised stainless steel spoon. It was then placed into sterile, 532 mL WhirlPak® bags (Nasco, Fort Atkinson, USA). Additional samples were placed into 15 mL, sterile, centrifuge tubes and fixed with 2 % (final concentration) formaldehyde for later analysis by microscopy. The unfixed samples were placed in a -20°C freezer, immediately upon return from the field and remained in a frozen state whilst transported to Sheffield, where they were also kept at -20°C until used in experiments.

2.1.2 Scott Turnerbreen

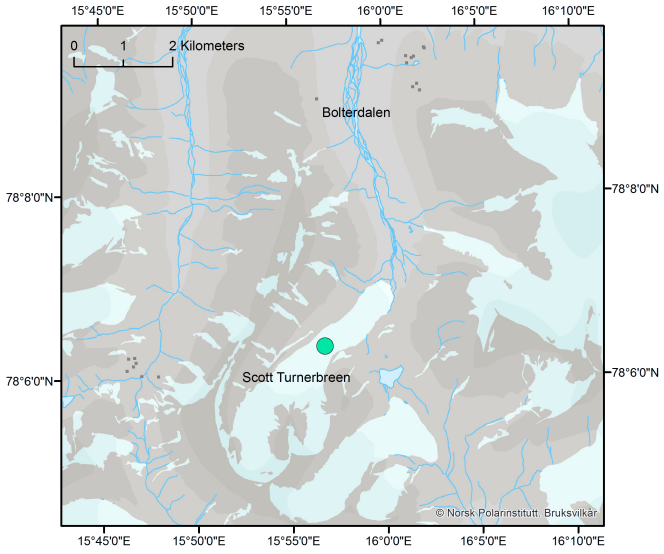

Figure 2.1.3: Scott Turnerbreen, Svalbard. The site of the thrust feature from which sediment was sampled was indicated by the green circle.

Scott Turnerbreen (N 78.45°, E 17.24°), hereafter ST, was a cold-based (Hodgkins et al., 1999) glacier located at the head of Bolterdalen in central Spitsbergen (Fig. 2.1.3). At the time of sampling, the glacier margin was *c.* 1 km from a prominent end moraine, formed by a surge event in the 1930's (Hagen et al., 1993). Bolterdalen lies in Tertiary strata of sandstones, shales and siltstones (Major and Nagy, 1972). It was one of many valleys in the area whose river feeds into Adventelva, a large braided river system dominating Adventdalen and flowing out into Isfjorden. Meltwater from ST was primarily conveyed by two marginal streams running through ice cored moraine into the proglacial river system.

Using ground penetrating radar and borehole temperature measurements, Hodgkins et al. (1999) determined that the presence of temperate basal ice was unlikely. A loss in ice thickness, following the 1930's surge, pushed ST below the minimum thickness required to sustain basal ice above the pressure melting point (Hodgkins et al., 1999). And so, as with many glaciers in Svalbard (Dowdeswell et al., 1995), following a combination of surge-thinning and increased post-Little Ice Age (LIA) temperatures, ST has undergone a shift in its thermal regime and dynamics.

Though decoupled from present-day hydrology in Bolterdalen, the subglacial sediment at ST still offers an interesting ecosystem to study. With a large number of polar glaciers thinning to the point of becoming cold based, the impact this has on sediment ecosystems should be explored. Not only is it probable that some bacteria will be able to maintain active metabolisms, as observed, for example, down to -20°C with permafrost bacteria (Rivkina et al., 2000) or with glacial isolates, down to -33°C So too, as these thinning glaciers are often retreating, microbial survival under cold based glaciers may later influence the deglaciated forefield ecosystem.

Sampling was conducted from a thrust fracture, containing poorly sorted sediment (see Fig. 2.1.3 for an overview, and Table 2.1 for the site coordinates). Striations visible on larger cobbles indicated a subglacial origin to the sediment. It was possible that basal sediment was forced upwards and entombed in an englacial cavity during the 1930's surge event. Surface sediment was removed until a uniform frozen sediment face was exposed. This was further excavated using a flame-sterilised stainless steel adze and blocks of frozen sediment were removed and placed directly into sterile, 532 mL WhirlPak® bags. Samples were taken and handled as for Vestre Grønfjordbreen (Section 2.1.1). The sediment extracted from ST (Fig. 2.1.6b) was well sorted sands and silts, with very

occasional pebbles also present.

2.1.3 Tellbreen

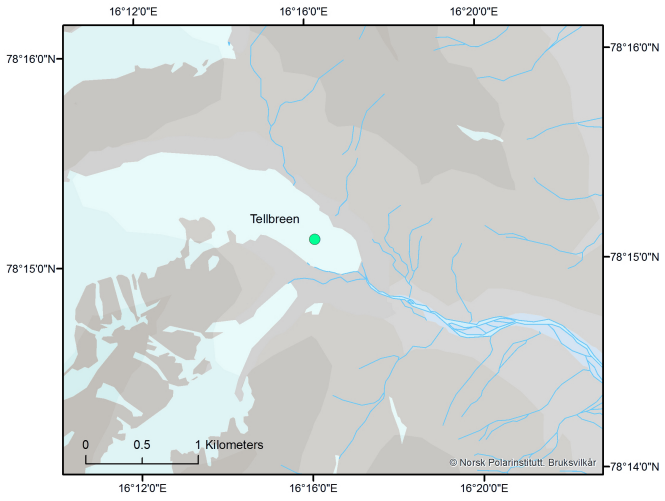

Figure 2.1.4: Tellbreen Glacier, Svalbard. The entrance to the subglacial meltwater channel from which a sample was taken is indicated by a green circle.

Tellbreen (N 78.25°, E 16.26°), hereafter TB, was a 3.5 km long valley glacier to the north of Adventdalen, Central Spitsbergen (Fig. 2.1.4). TB sits within Helvetiadalen, a valley consisting of Jurassic and Cretaceous sandstone and siltstone deposits, and dominated by a river system fed mostly from TB runoff. This river was a tributary to Adventelva, flowing out into Isfjorden. TB was a cold based glacier with an extensive, well mapped system of subglacial and englacial channels (Bælum and Benn, 2011). These have the capacity to store and transport liquid water throughout the year and are the source of TB's characteristic naled, which forms during the winter (Bælum and Benn, 2011). Mass balance for this glacier was negative, with thinning (0.6 $\pm$0.1 m/year), and a substantial retreat from its LIA moraine observed (Bælum and Benn, 2011). Because of the accessibility of the drainage system, TB gives a good opportunity to study sediment occupying the margins of channelised drainage systems. Sediments here potentially receive greater inputs of oxygen and any dissolved organic matter and nutrients, washed down from surface melt.

Sampling was conducted in Spring 2013 by Prof Andy Hodson. Sediment was

excavated from a sediment-rich ice facies of the main outflow of TB's channelised drainage system (see Fig. 2.1.4, and Table 2.1 for sampling location). Sediment was sampled into sterile WhirlPak® bags and transported to Sheffield, all in a frozen state. Once in Sheffield, a sub sample was removed and fixed in 2% final concentration formaldehyde whilst the remaining sample was kept at -20°C until immediately before use in experiments. The sediment extracted from TB (Fig 2.1.6c) was predominantly silty, though with some larger, darker pebbles also present.

2.1.4 Hørbyebreen

Hørbyebreen (N 78.75°, E 16.35°), hereafter HB, was a polythermal valley glacier located in Billefjorden, Spitsbergen (Fig. 2.1.5). It was a former surge type glacier and at the time of sampling in August 2012, was approximately 8 km^2 in area, with the glacial margin being approximately 3.5 km up valley of it's LIA moraine. Upper areas of the bounding valley comprise of Paleozoic limestone and Carboniferous sandstone and siltstone with the lower areas of the valley being composed of Devonian Old Red Sandstone, Precambrian orthogneiss and amphibolite (Dallmann, W et al., 2004).

Due to the nearby location of the Czech and Polish Research stations, HB has been well studied with respect to proglacial geomorphology (Evans et al., 2012), thermal regime and forefield ecology (Polar Ecology Conference, 2014). Ground penetrating radar has also been used to to study its thermal structure, with temperate ice having been observed in an overdeepening towards the front of the glacier (Jakub Małeck, Polar Ecology Conference, 2014). The proglacial zone was characterised by hummocked glacial till to the south, with fluvial deposits, debris ridges and linear eskers to the north, suggesting an area of increased meltwater pressure (Evans et al., 2012). A subglacial outflow on the northern, frontal margin feeds a large, braided river system which joins with rivers from other glaciers in Hørbyedalen and flows into Billefjorden.

Sampling was conducted by Dr Krystyna Kozioł and Emma Brown in July 2012 and focused on three locations (see Fig 2.1.5 for an overview, and Table 2.1 for coordinates) adjacent to the frontal margin in the northern part of the forefield. Sediment was excavated from underneath surface debris, and sampled in accordance to the methodology described for VG (Section 2.1.1). Sediment from HB (Fig. 2.1.6) was poorly sorted, containing mostly sands and silts, but also fine, to very coarse pebbles.

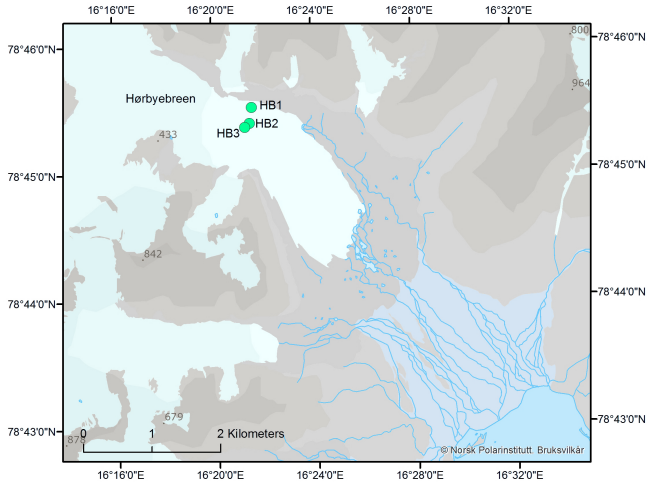

Figure 2.1.5: Hørbyebreen Glacier, Svalbard. Sampling sites are indicated by the green circles.

2.1.5 Von Postbreen and Brucebreen

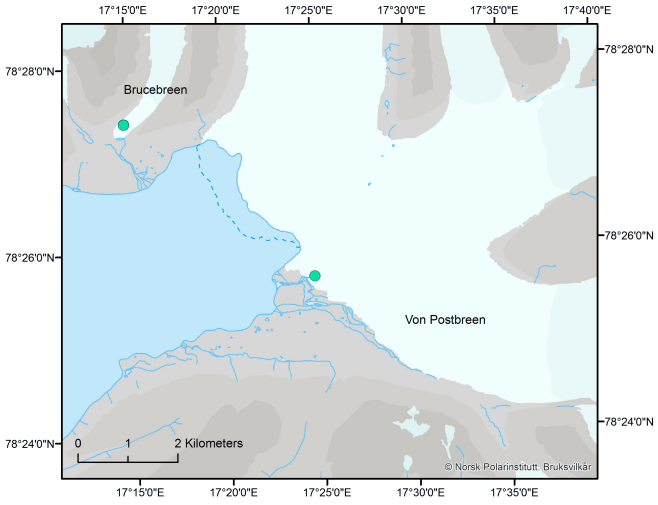

Figure 2.1.7: Von Postbreen and Brucebreen, Svalbard. The green circles indicate the locations from where sediment was sampled. Sampling was conducted at the 2012 glacial margin.

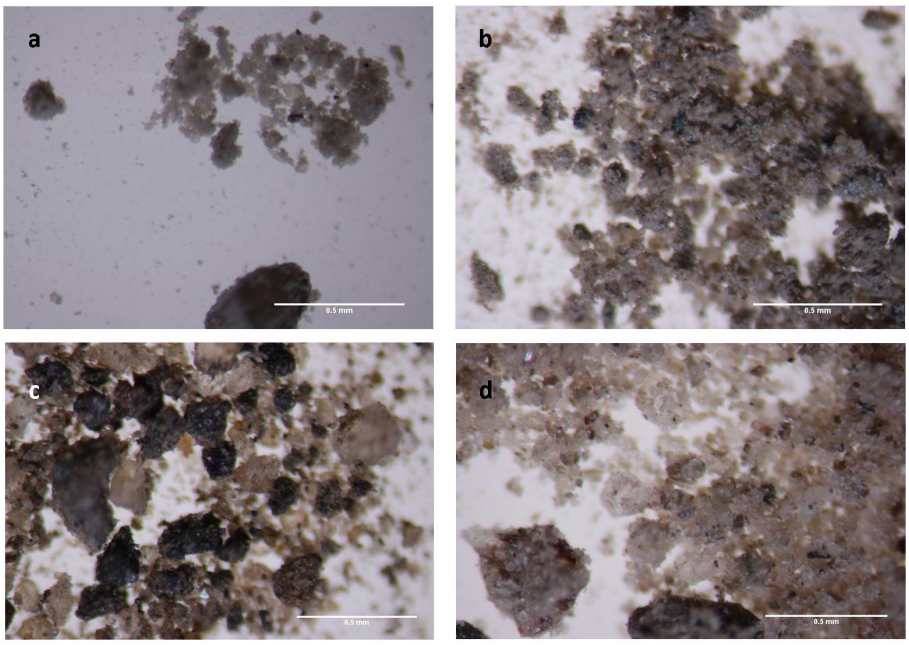

Figure 2.1.6: Sediments sampled from Spitsbergen. a) Vestre Grønfjordbreen, b) Scott Turnerbreen, c) Tellbreen, d) Hørbybreen. Scale bar shows 0.5 mm.

In addition to the above mentioned samples, opportunistic samples of subglacial till were taken from Von Postbreen (N 78.42°, E 17.41°), hereafter VP and Brucebreen (N 78.45°, E 17.24°), hereafter BB. Both glaciers lie at the head of Tempelfjorden, at the Easternmost point of Isfjorden, central Spitsbergen (Fig. 2.1.7). The geology of Tempelfjorden generally consists of Permo-Carboniferous carbonates, sandstones, cherts and siliciclastics (Blomeier et al., 2011). VP was a large (*c.* 15 km long), surge-type, polythermal glacier that converges with the tidewater glacier Tunabreen. Its last surge was in 1870 AD following which, it has been in retreat (Plassen et al., 2004), with its 2015 frontal margin approximately 2 - 3 km from the shoreline. BB was a small, steep glacier occupying the valley to the west of Tunabreen. A radar survey in 2012 indicated that it was cold based, but with active englacial and subglacial channels (H. Sevestre, unpublished data).

Sediment was sampled into 50 mL, sterile centrifuge tubes, from voids along the frontal margin of each glacier. These were immediately fixed using 2% final concentration formaldehyde for later microbial analysis. Both sediments were fine to coarse silts, with little larger material. Differences in colouration between

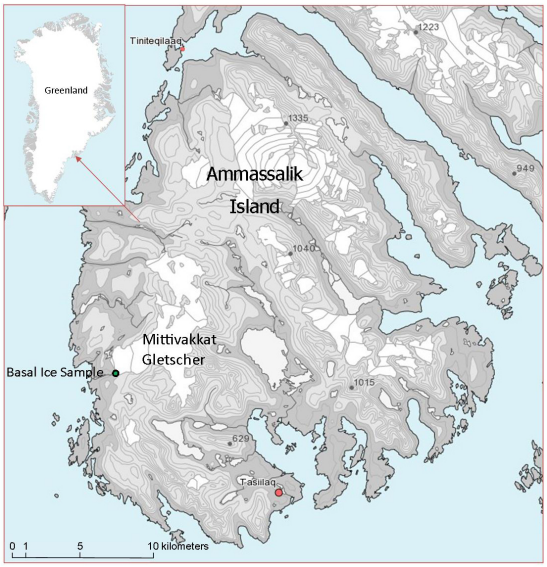

Figure 2.2.1: Mittivakkat Gletscher on Ammasillik Island, Southeast Greenland. The green circle shows the location of the basal ice sample.

VP (dull orange) and BB (light grey) sediments indicate a different mineralogy despite the close proximity of the glaciers.

2.2 Greenland

Sediment was collected from the Mittivakkat ice cap on Ammassalik Island, Southeast Greenland, in August 2013.

2.2.1 Mittivakkat

The Mittivakkat Gletscher (N 65.67°, W 37.87°), hereafter MK, was a temperate (Knudsen and Hasholt, 1999) glacier located on Ammassalik Island, Southeast Greenland. Sampling was conducted in August 2013, at which point, the forefield immediately in front of the glacial margin comprised of a flat outwash plain, constrained by steep valley walls and a proglacial river, exiting the glacier through a subglacial portal at 65° 40′ 58.4" N, 37° 52′ 35.8" W. Outflow from the glacier was predominantly into Sermilik Fjord, however, two ice dammed lakes to the north and south of the western outlet glacier also receive

subglacial water. The bedrock geology consists of garnet gneiss, basic charnockite complex and granites (Wright et al., 1973) with widespread iron staining on the bounding cliffs. Pyrite grains were visible in cryoconite and proglacial sediments. The LIA moraine was evident further down the valley and recession and thinning have been observed since the first observations in 1931 (Mernild et al., 2011, 2012). Due to the nearby location of Sermilik Research Station, MK was well studied, with projects investigating surface mass balance (Mernild et al., 2011), surface ice velocity (Mernild et al., 2012), as well as subglacial topography and ice thickness distribution (Yde et al., 2014).

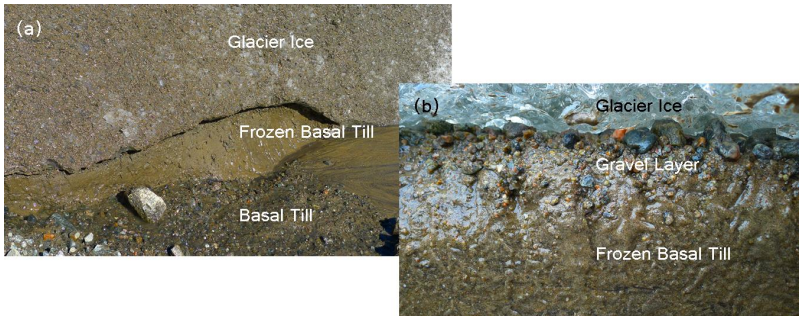

Figure 2.2.2: Basal ice sampled at Mittivakkat Gletscher, August 2013. (a) shows the exposed basal ice section; (b) shows the stratigraphy of the exposed section.

Sediment was collected from an exposed section of frozen basal till, located at the ice margin of the southern lobe of MK (see Table 2.1 for site coordinates). The exposed basal till section is shown in Fig. 2.2.2a, and was approximately 0.28 m at its thickest point and 1.55 m long. Stratigraphy is shown in Fig. 2.2.2b, and comprised of a top layer of glacial ice under which there was a boundary layer of gravel and stones. Under this, there was a solid ice phase containing sorted sandy sediments with one pure ice lens visible. Some mineral sorting was visible in the solid ice phase with signs of folding in the layer structure. The ground in front of the exposed section was frozen making further excavation difficult, however, observation of adjacent, unfrozen, deposits suggests that this sediment layer extends for several meters and contains bands of larger, sub-rounded, stones. It was stipulated that the basal ice was a glaciofluvial in origin, having been deposited subglacially in a meltwater channel.

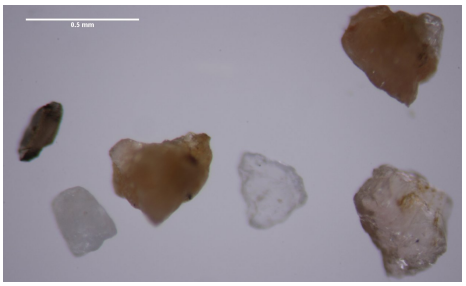

Figure 2.2.3: Sediment sampled at Mittivakkat Gletscher. Scale bar shows 0.5 mm.

The sediment in the basal ice layer was collected by carefully removing the surface defrosted layer and scooping the remaining thickness (*c.* 10mm) of unfrozen sediment directly into sterile, 50 mL centrifuge tubes, six centrifuge tubes of sediment were collected in total. Two 15 mL centrifuge tubes were also filled with sediment, which was immediately fixed in 2% (final concentration) formaldehyde. The sediment collected (Fig. 2.2.3) was characteristically well sorted, with medium to coarse sand-sized grains that were notably coarser, and more angular than the the fine-grained sedimentary silts sampled in Svalbard (Fig. 2.1.6).

Water was also sampled for use in biodegradation experiments (see Section 4.3.5). A 20 L sample of subglacial outflow was taken from the portal at 65° 40´ 58.4" N, 37° 52´ 35.8" W, directly in front of the ice margin. This was collected in a 20 L collapsible LDPE container that had been washed in 10% HCl and rinsed three times in 18 MΩ MilliQ and three times in sample. Snow samples were taken from patches of snow, in which the snow alga, Chlamydomonas nivalis, was clearly present (due to red colouration). These were collected in acid washed LDPE bottles. All samples were stored at *c.* 5°C and transported to Sheffield for further analysis and use in experiments.

2.3 Maritime Antarctic

2.3.1 South Georgia

2.3.1.1 Heaney Glacier

Heaney glacier (S 54.43°, W 36.249°), hereafter HN, was a *c.* 7 km long valley glacier located in St Andrew's Bay, South Georgia, Sub-Antarctica (Fig. 2.3.1).

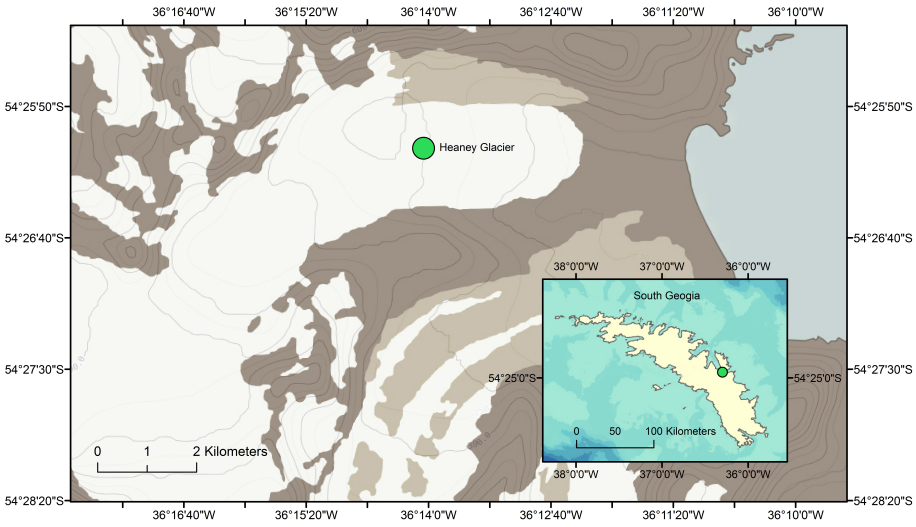

Figure 2.3.1: Heaney glacier sampling site (green circles), South Georgia.

St Andrew's Bay lies in the Sandebugten Formation of sandstone, siltstones and shales (Stone, 1980). Whilst there was little published relating to its hydrology or thermal state, there has been research performed investigating its mass balance, which indicates significant recession since its 1975, post-LIA maximum extent (Gordon and Timmis, 1992).

Samples were taken by Professor Andy Hodson and Dr Aga Novak during their Antarctic spring 2013 field campaign (see Fig. 2.3.1 for an overview, and Table 2.1 for the specific sampling location). Sediment was extracted from a sediment-rich ice facies of a meltwater channel and placed into sterile WhirlPak® bags. These were shipped back to Sheffield in cold storage whereupon a sub sample was fixed in 2% (final concentration) formaldehyde for microbial analysis. The remaining sediment was stored at -20^{o}C until it was required for experimentation. Sediment taken from HN, seen in Fig. 2.3.2, was poorly sorted, with silts, sands and fine pebbles all present.

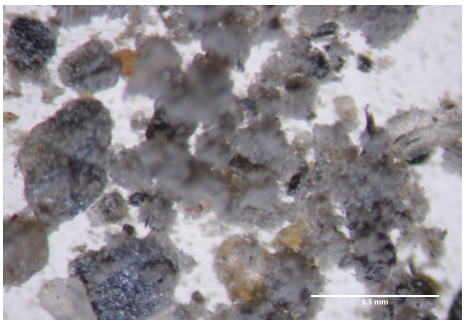

Figure 2.3.2: Sediment sampled from Heaney Glacier. Scale bar shows 0.5 mm.

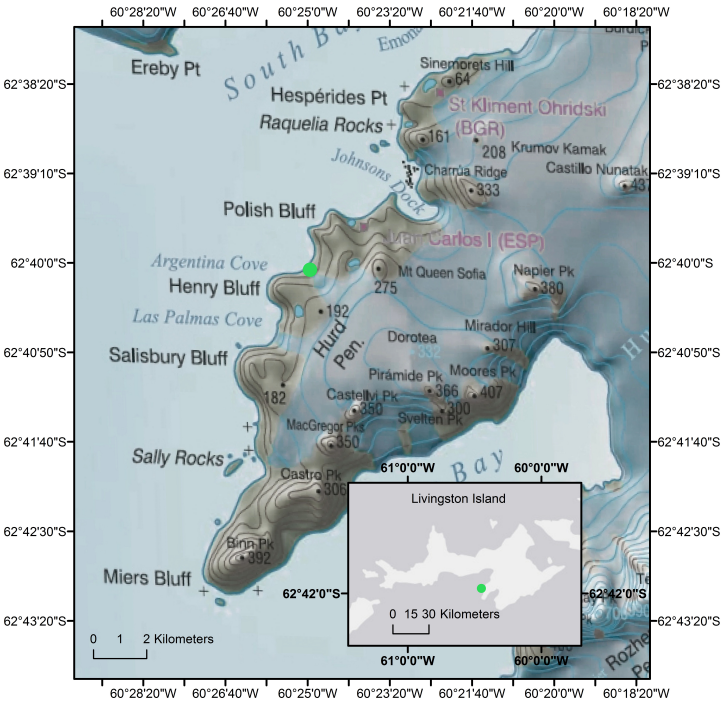

Figure 2.3.3: Sampling location (green circles) for glacial till taken from Argentina Glacier of the Hurd Ice Cap, Livingston Island, Antarctica.

2.3.2 Livingston Island

2.3.2.1 Argentina Glacier

Argentina Glacier (S 62.68°, W 60.41°), hereafter AG, was an outlet glacier of the Hurd Ice cap, located in the south of the Hurd Peninsula, Livingston Island, South Shetland Islands, Western Antarctica (Fig. 2.3.3). Local geology consists of shales, siltstones, arkosic greywackes and sandstones (Hobbs, 1968). At the time of sampling, in 2014, AG's frontal margin was approximately 0.4 km from the shoreline. Mass balance estimates of the Hurd Ice Cap suggest thinning and retreat of its outlet glaciers over the 1956 to present day time period (Molina et al., 2007). Radar surveying failed to detect temperate ice at AG, with ice thickness reaching a maximum of 80 m (Navarro et al., 2009). However, it diverges from the thickest section of the Hurd Ice Cap where an overdeepening contains temperate ice (Navarro et al., 2009). Little was known of the hydrology of the ice cap or its outlet glaciers. AG and HN offer excellent, southern hemisphere comparisons to the Svalbard glaciers, being both in the marine marginal zone, of similar size and overlying similar geology.

Sampling was conducted by Prof. Andy Hodson and Dr Aga Novak during a 2014 field campaign. The sediment was removed from a section of unfrozen glacial till, adjacent to the terminating margin of AG (see Fig. 2.3.3 for an overview, and Table 2.1 for the specific sampling location) and placed into sterile WhirlPak® bags. Sediment was shipped back to Sheffield in cold storage, whereupon a subsample was fixed in 2% (final concentration) formaldehyde for microbial analysis. The remaining sediment was stored at -20ºC until it was required for experimentation. Sediment taken from AG, seen in Fig. 2.3.4, was mostly well sorted silt with occasional fine to coarse sand-sized grains.

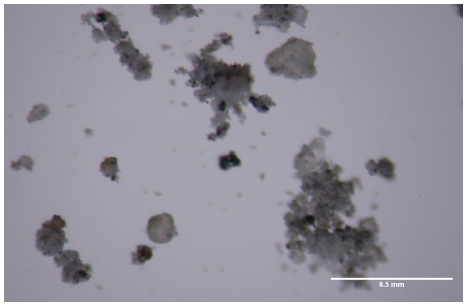

Figure 2.3.4: Sediment sampled from Argentina Glacier. Scale bar shows 0.5 mm.

2.4 Chapter Summary

Sampling of subglacial sediment was performed at six glaciers in Spitsbergen, one in Greenland, and two in the Maritime Sub-Antarctic. All of these glaciers were broadly similar, being Polar glaciers of approximately similar volume and with negative mass balance. They provided sediment from a range of geologies, predominantly sedimentary bedrock, through with granitic sediment also included. More, samples were removed from both distributed and channelised bedform features. Finally, the spread of sample locations offered biogeographical insight also, with comparison possible between Arctic and Sub-Antarctic glaciers, as well as smaller scale comparison between Svalbard glaciers. Table 2.1 summarises the glacial, geological and bedform attributes of each sample.

Table 2.1: A summary of sediment samples collected, their respective bedrock geologies, and from what glacial bedform feature they were removed.

Glacier	Sample ID	Sample Coordinates	Sediment Geology	Subglacial Bedform
Svalbard				
Vestre Grønfjordbreen	VG1	N 77.9475° E 14.2623°	Siltstone, calcareous sandstone.	Distributed sediments.
	VG2	N 77.9408° E 14.2595°		Distributed sediments.
Scott Turnerbreen	ST	N 78.4566° E 17.2471°	Sandstone, shale, siltstone.	Subglacial till entombed within thrust fracture.
Tellbreen	TB	N 78.2519° E 16.2692 °	Sandstone, siltstone.	Sediment-rich ice facies of meltwater channel.
Hørbyebreen	HB1	N 78.7585° E 16.3594°	Limestone, sandstone, siltstone.	Distributed sediments.
	HB2	N 78.7564° E 16.3578°		Distributed sediments.
Von Postbreen	VP	N 78.4283° E 17.4130 °	Carbonate, sandstone, chert, silicilastics.	Distributed sediments.
Brucebreen	BB	N 78.4566° E 17.2471°		Distributed sediments.
Greenland				
Mittivakkat	MK	N 65.6789° W 37.8792°	Gneiss, granite.	Refrozen, distributed subglacial till.
South Georgia				
Heaney	HN	S 54.4389° W 36.24986°	Sandstone, siltstone, shale.	Sediment-rich ice facies of meltwater channel.
Livingston Island				
Argentina	AG	S 62.6808° W 60.4152°	Shale, siltstone, sandstone.	Distributed sediments.

Chapter 3

Microbial ecology of subglacial sediments

This Chapter reports the work carried out to address Objective 1, and details the work carried out to enumerate and assess viability of microbial communities from a range of subglacial sediments.

3.1 Introduction

Research into the subglacial environment, summarised in Table 1.1 (Chapter 1), has shown that the freshly comminuted sediment underneath glaciers and ice sheets supports a diverse microbial ecosystem. Genetic and culture studies of subglacial microbiology (discussed in detail in Section 1.3.2) suggest strong linkages between the microorganisms present and geochemistry. Bacteria and archaea linked to nitrogen, iron, sulphur and methane cycling have been noted within a wide range of sediments (Sharp et al., 1999; Skidmore et al., 2000; Foght et al., 2004; Mikucki and Priscu, 2007; Lanoil et al., 2009; Yde et al., 2010b; Boyd et al., 2011; Stibal et al., 2012b), as have chemolithotrophs, capable of meeting their energy demands through the weathering of reduced mineral phases (Boyd et al., 2014; Christner et al., 2014). The ecosystem implied by these studies is well adapted to life in cold, nutrient poor glacial sediments, and which may be important in driving major biogeochemical cycles within the cryosphere. Directly establishing linkages between microbes and geochemical processes remains an important step towards understanding the adaptations

and importance of microbial life in the cryosphere.

The research conducted for this thesis aimed to investigate geomicrobial processes within subglacial sediments, and so make linkages between biology and geochemistry. The first step towards understanding the role of microbes within the sediments collected for this research project, was to establish their presence as viable cells, and to investigate whether geochemically important species were present. With samples of sediment from beneath nine glaciers (see Section 2), this study also aimed to compare microbial populations between glaciers, and in context of different subglacial conditions. The work conducted in this chapter also provided an ecological basis from which the investigations into carbon cycling (Chapter 4) and geochemistry (Chapter 5) could be considered.

Epifluorescence microscopy and flow cytometry, were used to assess viable and dead cells within each sediment. Targeted fluorescence *in situ* hybridisation (FISH) staining methods were also used to enumerate cells at a domain level, as well as investigating the relative cell concentrations of geochemically important bacterial sub-groups, commonly found in genetic analysis of glacial sediments (see Table 1.1). The wide range of samples utilised by this study, allowed direct comparison of domains and geochemically important groups of bacteria within Svalbard sediments, as well as comparing cell concentrations within sediments from Svalbard, Greenland and the Maritime Antarctic. This is also the first assessment in which viable subglacial cells have been enumerated, furthering our understanding of cell and carbon cycling within glaciers, as well as the microbial and geochemical potential within subglacial sediments.

3.2 Methodology

Microbial characterisation, detailed in the following section, was carried out upon sediments from: Vestre Grønfjordbreen (VG), Tellbreen (TB), Hørbyebreen (HB), Von Postbreen (VP) and Brucebreen (BB), Svalbard; Mittivakkat Gletscher (MK), Southeast Greenland; Argentina Glacier (AG), Livingstone Island, Antarctica; and Heaney Glacier (HN), South Georgia, Antarctica. Details relating to the sampling of these sediments, as well as their mineralogy and morphology are listed in Table 2.1, Chapter 2.

3.2.1 Cell Concentrations

Enumeration of cells within the sediment samples was performed using epifluorescence microscopy and flow cytometry techniques.

3.2.1.1 Cell-Mineral Separation

To enumerate cells, one must first be able to detect them. This posed a challenge in the poorly sorted mineral matrix of subglacial sediments, as mineral grains obscured the cell from view and introduced background fluorescence which reduced the contrast between a stained cell and the filter upon which it sat. For this reason, a protocol in which sediment-bound cells were dispersed into solution for analysis was produced, based on the work conducted in Kepner and Pratt (1994). A variety of treatments were tested to optimise cell recovery from the sediment slurries. Treatments involved the use different ionic surfactants (100mM EDTA, Methanol or Triton X-100) and/or ultrasound to dislodge and disperse cells into solution.

The recovery of cells using each treatment was tested using a forward contamination method. For this, live sediment cells that had been extracted into solution, were placed onto a low nutrient, yeast agar medium and left to grow for 1 week. A colony was then removed and suspended in sterile phosphate buffered saline (PBS) containing 2% final concentration formaldehyde. This suspension of cells underwent ultrasound (2 minutes) and was vortexed before being diluted into: 1/1, 1/10, 1/100 and 1/1000 concentrations. HB sediment was chosen to test recovery, and was inoculated in triplicate with each concentration of cell suspension. Each cell extraction protocol was then performed on the inoculated HB sediment, with the cell concentration of inoculated sediment, uninoculated sediment and each cell suspension analysed using flow cytometry (see 3.2.1.3 for more information).

The results from this study are displayed in the Appendix (Section 7.1) and led to the combined use of EDTA and ultrasound to extract cells for analysis. This method returned 83.7% ($\pm$ 14.4%) of the inoculated cells, though, as with the other methods, the 1/1000 cell suspension's cell count was within the range of error. For the adopted protocol, sediment was fixed in 2% final concentration formaldehyde (analytical reagent grade, Fisher Chemical) and made into a 10 % w/v suspension through the addition of sterile PBS and 100 mM EDTA (final concentration). This was homogenised in a rotary shaker for 30 minutes and placed in an ultrasonic bath for 3 minutes. The suspension was centrifuged at

3000 x g for 10 minutes and the supernatant removed. The pellet was resuspended in 1 mL of PBS and the homogenisation, ultrasound and centrifuge steps repeated. Supernatant from the secondary extraction was added to the first batch and this was then centrifuged at 5000 x g for 10 minutes to create a pellet of cells. The supernatant was removed and the pellet resuspended in 1 mL of sterile PBS for analysis.

3.2.1.2 Total Cell Counts - DAPI Staining

Cell counts were made using the nucleic acid stain 4',6-diamidino-2-phenylindole (DAPI). 1 mL of the extracted cell suspensions were placed into sterile 1.5 mL Eppendorf tubes with 0.5 µL of the DAPI stain. These were incubated at 4^oC for 5 minutes before being filtered through a 0.22 µm black polycarbonate filter. The filter was rinsed with 18 mΩ ultrahigh quality (UHQ), deionised water and mounted onto a microscope slide. Cell counts were made on a Olympus BH-2 epifluorescence microscope at 1000x magnification using a DAPI filter cube. Blanks of PBS were also analysed in in the same manner as the cell suspensions. Twenty fields of view were recorded per slide and the cell concentration calculated using Equation 3.2.1.

$$Cells\,per\,g\,(dry\,mass) = \frac{n(\frac{a_f}{a_{fov}})}{m} \tag{3.2.1}$$

Where: n, is the mean cell count per field of view; a_f, is the area of the filter membrane; a_{fov}, is the area of the field of view and m, is the dry mass of the sediment analysed. Five replicates were performed for each sediment.

3.2.1.3 Live/Dead staining - Flow Cytometry

Live/Dead cell counts of the cell extracts were made using a Partec CyFlow® SL flow cytometer equipped with a 20 mW at 488nm blue solid state laser. Detailed protocols for the analysis of bacteria and viruses in environmental samples are available elsewhere (e.g. (Gasol et al., 2000; Marie et al., 1999, 2001)). Two nucleic acid stains were used to assess cell viability in the samples. SYBR Green I fluoresces green under excitation and is membrane permeant, whereas propidium iodide (PI) fluoresces red under excitation and is membrane impermeant. By staining the samples with both SYBR Green I and PI, it was possible to make counts of cells with intact membranes, visible on the green-fluorescence channel, and of cells with damaged membranes, on the red-

fuorescence channel of the flow cytometer.

Briefly, a 997 µL aliquot of the fixed cell suspension, prepared using the methodology described in Section 3.2.1.1, was placed into a flow cytometry vial and incubated with 1.5 µL of SYBR Green I (Molecular Probes) at 37^{o}C in the dark. After this period, 1.5 µL of 30 mM propidium iodide was also added, and the sample incubated at room temperature for a further 15 minutes. FCS files were analysed using FlowJo software (Treestar, Inc., San Carlos, CA). Gates were applied to live and dead cells, viewed as distinct cell clusters on a dot-plot of green versus red fluorescence, and population data extracted from these gated regions. Blanks of stained and unstained PBS were also analysed in the same manner as the cell suspension. Five replicates were performed for each sediment.

In addition to collecting data relating the excitation/emission of stained cellular material, autofluorescent particles within the cell extracts were also quantified cytometrically. The FL2 channel of the CyFlow® SL was used to detect and count particles containing the phycobiliprotein phycoerythrin, a pigment that is present in the red algae and cyanobacteria common to the supraglacial ecosystem (Sattler et al., 2012; Samsonoff and MacColl, 2001). The proportion of FL2 counts that had also bound with the SYBR Green I fluorochrome was also recorded, and interpreted as intact, autofluorescing cells.

Estimations of cellular carbon equivalents were made using the cytometric enumerations. FL1 and FL2-compensated PI stained cell counts were used as an estimate of dead bacterial biomass, counts were converted into carbon equivalents using the widely adopted assumption that one bacterial cell contains 20 fg of carbon (Fukuda et al., 1998). FL1-compensated FL2 counts were converted into dead algal carbon equivalents, using the conversion factor of 0.02 mg C μL^{-1} of algal cells and a cell diameter of 10 μm (Fogg, 1967) per autofluorescent particle.

3.2.1.4 Fluorescence *in situ* Hybridisation

Fluorescence *in situ* hybridisation (FISH) was performed upon sediment from Svalbard glaciers (HB, VG, ST, VP, BB and TB) only. This was due to the availability of the oligonucleotide probes and microscope whilst in Svalbard, which allowed hybridisation and analysis to be performed within 48 hours of sampling. The hybridisation efficiency of fixed samples was significantly reduced after c. 48 hours in 4°C storage, with little to no hybridised cells observed in MK, HN and

AG sediments when analysed in Sheffield. Cells were brought into solution using the method described in 3.2.1.1. The resulting suspension was filtered through a 0.2 μm, black, polycarbonate filter on a glass filter stage using a hand pump and keeping the pressure on the filter membrane below 20 psi. The filter membrane was cut into 6 sections with a sterile surgical bade, and each membrane section placed into a sterile Petri dish for staining. The oligonucleotide probes used in this study are detailed in Table 3.1, and were chosen to correspond with the three domains, to give a good broad comparison of bacteria, archaea and eukaryotes concentrations within these samples. Subgroups of bacteria, identified within phylogenetic analysis of subglacial sediments (Stibal et al., 2012b; Gaidos et al., 2009; Boyd et al., 2011; Skidmore et al., 2005), and with similarity to species common within geochemical weathering processes, were also selectively targeted using BET42a, EPSY549 and BAC303 probes. All probes were bound to a CY3 dye for analysis by epifluorescence microscopy.

Table 3.1: Oligonucleotide probes used in this study

Probe Name	Specificity	Target Sequence
EUB338 (Bonkowski, 2004)	Most Bacteria	GCTGCCTCCCGTAGGAGT
EUK1209 (Lim et al., 1993)	Eukarya	GGGCATCACAGACCTG
ARC344 (Raskin et al., 1994)	Archaea	TCGCGCCTGCTGCICCCCGT
BET42a (Manz et al., 1992)	β-Proteobacteria	GCCTTCCCACTTCGTTT
EPSY549 (Lin et al., 2006)	ε-Proteobacteria	CAGTGATTCCGAGTAACG
BAC303 (Manz et al., 1996)	Bacteroidaceae	CCA ATG TGG GGG ACC TT

Staining was performed by diluting 1 µL of each probe listed in Table 3.1 in 16 µL of hybridisation buffer (0.9 M NaCl, 20 mM Tris-HCl and 0.01% SDS) and then pipetting the diluted probe directly onto each filter section. Excess hybridisation buffer was pipetted into the Petri dish to maintain saturation. The Petri dish was sealed with parafilm and placed in a thermostatically controlled incubation chamber at 46°C for 90 minutes. After hybridisation, unincorporated probe was removed by rinsing the filter sections with 500 µL of washing buffer (20 mM Tris-HCl 5 mM EDTA, 0.01% SDS and 0.9 M NaCl) for 15 minutes at 48°C. The filter sections were then mounted on glass microscopic slides and analysed immediately. Blanks were also prepared using the same protocol, but flushing the PBS that was used in the cell separation method through the filter membrane. Analysis was performed at 1250 x magnification on a Leitz Labalux

epifluorescence microscope equipped with a 50W mercury lamp and a CY3 filter cube (41007A, Chroma, USA). Twenty fields of view were recorded for each section of stained filter membrane, and cell counts calculated using Equation 3.2.1. Five replicates were performed for each sediment.

3.3 Results

3.3.1 Cell Counts DAPI

Total cell counts made using DAPI stain are displayed in Table 3.2. Results ranged from 7.35×10^4 cells g^{-1} in MK sediment to 2.95×10^6 cells g^{-1} in ST sediment, with the majority of sediments containing *c.* 10^5 cells g^{-1}. These results are of similar magnitude to those published elsewhere (see Table 1.1 for a comprehensive list of other studies), and are of the same order of magnitude as other studies from Svalbard (Kaštovská et al., 2006). Fig. 3.3.1 shows micrographs of typical fields of view observed during analysis. The cells observed in all samples were typically coccoid in shape with vibrio cells also common. VG, ST and HN sediments were notable for the presence of several streptococci arrangements. Sub-micron fluorescing particles were also recorded, thought to be virus like particles (VLPs), though observation of these was uncommon.

The high errors observed for ST, BB and HN sediments indicated heterogeneity within these samples, some replicates returning values that were an order of magnitude lower than median cell concentrations. As approximately 100 cells were recorded for each replicate, the statistical power for reported cell counts was sufficient. Instead, the majority of variation arose following conversion of cell counts to cell concentrations, likely arising from variation in surface area to mass ratios between each aliquot of sediment analysed. Though error was reduced when cell counts were normalised by volume, normalising by mass offers greater insight into the process driven questions dealt with in the following chapters.

3.3.2 Cell Counts: Live/Dead

Total cell concentrations measured using PI stain (Table 3.3) ranged from 5.33×10^4 cells g^{-1} of AG sediment to 7.43×10^5 cells g^{-1} of ST sediment, again,

Table 3.2: Mean (μ) and standard deviation (σ) of five replicate cell counts for each subglacial sediment.

	Cells g^{-1} (dry mass) sediment	
Glacier	μ	σ
VG	491000	*76200*
HB	251000	*77900*
ST	2760000	*1410000*
TB	633000	*477000*
VP	463000	*76700*
BB	435000	*218000*
MK	73500	*30400*
HN	410000	*234000*
AG	83500	*1920*

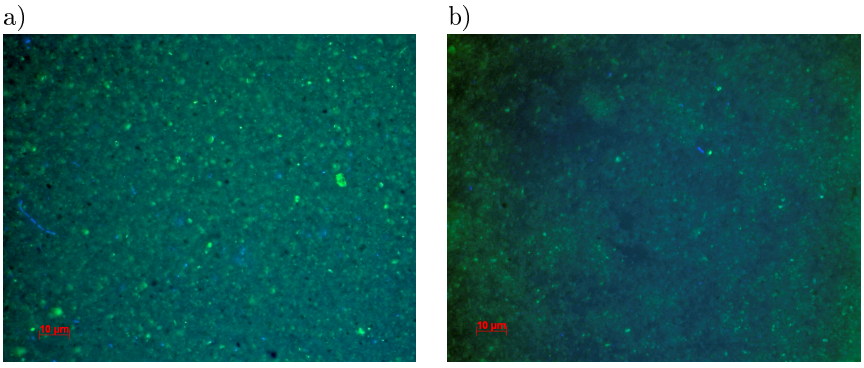

Figure 3.3.1: Example fields of view after extraction and staining with DAPI. a) shows cell extracts from HN and b) from TB.

Table 3.3: Mean (μ) and standard deviation (σ) of triplicate total cell counts and live cell counts made using flow cytometry.

	Cells g^{-1} (dry mass)			
	Total Cells		Live Cells	
Glacier	μ	σ	μ	σ
VG	115000	*54500*	860	*451*
HB	59400	*11600*	518	382
ST	742000	*22500*	3540	*1400*
TB	64600	*22300*	1280	862
VP	112000	*29100*	498	*259*
BB	113000	*42700*	680	*94*
MK	62600	*28200*	588	328
HN	191000	*30400*	735	*562*
AG	53300	*34400*	2760	*1240*

falling within the ranges observed for polar glaciers elsewhere (Kaštovská et al., 2006; Lanoil et al., 2009; Stibal et al., 2012c,a; Pearce et al., 2013). Whilst DAPI cell concentrations were typically 2× to 4× larger then cell counts conducted with the PI stain, with the exception of TB sediment, there was a strong correlation between methods ($R^2 = 0.95$) indicating systematic under or over estimation. This difference likely occurred because of the gating applied to exclude events with low forward and side scatter within the flow cytometry data. As a result of this processing, fluorescing VLPs and cell clusters that would have been included in DAPI cell counts would have been excluded by gating. However, by gating in the FL1 region and then sorting based on event size and granularity, flow cytometry reduces uncertainty from non-specific staining of organic and mineral debris, present when analysing stained micrographs. As mineral debris was apparent in all DAPI stained micrographs, whereas VLPs and cell clusters were less common, the conservative cell concentrations provided by flow cytometry would appear more appropriate for providing enumeration data in this case. Though error was relatively high for both methodologies, standard deviation was typically lower for PI-stained mean cell counts ($\sigma_\mu = 34\%$ compared with 42% for DAPI).

Cells with intact cell membranes were detected at several orders of magnitude lower concentration than that of total cells. Live cells, shown in Table 3.3, ranged from 498 cells g^{-1} of VP sediment to 3535 cells g^{-1} of ST sediment. It is of note here that despite having the lowest total cell concentration, AG sediment contained the second highest concentration of live cells, giving it the

Table 3.4: Mean (μ) and standard deviation (σ) of triplicate autofluorescing (FL2 band) particle counts and autofluorescing cell (FL1 counts in the FL2 gated region) counts made using flow cytometry.

	Autofluorescing Particles g^{-1} (dry mass)		Autofluorescing Cells g^{-1} (dry mass)	
Glacier	μ	σ	μ	σ
VG	91	*80*	36	*53*
HB	108	*116*	19	*25*
ST	4680	*2290*	285	*242*
TB	64	*98*	5	*7*
VP	114	*166*	20	*29*
BB	212	*154*	72	*56*
MK	31	*44*	0	*0*
HN	37	*64*	10	*18*
AG	446	*411*	24	*22*

the highest overall proportion of live cells to total cells (18× more total cells to live cells compared to a group average factor of 141). As all sediments were fixed upon sampling, cell morphology was likely preserved during the extraction process (Goldstein et al., 2003; Griebler et al., 2001), however, as this was not tested, it is possible that rupture during extraction has artificially lowered live cell counts. Relative standard deviations for live cell counts were high, ranging from 13% to 76%, but with an average of 51%.

Cells with intact membranes were typically of similar morphology, being tightly clustered with respect to cell size and granularity (Fig. 3.3.2) Total cell populations, however, usually had two or more separate clusters indicating multiple populations. MK was an exception here, being tightly clustered for both live and total cell counts, indicating less variable, or fewer cell morphologies.

FL2 analysis is shown in Table 3.4, and indicated that every sediment contained autofluorescing material such as phycoerythrin. Concentrations were generally low, with a group median of 108 particles g^{-1} of sediment. The concentration of autofluorescent particles that were also detected in the FL1 channel were also low (see Table 3.4), with a group median of 51 (± 90) cells g^{-1}. Autofluorescing cells typically accounted for 14.55% (± 10.43%) of mean observed autofluorescing particles, and 3.55% (± 3.87%) of SYBR Green I stained cells.

Carbon equivalents of dead cells within the sediments are shown in Table 3.5. MK sediment had the lowest total cellular carbon equivalent, containing 1.56 (± 1.02) ng C g^{-1} of sediment whereas AG contained the largest equivalents,

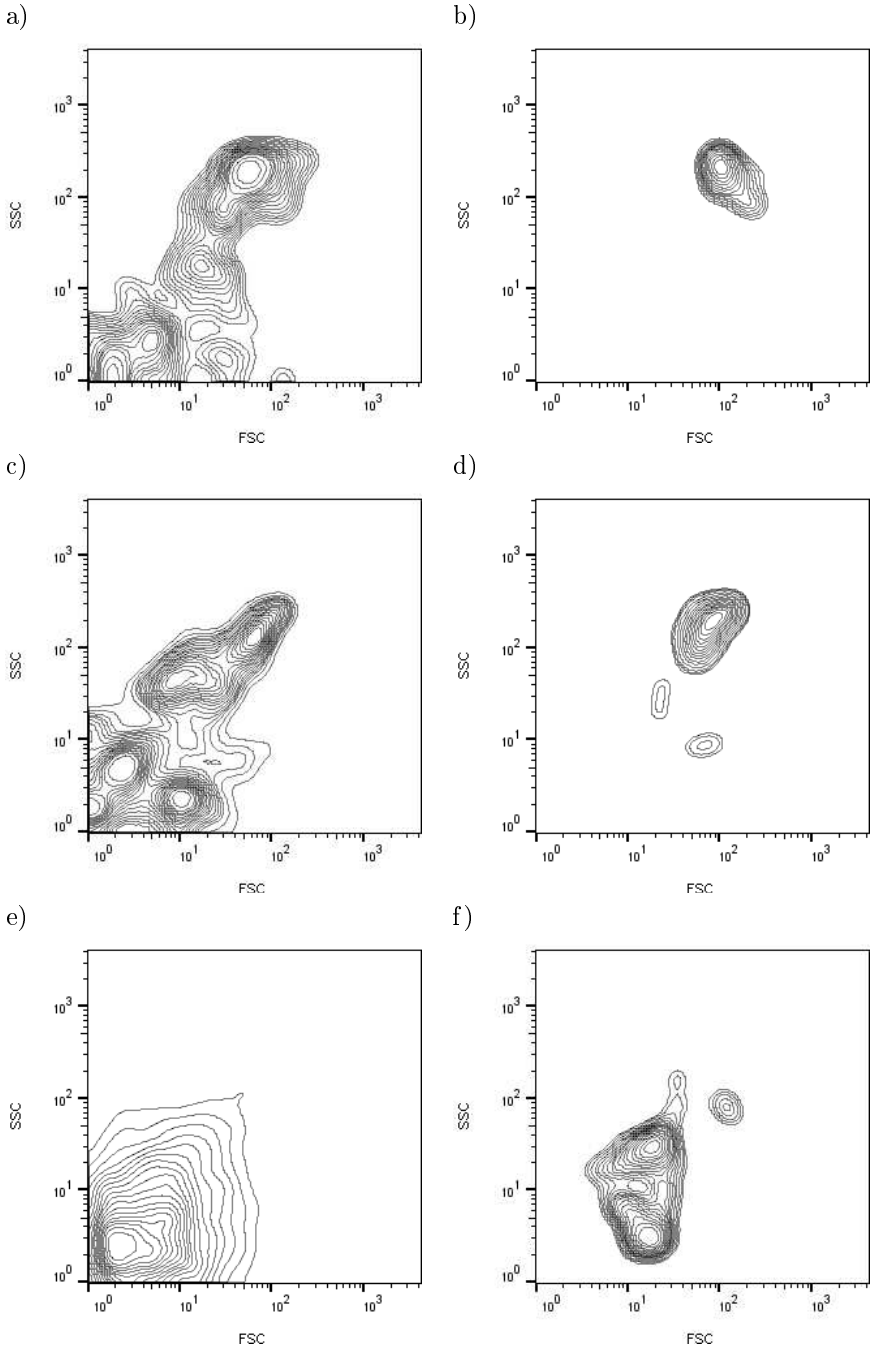

Figure 3.3.2: Contour plots comparing FSC/SSC distribution intensity of total cells (a) and live cells (b) for TB sediment, total cells c) and live cells d) for AG sediment and total cells e) and live cells f) for MK sediment.

Table 3.5: Mean (μ) and standard deviation (σ) carbon equivalents for dead bacterial cells, autofluorescing cells and non-viable cells in total. Concentrations given in ng C g^{-1} (dry mass).

	Bacterial biomass		Algal biomass	
Sample	μ	σ	μ	σ
VG	2.28	*1.09*	0.87	*0.67*
HB	1.18	*0.23*	0.93	*1.21*
TB	1.27	*0.44*	0.61	*1.03*
VP	2.22	*0.58*	0.98	*1.74*
BB	2.24	*0.85*	1.91	*1.29*
MK	1.24	*0.56*	0.32	*0.46*
HN	3.81	*0.61*	0.27	*0.67*
AG	1.00	*0.68*	4.42	*4.31*

with a cellular carbon concentration of 5.43 (± 4.98) ng C g^{-1}.

3.3.3 FISH

Fig. 3.3.3 shows micrographs of hybridised bacteria (a) and archaea (b). These micrographs were taken upon return to Sheffield where a microscope with a camera stage was available. Hybridisation efficiency had greatly reduced by this point and the low cell concentrations apparent in Fig. 3.3.3a was not representative of the numbers of EUB338-stained cells observed straight after sampling, where tens of cells were commonly visible per field of view. For the other probes, however, cell numbers were typically low and with low intensity relative to the EUB338 stain (see Fig. 3.3.3 for a comparison). In some cases, 10 or fewer cells were recorded per sediment and so the reliability of cell concentrations derived from these probes (excluding EUB338) was low and should instead be used as a qualitative indicator of target presence, and as a relative measure within this study only.

With this in mind, tentative cell concentrations derived from FISH analysis are shown in Tables 3.6 and 3.7. Bacteria was the most abundant domain in all sediments, occupying an average of 68% of total hybridised cells. EUB338 counts ranged from 13708 cells g^{-1} of HB sediment to 636625 cells g^{-1} of ST sediment. HB, TB, VP and BB sediment each contained more archaea than eukaryotes (20% compared to 18%; 4% compared to 1%; 23% compared to 14%, and 21% compared to 15% respectively) whilst VG and ST sediments contained a greater

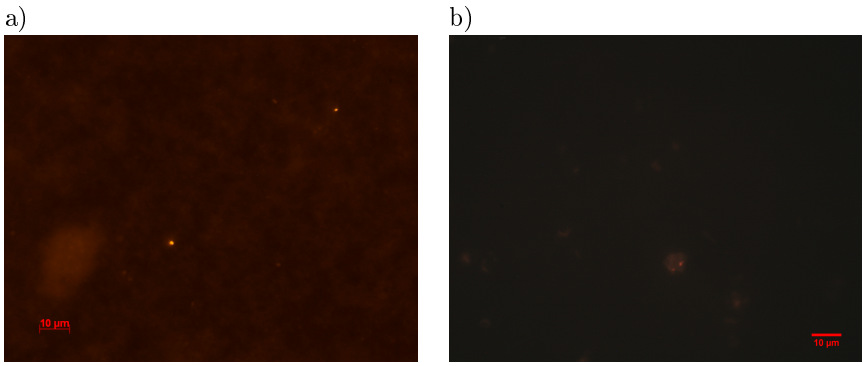

Figure 3.3.3: Example fields of view of FISH microscopy. a) Shows VG sediment stained with EUB338 probe. b) shows VG sediment stained with ARC344 probe.

proportion of eukaryotes compared to archaea (20% compared to 15%, and 26% compared to 14% respectively). Morphology of cells stained by the EUK1209 probe were typically unicellular, *c.* 5-10 μm and oval in shape, though occasional *c.* 100 μm coenocytic filaments were also observed. Uptake of the ARC344 probe was only evident in sub-micron coccoid cells.

Cell counts of bacterial subgroups are shown in Table 3.7. β-Proteobacteria were the most abundant bacteria in VG sediment, with the BET42a stain accounting for 83% of the cell count from the EUB338 stain and were typically present as *c.* 5 μm rod shaped cells. ε-Proteobacteria were present in all analysed sediments, accounting for 8 to 20% of the EUB388 cell count. Bacteroides, were most prevalent in ST sediment, accounting for 34% of ST's EUB388 cell counts.

3.4 Discussion

The work conducted for this Chapter sought to address Objective 1, to characterise and enumerate microbial communities within different subglacial sediment ecosystems. The sediments analysed were taken from underneath a variety of polar glaciers in Svalbard, Greenland and the Maritime Antarctic (see Chapter 2 for more detail). All contained active microbial populations in which bacteria were the most common domain, though archaea and eukaryote were also present. A finding which adds to the growing body of research into subglacial microbes (see Table 1.1), showing that comminuted rock underneath glaciers

Table 3.6: Mean (μ) and standard deviation (σ) fluorescence *in situ* hybridisation cell counts of bacteria, eukaryotes and archaea for Svalbard subglacial sediments. *n.d.* indicates sediments where no cells of a certain type were detected. *n.a.* indicates that no analysis took place due to probe availability.

	Cell Concentration (cells g^{-1})					
	EUB338		EUK1209		ARC344	
Sample	μ	σ	μ	σ	μ	σ
VG	180000	*52400*	49500	*13800*	36400	*7780*
HB	13700	*6220*	4090	*1600*	4460	*291*
ST	637000	*162000*	282000	*136000*	149000	*38000*
TB	52900	*62500*	633	*901*	2220	*2700*
VP	237000	*106000*	50200	*18700*	73100	*61000*
BB	115000	*55200*	27000	*14100*	38100	*19800*

Table 3.7: Mean (μ) and standard deviation (σ) fluorescence *in situ* hybridisation cell counts for β-Proteobacteria, ε-Proteobacteria and Bacteroidaceae in Svalbard subglacial sediments. *n.d.* indicates sediments where no cells of a certain type were detected. *n.a.* indicates that no analysis took place due to probe availability.

	Cell Concentration (cells g^{-1})					
	BET42a		EPSY549		BAC303	
Sample	μ	σ	μ	σ	μ	σ
VG	161000	*83000*	48600	*66500*	41000	*14300*
HB	1700	*352*	2520	*588*	*n.d.*	
ST	*n.d.*		83600	*31700*	364000	*207000*
TB	*n.a.*		*n.a.*		*n.a.*	
VP	66400	*2700*	54000	*16600*	28000	*5630*
BB	2260	*1870*	16900	*9580*	14200	*22000*

and ice sheets supports a diverse range of prokaryotic and fungal life.

In this study, the adopted cell extraction method recovered approximately 84% of cells from the sediment (calculated during method development using a forward contamination study), and so the cell concentrations herein reported likely underestimate actual cell concentrations. Furthermore, it is unknown whether the extraction protocol used favours certain sediment communities, and, with many microbes depending upon direct mineral contact for weathering to occur (Ehrlich and Newman, 2009), bias may be introduced whereby these adhered cells are not effectively removed for analysis. Nevertheless, every sediment examined contained live microbial populations, with cells that were intact (based upon SYBR Green uptake) and synthesising ribosomal RNA (based upon numbers of cells able to hybridise with the FISH probes).

Total cell concentrations observed within these sediments were of similar magnitude to those reported for polar glaciers elsewhere (Kaštovská et al., 2006; Lanoil et al., 2009; Stibal et al., 2012c,a; Pearce et al., 2013) whilst being below concentrations noted underneath Alpine glaciers (Sharp et al., 1999; Foght et al., 2004). This perhaps suggests that polar glaciers, existing in colder conditions, having shorter melt seasons and so typically being cold-based or polythermal, have a lower potential for supporting microbial life. Although differences were noted between the sediments sampled for this project, they could not be attributed to differences in geographical locations, geology or bedform morphology. As error was typically high between replicate cell counts, it was determined that cells were distributed heterogeneously throughout the sediment. It was probable, therefore, that within such a small set of samples, differences affected by geography, geology or morphology would be obscured by the small scale spatial variability in cell concentrations.

ST sediment had the highest cell counts across methodologies, with 4.4x and 2.7x more cells than group mean total and live enumerations respectively. A high number of events in the FL2 channel (see Table 3.4) indicated probable contamination from surface runoff here. ST sediment contained 4680 $\pm$ 2288 autofluorescing particles g^{-1}, 51x greater than the group mean of 91. It is likely, therefore, that whilst entombed, the sediment received inputs of surface snow melt and hence, inputs of supraglacial algal and bacterial communities also. For this reason, ST sediment was excluded from further study. It did, however, provide a good illustration of surface contaminated subglacial sediment, against which the other samples could be validated.

Some insight into cell origin and survival within the sediment samples was

gained using the live/dead cell counts in combination with phycoerythrin data. A degree of connectivity with supraglacial snow and ice was observed in all cases due to the presence of autofluorescing particles (Table 3.4), phycoerythrin being accessory to the chlorophyll pigments responsible for photosynthesis (Mehrotra and Sumbali, 2009). However, excluding ST results, only a small percentage (0% (MK sediment) to 30% (BB sediment)) of the FL2 triggered particles also presented as SYBR Green stained cells and the majority of autofluorescing particles were interpreted as degraded cellular material or extracellular polysaccharides (Samsonoff and MacColl, 2001). Intact autofluorescing cells were possibly cyanobacteria, as observed in Svalbard subglacial sediment by Kaštovská et al. (2006).

Low cell viability was also observed using the live/dead assay, as cells with intact membranes typically accounted for less than 1% of total cytometrically measured cells, with the exception of TB and AG sediments (2%, and 5% respectively). This proportion was less than observed in supraglacial ecosystems, where 10 - 80% cell viability has been reported (Stanish et al., 2013), and differs from findings in Miteva et al. (2004), in which a 5:1 ratio of live to dead cells was observed in "silty" ice, from a GISP 2 ice core section.

RNA is also sometimes used to assess *in situ* cell viability (Keer and Birch, 2003), as it typically degrades more rapidly than DNA following cell mortality (Hofreiter et al., 2001; Fordyce et al., 2013; Dubelman et al., 2014). The proportion of total cells observed to be active in rRNA synthesis (combined domain cell counts from Table 3.6) relative to DAPI cell counts was higher (9 - 78%) than the live/dead results. However, little is known about RNA persistence and degradation in the glacial environment, and the possibility of supraglacial RNA being preserved in the low temperature/light subglacial environment is supported by several studies that have recovered ancient RNA genomes from ice cores and permafrost (Castello et al., 1999; Castello and Rogers, 2005; Ng et al., 2014). Along with uncertainty in the absolute values reported for eukaryote and archaea cell concentrations, use of the live/dead assay appears to be the better method for assessing cell viability here.

The carbon equivalents shown in Table 3.5 represent a potential available pool of organic carbon for subglacial microbes. Whereas the autochthonous and allochthonous inputs in the bacterial pool cannot be distinguished, the carbon available from autofluorescing cells most likely originate from the surface. Comparing these two inputs, bacterial carbon equivalents are greater than that of algal cells in all sediments except AG, where larger concentrations of

autofluorescing particles were observed. However, even accepting the assertion that autofluorescing cells were allochthonous in origin, and dead bacterial cells autochthonous, surface derived material still accounted for 40.6% (± 24.6%) of total, cell derived carbon in the sediments analysed; a potentially important source of carbon for *in situ* organotrophic communities.

The FISH analysis showed a dominance of bacterial cells in the analysed sediments, but also indicated the presence of active eukaryotic and archaea communities. Whilst no further classification of identified eukaryotes and archaea beyond domain level was made, their presence is not widely recorded in earlier subglacial literature. Perhaps this is because of a tendency towards molecular studies that use bacterial primers and 16s rRNA analysis.

Allochthonous algal cells and fungi are the most likely unicellular eukaryotes to be present here, and fungi have been found in a handful of papers investigating accretion ice (D'Elia et al., 2008), subglacial ice (Sonjak et al., 2006) and sediments (Kaštovská et al., 2006), the latter of which also observed algal cells. As average autofluorescing cell counts only accounted for 0.29% (± 0.31%) of eukaryotic cell counts, it is probably that fungi were the dominant eukaryote present within these sediments. With EUK1209 stained cells ranging from 1% (± 1%; TB sediment) to 19% (± 25%; VG sediment) of total FISH cell counts, fungi may, therefore, comprise a significant proportion of the measured subglacial community. And, as fungi are often considered to be geomicrobially important, and can be well adapted to utilising more recalcitrant forms of organic carbon (Ehrlich and Newman, 2009), the need for further investigation into their ecological role, if any, becomes apparent.

Archaea have been reported in Subglacial Lake Whillans (Christner et al., 2014) as well as in subglacial sediments from Antarctica, Greenland (Stibal et al., 2012b,c) and Arctic Canada (Boyd et al., 2010). In the samples measured here, archaea constituted an average of 16% (± 7%) of total FISH cell counts across all sediments. With Boyd et al. (2010); Stibal et al. (2012b) and Stibal et al. (2012c) all finding that methanogenic phylotypes dominate their archaeal clone libraries, the detection of significant archaeal communities in these Svalbard sediments could hint at the methanogenic potential in these glaciers also. Whereas only one sample from sediment adjacent to a meltwater channel was analysed for archaea, it is of note that this sediment, TB, contains the lowest proportion of archaeal cells (4% compared to a group average of 16%). It is, therefore, suggested that this could be a result of greater oxygenation and shorter residence time of the channelised sediments, preventing the formation of favourable conditions for

methanogenesis to occur.

With the exception of VG sediment, in which betaproteobacteria dominated, with BET42a hybridised cells accounting for 83% of EUB338 hybridised cells, β-Proteobacteria and ε-Proteobacteria were recorded in broadly similar proportions in each sediment. Bacteroides were recorded in slightly smaller proportions. The presence of such bacterial classes within these sediments, suggests a hypothesis of *in situ* geomicrobial activity. This is supported by phylogenetic studies, that have have shown subglacial proteobacterial OTUs to cluster with a diverse range of chemotrophic, sulphur, iron and nitrogen cycling bacteria (Gaidos et al., 2009; Stibal et al., 2012b; Thór Marteinsson et al., 2012; Pearce et al., 2013).

3.5 Conclusions

The ecology of subglacial sediments was investigated in samples taken from nine glaciers across Svalbard, Greenland and the maritime Antarctic. All were found to contain active microbial populations in which bacteria were the most abundant domain present, with smaller proportions of eukarya and archaea also identified in every sediment. Photosynthetic particles, some of which were present as potentially viable cells, were also found at every site (with the exception of MK sediment, in which no viable autofluorescing cells were identified) indicating connectivity with supraglacial ecosystems, either through subglacial meltwater transport, or, with latency, through basal melting. When comparing sediments by provenance, it was notable that there was no clear pattern in live or dead cell concentrations between different glacier locations, sediment geology or between channelised versus distributed sediments.

Whilst active microbes were found at every site, the ratio of live versus dead cells was low. This could be a result of an allochthonous cell origin, whereby a large proportion of subglacially transported cells were unable to adapt. Another explanation could relate to the sediment sampling location. Due to sampling limitations, sediments were removed only from glacial margins. As all glaciers sampled were polar, and were polythermal or cold based, it was assumed that their frontal ice margins would have frozen to the bed during recent winter seasons. In such a scenario, the overwintering survival of the sediment ecosystem is unknown, as is how well this represents the ecology of more seasonally stable temperate ice.

In MK sediment, which was recovered from a frozen till layer, the discovery of viable microbes suggests partial survival of its ecosystems as the sediment froze to the glacier bed. This was interesting, as it highlighted the possibility for ecosystems to be remain active for long periods when seemingly entombed in ice. However, it also suggested a limitation of the sampling strategy adopted for this study, as well as many other studies which investigate subglacial microbiology. Though viable and geomicrobially active cells have been found, it is uncertain what community shifts may have occurred during changes in the overlying glacial morphology. As a result, it was difficult to determine how representative some of the samples within this study were with respect to their original conditions under distributed or channelised flow. Though the samples investigated here encompassed sediments from both of these hydrologies, variability in absolute cell counts precluded strong conclusions being drawn about hydrological controls upon ecology. With this in mind, a way forward for ecological studies is suggested. Better representation of differing sediment morphologies needs to be accounted for, both at a glacier scale, and at a smaller scale, over which micro catchments of aerobic or anaerobic sediment may produce great heterogeneity and diversity.

The results reported in this study gave a unique perspective into the connectivity of supraglacial and subglacial ecosystems and highlight the potential importance of both archaea and fungi in a wide and varied range of subglacial sediments. Though slight differences were noted between different sediment types within this study, the techniques used were somewhat non-specific with respect to defining community shifts, and so a genetic approach is suggested as a future improvement. Highlighted by the FISH survey within this study, a genetic approach should target species from all domains, this could then be encompassed into a more directed study about small- and large-scale community changes using FISH. Adoption of catalysed reporter deposition (CARD) FISH in future studies may also help to improve hybridisation of these sediment microbiota. Presently, a range of subglacial sediments have been well characterised with respect to bacterial diversity (Table 1.1), however, little is still known about the spatial variability of different taxa under glaciers, and what impact this may have for sediment geomicrobiology.

Chapter 4

Carbon Cycling and Metabolism in Subglacial Sediment

4.1 Introduction

Carbon has received much recent attention within glacial research, and not only with respect to climate change. A surge of research into supraglacial ecology has been followed with the reclassification of glaciers as biomes, and consequently, with the cryosphere being factored into the global carbon cycle. Though supraglacial ecosystems have been fairly well characterised with respect to metabolism and carbon fluxes (Hodson et al., 2007; Anesio et al., 2010; Hodson et al., 2010a; Yallop et al., 2012; Lutz et al., 2014), more yet needs to be done to constrain biological carbon fluxes within subglacial environments. Subglacial sediments contain microbial communities which comprise a diverse range of species and trophic strategies (see Table 1.1 and Section 1.3.3.1, Chapter 1, for a summary of literature and Chapter 3, for microbial analysis of the sediments utilised in this study). Little is known of their involvement in the cycling of energy or matter, however.

The majority of research into subglacial carbon cycling has focused upon methanogenesis (Wadham et al., 2008; Mikucki et al., 2009; Boyd et al., 2010; Bárcena et al., 2011; Stibal et al., 2012c), or has inferred metabolic potential

from culture or metagenomic studies (Skidmore et al., 2000; Foght et al., 2004; Kastovská et al., 2005; Stibal et al., 2012b). Methanogenesis is a logical anaerobic metabolism within sub-ice sheet systems, as long water residence times would promote anoxia across large areas of sediment. Underneath smaller glaciers, such as the ones sampled for this study, however, suboxic conditions are thought to dominate (Tranter and Skidmore, 2005; Wynn et al., 2006; Irvine-Fynn and Hodson, 2010), with strong redox gradients providing a range of conditions for different microbial metabolisms (Tranter and Skidmore, 2005). There is limited evidence for sulphate or iron reduction within subglacial sediments (Skidmore et al., 2000; Wadham et al., 2004; Mikucki and Priscu, 2007), as well as denitrification (Wynn et al., 2007; Yde et al., 2010b), and so different terminal electron accepting processes (TEAP), whether respiration using O_2, NO_3^-, Fe^{3+} or SO_4^{2-}, have the potential to be important subglacially. By considering these processes together, and through their direct measurement in sediments, this chapter hopes to gain a fuller understanding of the importance of different metabolisms within the subglacial carbon cycle.

A greater understanding of subglacial carbon cycling would, foremost, provide insight into questions relating to the potential, growth and limitations of/to microbial life here. In turn, a greater understanding of these fundamental processes may direct research into the extent, diversity and adaptations of life within subglacial ecosystems. Once more is revealed of the complexity of subglacial carbon cycling, then its place in context of cryospheric or even global carbon cycles can be better considered. Carbon released by subglacial respiration or methanogenesis has the potential to contribute significantly to glacial carbon budgets, with the volume of sediment able to support life under glaciers, exceeding that of supraglacial cryoconite ecosystems (Boetius et al., 2014). More needs to be done to characterise the magnitude of subglacial biological carbon fluxes, and to determine the factors which influence productivity there.

This Chapter sought to address the 2nd Objective of this thesis, to assess microbial activity within subglacial sediments across a range of conditions, and investigate how rates and growth strategies were affected by carbon or electron acceptor availability. This was approached using microcosm experiments, in which sediments from different glaciers were incubated with controlled electron donor and acceptor conditions. Fourier transform infra-red (FTIR) spectroscopy was employed for the first time within the study of subglacial sediments, to investigate the quality of organic compounds within subglacial sediments. Thus, measured bacterial production could be better considered in context of available

sediment organic carbon sources.

4.2 Methodology

The sediment utilised for this study was sampled as described in Chapter 2. A combination of direct measurements, batch incubations and microcosm experiments were then used to address the aim of this Chapter.

4.2.1 Field Sites

Organic carbon and biological activity was assessed in sediments sampled from Vestre Grønfjordbreen (VG), Tellbreen (TB), Hørbyebreen (HB), Mittivakkat Gletscher (MK), Argentina Glacier (AG) and Heaney Glacier (HN). Details relating to the sampling of these sediments, as well as their mineralogy and morphology are listed in Table 2.1, Chapter 2.

4.2.2 Characterising Sediment Organics

4.2.2.1 Nutrient Analysis

Air-dried, powdered sediment was analysed for organic carbon and nitrogen content using a Vario EL cube CN analyser (Elementar, Hanau, Germany). Further samples of sediment were air dried at 4°C and $<$ 2 mm sieved. The fine fraction was then analysed for sediment organic carbon (SOC) using a loss on ignition (LOI) approach (Radojevic and Bashkin, 1999). Dry mass was established after 6 hours in the furnace at 105°C (m_{105}), after which, the mass of the mineral fraction was recorded following 18 hours in the furnace at 450°C (m_{450}). The organic matter fraction was determined using Equation 4.2.1.

$$\%LOI = \frac{(m_{105} - m_{450})}{m_{150}} \times 100 \tag{4.2.1}$$

4.2.2.2 Fourier Transform Infra-Red Spectroscopy

Fourier transform infra-red spectroscopy (FTIR) was used to characterise the composition of organic carbon in the glacial sediments. An established, and sensitive method, FTIR detects the characteristic infra-red absorption wavenumbers of different classes of biomolecule (Reitner et al., 2010), allowing the identification of organic compounds, even when present in low concentrations.

To avoid mineral-absorption interference, the organic carbon extraction and purification procedure used by Giovanela et al. (2010) was carried out prior to measurement. Using the organic carbon concentration calculated for each sediment during C:N analysis (Section 4.2.2.1), freshly defrosted sediment was weighed out to ensure enough organic carbon would be extracted for analysis. Sediment was pre-treated with 0.1 M HCl by mixing on a rotary shaker for 1 h and leaving to stand at 4°C for 24 h. Following this, humic acid was extracted by mixing the pre-treated sediment with 1 M NaOH solution for 1 h and then leaving it to stand for 24 h at 4°C. The suspension was centrifuged, and the supernatant removed and buffered to pH 2.0 using 6 M HCl to precipitate the humic fraction. This was separated from the supernatant by centrifuge and freeze-dried. The resulting powder was scanned using a Perkin Elmer, Spectrum One spectrometer. 50 scans were recorded per sample, with a wavenumber range of 600 to 4000 cm^{-1}, at 4 cm^{-1} resolution.

The raw scan data was baseline corrected, normalised and smoothed using the Perkin Elmer "Spectrum" software, before peak analysis was conducted using KnowItAll® Informatics System (Bio-Rad) software. Peak assignments were made following Tipson (1968); Griffiths (1992) and Pavia et al. (2001). Control samples, produced in the same manner as the sediment extracts, but without sediment, were also analysed. These provided spectral information about the extractant, and any mineral peaks that may have caused interference with organic peaks.

4.2.3 Microbial Activity Measurements

Initial measurements of bacterial production and autotrophic activity were made upon all sediments after return to Sheffield. This was done 24 hours after transferral from -20°C storage freezers to 4°C Panasonic cooled incubators (MIR-254-PE). The interval between sampling and measurement was *c.* two, four and six months post-sampling, for MK, Svalbard and maritime Antarctic sediments respectively. During this time, frozen conditions were maintained.

4.2.3.1 Bacterial Production

Bacterial production under aerobic conditions were determined by measuring [^{3}H] labelled leucine uptake into trichloroacetic acid (TCA) precipitable material. The methodology from Buesing and Gessner (2003) was adapted for the experimental conditions used in this study. Optimum incubation time was

determined by testing the linearity of leucine uptake. This was achieved by incubating sediment for 0.5, 1, 2 and 4 hours and observing whether production rate was asymptotic as a function of incubation time. It was also established that the addition of labelled leucine was not influencing bacterial production by measuring the uptake of labelled leucine in incubations containing 10, 25, 50 and 100 μm additions of unlabelled L-leucine. The results of these initial studies led to the adoption of the following protocol.

Aliquots of defrosted sediment slurry were removed and placed into 1.5 mL Eppendorf tubes. Five live samples were incubated alongside two controls, prepared through the addition of 2% (final concentration) formaldehyde to live sediment. Defrosted sediments contained enough water to enable mixing of labelled leucine throughout the sediment. This allowed incubations to be performed without the addition of media or water, reducing environmental changes upon the sediment ecosystem. Each sediment aliquot was inoculated with $1\mu L$ (37 kBq), L-[4, 5-^{3}H(N)]leucine (MP Biomedicals, specific activity: 5.42 TBq mmol^{-1}), shaken and left to incubate in the dark at 5°C.

After 30 minutes, incubations were terminated through the addition of 5% v/v (final concentration) TCA and placed back in the fridge for 10 minutes to allow proteins and nucleic acids to precipitate. Ultrasound was then used to disrupt the aggregates of sediment before the samples were placed in the centrifuge at 13000 × g for 10 minutes to separate unincorporated leucine, still in solution, from the sediment. The supernatant was discarded and the pellet taken through a series of cleaning steps to remove any remaining unincorporated leucine. Cleaning was performed by re-suspending and agitating the pellet before further centrifuging and discarding the supernatant. This was done sequentially, using 5% TCA, 98 % ethanol and UHQ deionised water. After cleaning, proteins were redissolved by suspending the pellet in an alkaline solution of 0.5 M NaOH, 25 mM EDTA and 0.1 % sodium dodecyl sulphate, and incubating for 60 minutes at 80°C. The resulting suspension was brought back to room temperature before being centrifuged at 13000 × g for 10 minutes. 100 μL aliquots of the clarified protein extracts were added to 10 mL of Monophase S (PerkinElmer LAS (UK) Ltd.) liquid scintillation cocktail, and radioasseyed using a Packard Tri-Carb 3100 TR Liquid Scintillation Analyzer.

Disintegrations per minute (DPM) values from the sterilised control were subtracted from that of the live samples to give: disintegrations per minute of incorporated leucine ($\mathrm{DPM}_{INC_{BP}}$). Bacterial production (BP) in μg of C, per gram of dry sediment, per hour was then calculated using the following

Equations:

$$mmol\ LEU_{INC} = \frac{DPM_{INC_{BP}}}{SA \times 60 \times m \times t} \tag{4.2.2}$$

$$BP\ (\mu gCg^{-1}h^{-1}) = 0.86 \times mol\ LEU_{INC} \times 131.2 \times i \times 100/7.3 \tag{4.2.3}$$

Where: $mmol\ LEU_{INC}$ is amount of leucine incorporated into protein (mmol); DPM_{INC} is disintegrations per minute (DPM) (direct output from the scintillation counter); SA is the specific activity of the L-[4, 5-^{3}H(N)]leucine (Bq); *60* converts between DPM and Bq; m is the dry mass of sediment inoculated with leucine (g); t is incubation length (hours); BCP is bacterial carbon production (µg C $g^{-1}h^{-1}$); *0.86* converts from bacterial production to bacterial carbon production (Simon and Azam, 1989); *131.2* is the molecular mass of leucine; i is the isotope dilution factor, 1.5 (Kirchman, 1993), and *100/7.3* is the molar percentage of leucine in protein (Simon and Azam, 1989).

As microbial geochemical processes were being assessed using long term batch incubations (see Chapter 5, Section 5.2.2.1), acclimation of bacteria to experimental conditions was concurrently measured in sediments from both VG sites and both HB sites (VG1, VG2, HB1, HB2). Aqueous samples were removed for chemical analysis at 4, 18, 30 and 100 day intervals, at which point between 10 and 20 mg (dry mass) of sediment were harvested also. These were transferred into 1.5 mL Eppendorf tubes with 0.5 mL of the incubation medium they were removed from. In total, five Eppendorfs containing active sediment were incubated alongside two sterile controls, provided by the dry-heat sterilised controls utilised by the geochemical survey, and by addition of 2% (final concentration) formaldehyde. Bacterial production was determined in these sediments in the same manner as initial production measurements.

4.2.3.2 Primary Production

Levels of dark inorganic carbon fixation were measured in incubations concurrent to those measuring bacterial production. Incubation vessels (1.5 mL Eppendorf tubes) were set up as in Section 4.2.3.1, and were inoculated with 0.5 μL (37 kBq) sodium bicarbonate [^{14}C] (MP Biomedicals, specific activity: 2 GBq $mmol^{-1}$). Incubations were for 4 hours in the dark at 5°C and were terminated through the addition of 5% v/v (final concentration) TCA, causing un-

incorporated radio label to degas as CO_2. Each vessel was then freeze-dried, and approximately 20 mg of dry sediment weighed into Combustopad-lined Combustocones, which were oxidised using a Packard 307 Sample Oxidizer (PerkinElmer LAS (UK) Ltd.). CO_2 released upon combustion was captured into a scintillation cocktail consisting of 10 mL Carb-O-Sorb (PerkinElmer LAS (UK) Ltd.), 10 mL Permafluor (PerkinElmer LAS (UK) Ltd.) and 2 mL deionised water. Recovery of the sample oxidiser was tested using ^{14}C High DPM Spec-Chec (PerkinElmer LAS (UK) Ltd.). Blank, non-active tissue was used to determine background levels of radiation and were also oxidised in-between every sample to ensure that there was no carry-over of CO_2 from one sample to the next. Scintillation vials containing oxidised sample were radioasseyed using a Packard Tri-Carb 3100 TR Liquid Scintillation Analyzer.

DPM values of the sterile control were subtracted from the live samples to give a value of incorporated DPM ($DPM_{INC_{PP}}$). Primary production was then calculated using Equation 4.2.4.

$$PP\,(\mu g\,C\,g^{-1}\,h^{-1}) = \frac{DPM_{INC_{PP}} \times 1.05}{DPM_{TOT} \times m \times t} \tag{4.2.4}$$

Where: PP is primary production in (µg C $g^{-1}h^{-1}$); $DPM_{INC_{PP}}$ relates to disintegrations per minute incorporated into biomass (DPM); *1.05* is a discrimination factor to account for slower ^{14}C uptake relative to ^{12}C (Peterson, 1980); DPM_{TOT} is the total concentration of labelled carbon added to the incubation vessel (DPM); m is the dry mass of the sediment inoculated with sodium bicarbonate [^{14}C] (g), and t is incubation length (*hours*).

4.2.4 Carbon cycling and limitation

Organic carbon limitation within the collected sediments was investigated through a set of batch microcosm experiments, in which carbon concentration and composition were introduced as variables. The sediments incubated for this experiment represent a range of organic carbon contents (see Table 4.1) and allowed comparison between relative low- (MK), medium- (HN, AG) and high- (VG) carbon sediments.

Sediments were incubated in batch microcosms, containing water sampled from a subglacial outflow channel at MK Gletscher. Sampled in August 2013, to preserve its dissolved organic carbon (DOC) content, but remove sediment particles, this water was 0.45 µm filtered through a polysulfone membrane and

stored at -20°C until use, at which point, DOC concentration was 0.2 mgL^{-1} ($\pm$0.016). Amendments of DOC were made to the MK water, producing two additional media that reflect potential inputs of snowpack DOC into the subglacial environment and test carbon limitation in the different sediments. The snow-DOC amended media was produced by taking snow with a visible algal population from MK Gletscher, letting it melt and filtering it through a 0.45 µm nylon membrane. The resulting liquid was added to a 3 L aliquot of the portal water to give a final DOC concentration of 2 mgL^{-1}. Glucose was added to a second 3 L aliquot of the MK water to create a microcosm rich in labile carbon with a final DOC concentration of 2 mgL^{-1}.

The microcosm vessels consisted of 10% HCl washed and autoclaved 100 mL amber glass bottles. Three replicates and two controls, in which sediment was sterilised using dry heat (120°C for 72 hours) or autoclave (121°C for 45 minutes), were incubated per sediment. Triplicate controls, containing media without sediment, were incubated alongside the sediment microcosms. Aliquots of media were extracted from the incubation vessels at 1, 5, 15, 39 and 40 day intervals, being replaced with each microcosm's respective media to prevent gaseous exchange within a headspace. Dilution effects were accounted for in all subsequent analyses.

Total dissolved inorganic carbon (TDIC) was used to measure of net respiration, and was assayed immediately after sampling using a PP Systems EGM-4 infra-red gas analyser (IRGA) in static sampling mode. For this, a 1 mL aliquot of the extracted media was shaken for one minute inside the extraction syringe with a 9 mL headspace (drawn in through a soda-lime CO_2 scrubber to remove atmospheric CO_2) and 0.5 mL of 5 % HCl. Any CO_2 gas in the resultant headspace was derived from inorganic carbon within the media sample (Hodson et al., 2010a) and was injected into the IRGA in three 3 mL aliquots. TDIC concentrations were calculated from the CO_2 concentrations using $NaHCO_3$ standards prepared on the day of sampling. A 1.5 mL aliquot of the removed sample was 0.45 µm filtered through a cellulose nitrate membrane and analysed for Ca^{2+} and Mg^{2+} concentrations using ion chromatography.

Respiration rates ("R" within equations) within the sediments were determined using Equation 4.2.5:

$$R\,(\mu g\,C\,g^{-1}\,h^{-1}) = \frac{\delta TDIC_{tot} - \delta TDIC_{[Ca^{2+}+Mg^{2+}]} - \delta TDIC_{con}}{m \times t} \qquad (4.2.5)$$

Where $\delta TDIC_{tot}$ relates to the measured change in TDIC concentration; $\delta TDIC_{[Ca^{2+}+Mg^{2+}]}$ was the change in TDIC attributed to carbonate weathering, determined from the concentration change of Ca^{2+} and Mg^{2+}ions; $\delta TDIC_{cont}$ was the TDIC change in control samples, corrected for $\delta TDIC_{[Ca^{2+}+Mg^{2+}]}$ and changes in sediment-free incubations; m was the mass of sediment incubated and t was the time, over which the TDIC change was measured. The precision error of this methodology, at the concentrations of carbon observed within VG, HN and AG incubations, was below 1%, though a decrease in precision was noted at TDIC concentrations similar to those observed in MK incubations (8%).

After 40 days of incubation, BP within sediment from each microcosm was also measured. For this, the vessels were agitated, and 0.5 mL aliquots of sediment-media suspension transferred to 1.5 mL Eppendorf tubes. These were then inoculated with $1\mu L$ (37 kBq) of L-[4, 5-^{3}H(N)]leucine before undergoing a 30 minute incubation period. Incubations were terminated, and the uptake of ^{3}H into protein determined, using the methodology described in Section 4.2.3.1. BP and respiration, calculated using the difference in TDIC between days 39 and 40, were then used to estimate bacterial growth efficiency (BGE) in each microcosm with Equation 4.2.6.

$$BGE = \frac{BP}{R + BP} \tag{4.2.6}$$

4.2.5 Terminal Electron Accepting Processes

Anaerobic metabolism, and dominant terminal electron accepting processes (TEAP) within the subglacial sediment samples, were investigated using anaerobic microcosms. Experimental design was based upon that of Chapelle et al. (1996), with sediments incubated in the absence of oxygen, but with an abundance of a single electron acceptor. Different TEAP were then monitored by tracking the consumption of electron acceptors as well as the concentration of reaction products over the course of the experiment. Microcosms were assembled using VG, AG and HN sediments, and using either unamended media, or, media amended with nitrate, sulphate or ferric iron.

Following the trace metal-clean procedures outlined in Statham and Hart (2005), 60 mL glass, crimp top serum bottles were used as incubation vessels, having been autoclaved, acid washed in 50 % (v/v) hydrochloric acid for one week and then 10 % (v/v) nitric acid for one week, before being rinsed 10 times in UHQ deionised water. Six grams of freshly defrosted sediment was placed

directly into each incubation vessel using a sterile nickel spatula, and a slurry was formed using UHQ deionised water. Vessels were then either left unamended, being topped up with UHQ, or, were amended with either $MgSO_4$, $NaNO_3$ or Fe_2O_3, to a final electron acceptor concentration of 5 mM. For each electron acceptor amendment, a secondary batch of microcosms was prepared with an electron donor amendment, of 5 mM sodium acetate. After the media had been added to the microcosms, each was shaken and sparged with DOC-free N_2 gas for 3 minutes to bring dissolved oxygen concentrations to < 0.01 mg L^{-1}, before being crimped closed with a gas-tight rubber stopper. For each treatment, three replicates and two sterile controls (dry heat: 120°C for 72 hours or addition of a 10% $ZnCl_2$ solution) were incubated. Incubations were run in a Panasonic MIR-254-PE Cooled Incubator at 4°C for 50 days.

Sampling was conducted at 1, 5, 10, 20 and 50 day intervals. At each interval, sterile, stainless steel needles connected to gas-tight syringes were used to extract an aliquot of the incubation medium for analysis. Immediately after sampling, replacement, oxygen-free media of known TDIC and electron acceptor composition was drawn into the vessel under the vacuum left by the removed aliquot. This method prevented the formation of a headspace in the incubation vessel into which dissolved inorganic carbon could be lost as CO_2, whilst maintaining pressure, and oxygen-free conditions. Dilution effects were accounted for in all subsequent analyses. Respiration was measured through total dissolved inorganic carbon (TDIC) change, which was analysed immediately after sampling using the methodology described in Section 4.2.4.

Of the rest of the removed aliquot of media, 1.5 mL was filtered through a 0.45 μm cellulose nitrate membrane and analysed for major ion concentrations using ion chromatography (see Section 5.2.2.1). In the case of the Fe^{3+}-amended and unamended incubations, a further 1.5 mL aliquot of the filtered sample was analysed for Fe^{2+}(s) using the Ferrozine assay. Briefly, 100 μL of FerroZine® Iron Reagent (Hach Lange, UK) was mixed into the sample. After 5 minutes to allow the magenta solution to develop, the sample was transferred to a quartz cell and absorbance analysed at 562 nm on a Shimadzu UV-1800 UV-VIS spectrometer. Standards were prepared on the day of analysis using ferrous ammonium sulphate hexahydrate (Sigma-Aldrich). Sediment ferrihydrite concentrations were also monitored, before and after incubation, in the Fe^{3+} and unamended microcosms using the method described in 5.2.2.2.

Dissolved sulphides were analysed in the aliquots removed from sulphate-amended and unamended incubations using the methylene blue method.

Here, a 10 mL unfiltered aliquot was mixed with 0.5 mL N,N-dimethyl-p-phenylenediamine sulfate (Sulphide 1 reagent, Hach Lange, UK) and then buffered with 0.5 mL potassium dichromate (Sulphide 2 reagent, Hach Lange, UK). Five minutes were allowed for the methylene blue colour to develop before absorbance was measured at 665 nm on a Shimadzu UV-1800 UV-VIS spectrometer. Concentrations were determined using freshly prepared standards made using washed sodium sulphide crystals that had been dissolved in UHQ.

Concentrations of TDIC and electron acceptor within the supernatant of each live incubations vessel, were corrected so that biotic processes could be considered in isolation from total solute changes. This was done by subtracting average TDIC and electron acceptor concentrations within sterile incubations from concentrations in live incubations. Biotic concentrations are reported here.

All reported statistics were performed using IBM SPSS Statistics 22, with p values generated using one-way multivariate analysis. Post-hoc Scheffe tests were used to infer differences between factors. The precision of all analytical methods was below 5%.

4.3 Results

4.3.1 Sediment organic matter

Table 4.1 shows SOC contents calculated from LOI data. MK's granitic sediment contained the lowest concentration of organic matter when compared to the sedimentary geology of till taken from HN, AG and Svalbard glaciers. The cellular carbon concentrations, which were modelled using cell enumerations (reported in Table 3.5, Chapter 3), made up 0.0002% (TB sediment) - 0.05% (MK sediment) of these gravimetrically measured carbon concentrations. C/N, shown in Table 4.1, varied considerably by glacier, with a very high C/N of 62.6 in VG sediment. Other values were more typical, ranging from 3.77 in MK sediment to 23.2 in HB sediment.

Table 4.1: Mean (μ) and standard deviation (σ) values for sediment organic carbon concentrations, and C/N in subglacial sediments. $n = 3$.

	Carbon (mg g^{-1})		C/N	
Sample	μ	σ	μ	σ
VG	24.2	*0.9*	62.6	8
HB	8.69	*0.004*	23.2	*0.9*
TB	19.0	*0.05*	19.0	*0.7*
MK	0.121	*0.04*	3.77	*0.2*
HN	2.79	*0.3*	7.46	*0.5*
AG	1.98	*0.06*	9.00	*0.9*

4.3.2 FTIR Spectroscopy

Figure 4.3.1 shows spectra for NaOH-extracted sediment organic matter at each site. Peaks typical of organic functional groups were distinct from the NaOH control spectra, which showed weak banding between 1500 - 1000 cm^{-1}, and an intense peak at *c.* 3000 cm^{-1} from O-H stretch. O-H stretch of water was evident in all samples within the 3700 - 3000 cm^{-1} region. Aliphatic groups, present within the 3000 - 2800 cm^{-1} region were only evident in Svalbard sediments, with low intensity peaks at *c.* 2928 and 2850 cm^{-1} evident in VG, TB and HB extracts. In VG, TB, AG, HN and HB extracts, a peak was observed at 1711 cm^{-1}, from C=O stretch of COOH, ketones or aldehydes. Amide I bands (*c.* 1656 cm^{-1}) were evident in all extracts, whereas amide II bands (*c.* 1458 cm^{-1}) were observed in VG, TB, HB and HN extracts only. Amide groups were also evidenced by the presence of peaks from C-N stretch (at *c.* 1341 cm^{-1}) in all extracts. C-O stretch at *c.* 1295 cm^{-1} and O-H bending at *c.* 953 cm^{-1} indicated carboxylic acids in VG, TB, AG, HN and HB sediments. All samples excluding TB, exhibited a broad peak between 1150 and 1000 cm^{-1} that was characteristic of Si-O-Si stretch, and may have obscured peaks in the region characteristic of carbohydrate functional groups. Bands from C-O stretch, characteristic of polysaccharides were evident in all samples, however, distinct at 1145 cm^{-1}, on the shoulder of the broad Si-O peak.

4.3.3 Microbial Activity

After one day of incubation, median rates of bacterial production (BP) in the sediments (shown in Fig. 4.3.2) ranged from 2.49x10^{-6} $\mu gCg^{-1}h^{-1}$ in TB sediment to 1.95x10^{-5} $\mu gCg^{-1}h^{-1}$ in VG sediment. ^{3}H recovery from control

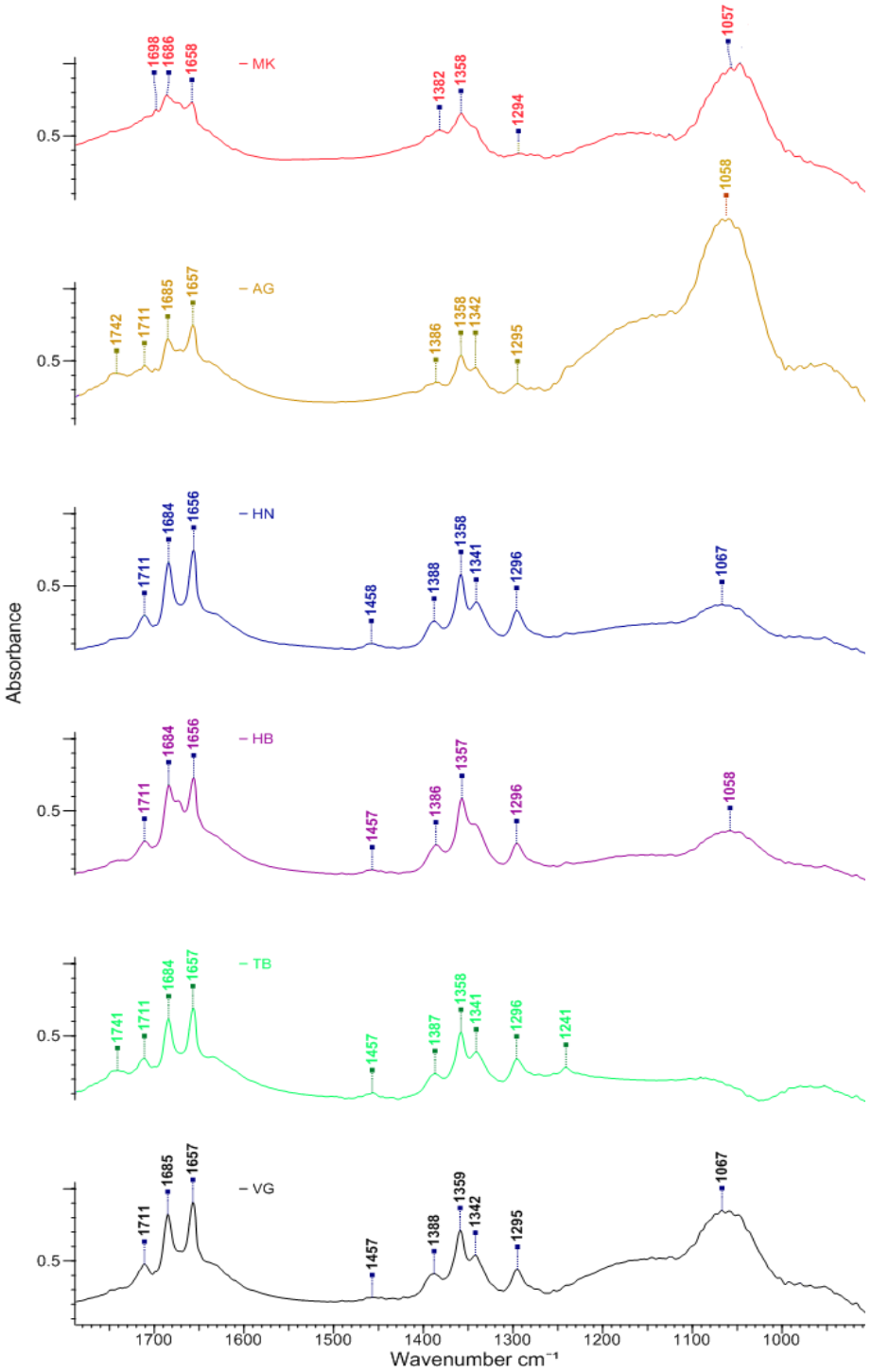

Figure 4.3.1: FTIR spectra of NaOH extracted sediment organic matter. Peaks shown from 900 from 1800 cm^{-1}. Scan number = 50.

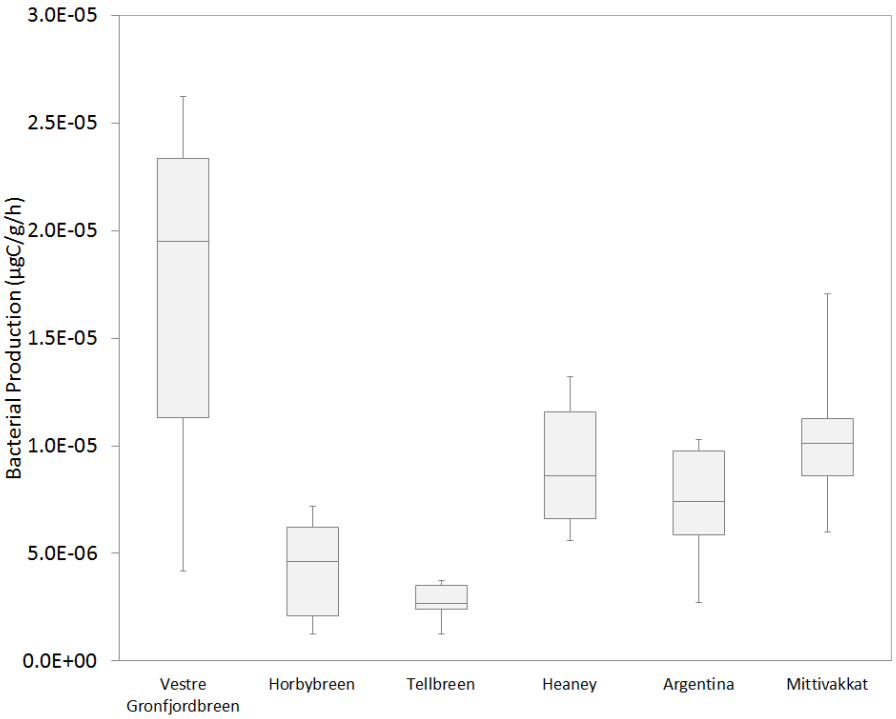

Figure 4.3.2: Rates of bacterial production in subglacial sediments, determined by L-[4, 5-^{3}H(N)]leucine incorporation into nucleic acid. Shown are minimum, Q1, median, Q3 and maximum values; $n = 5$.

samples was typically an order of magnitude lower than live sediments, with direct DPM counts from sterilised incubations averaging 5.41% that of active samples.

Rates of bacterial production were lowest just after defrosting, but had increased by an order of magnitude (to *c.* $10^{-5} \mu g C g^{-1} h^{-1}$) after 18 days of incubation in the case of HB1 and VG1 sediments, 30 days, in the case of VG2 sediment, and 100 days, in the case of HB2 sediment (see Fig. 4.3.3). Sterilised controls maintained low levels of leucine incorporation (*c.* 10^{-7} $\mu g C g^{-1} h^{-1}$) throughout the 100 day acclimation experiment, probably a result of leucine adsorption to sediment particles (dos Santos Furtado and Casper, 2000). Similarity between dry heat sterilised and formaldehyde killed controls was also observed, with an average coefficient of variation between sterilisation methods of 37%, throughout the incubation period.

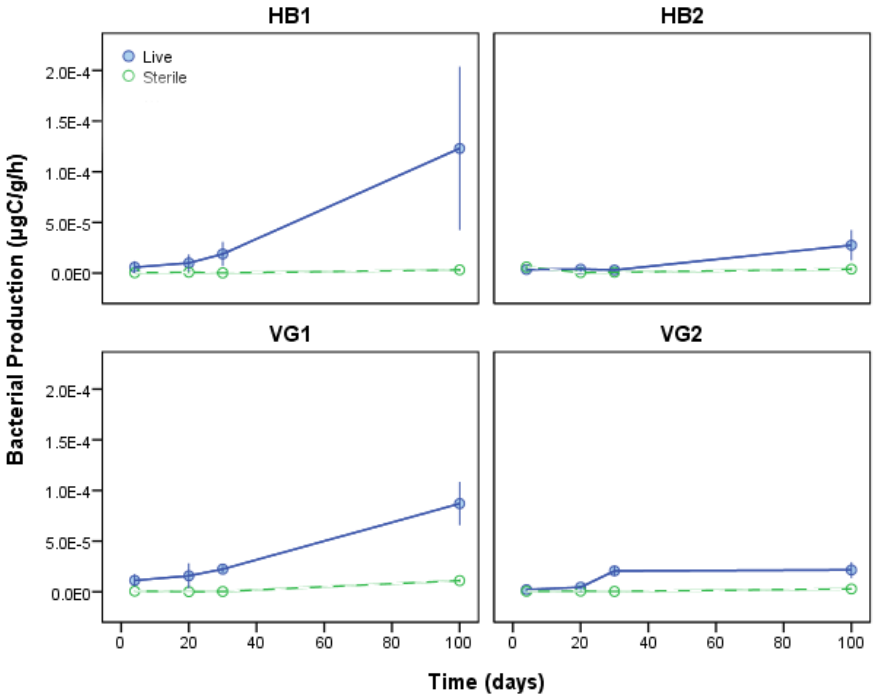

Figure 4.3.3: Acclimation of sediment heterotrophic communities. Rates of bacterial production determined by L-[4, 5-^{3}H(N)]leucine incorporation after number of days incubating at 4°C in the dark. Error bars show one standard deviation; $n = 5$.

4.3.4 Primary Production

Median rates of cellular incorporation of inorganic carbon by chemoautotrophic activity, shown in Fig. 4.3.4, ranged from 4.16x10^{-4} $\mu gCg^{-1}h^{-1}$ in sediment from the second VG site visited (VG2), to 1.14x10^{-3} $\mu gCg^{-1}h^{-1}$ in sediment taken from the first site visited (VG1). ^{14}C recovery from control samples averaged 12.19% of live sediments and was typically the same magnitude as background radiation (comparing direct DPM). Compared to measurements of bacterial production, rates of primary production changed little over the course of 100 days incubation (see Fig. 4.3.5), with no observable acclimation period.

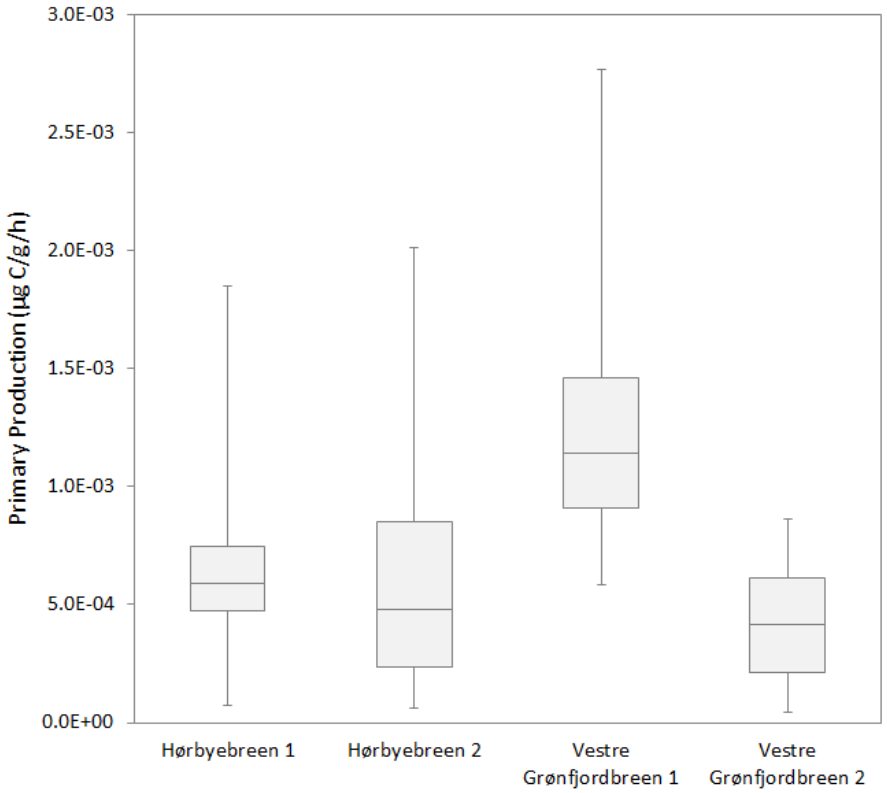

Figure 4.3.4: Rates of chemoautotrophic primary production, determined by cellular incorporation of sodium bicarbonate [^{14}C]. Shown are minimum, Q1, median, Q3 and maximum values; $n = 20$.

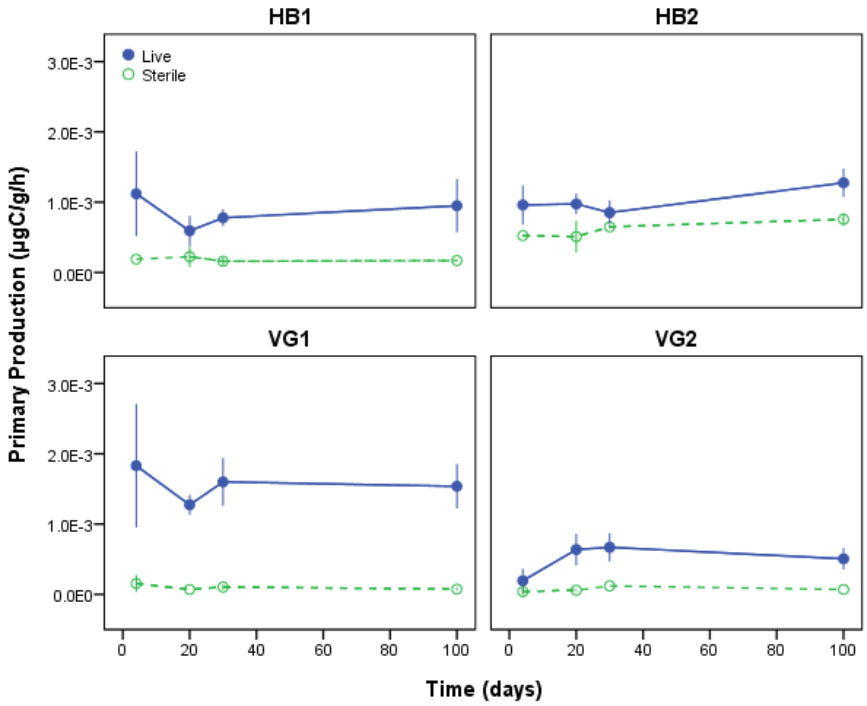

Figure 4.3.5: Acclimation of sediment autotrophic communities. Rates determined by cellular incorporation of sodium bicarbonate [^{14}C] after number of days incubating at 4°C in the dark. Error bars show one standard deviation; $n = 5$.

4.3.5 Carbon Cycling and Limitation

Fig. 4.3.6 shows the evolution of TDIC, as a result of biotic processes, for each sediment and carbon amendment. The largest increases in TDIC concentrations were observed in the VG incubations, whereas little increase occurred over the course of the MK incubations. In MK, AG and HN sediments, the glucose amendment produced the largest relative change in TDIC concentration, with little observable increase in the unamended incubations. Algal DOC-amended incubations saw greater TDIC increases relative to the unamended AG and HN microcosms. VG incubations had the opposite pattern, with TDIC increases greatest in unamended and algal DOC-amended microcosms.

Variation between replicates was generally low, with an average coefficient of variation of 5% for corrected TDIC values. No calcium or magnesium was detected in MK incubations, but contributions of TDIC from carbonate weath-

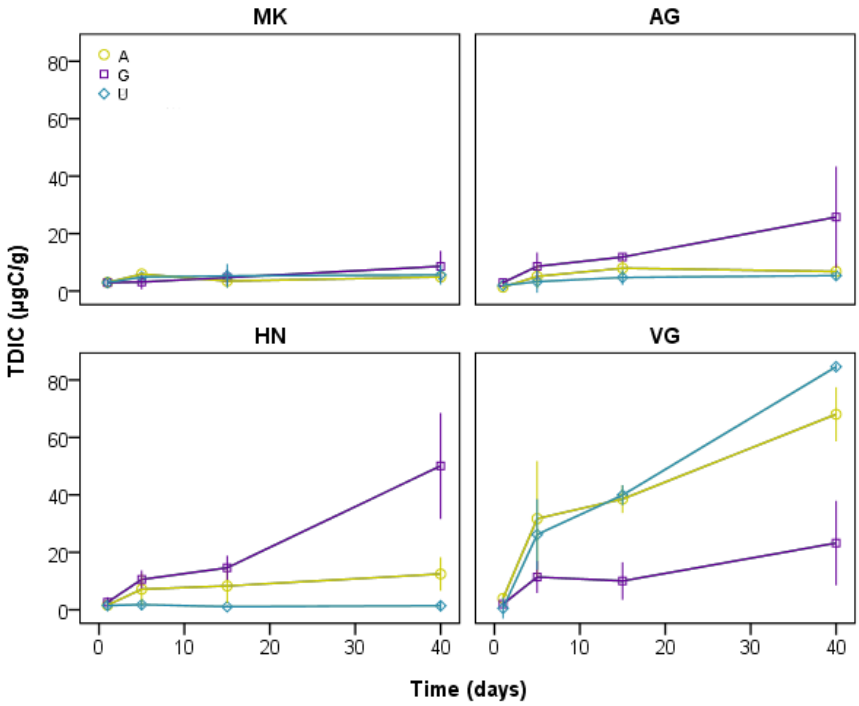

Figure 4.3.6: Temporal evolution of aqueous TDIC concentrations, normalised for sediment mass (μg Carbon g^{-1} sediment) and corrected for calcite weathering and abiotic processes. Microcosms contain sediment from: MK, AG, HN and VG glaciers; incubated in: unamended subglacial outflow (U), glucose-amended subglacial outflow (G) and algal DOC-amended subglacial outflow (A). Error bars show one standard deviation; $n = 3$.

ering accounted for 13.2% (±6.2), 22.7% (±8.6) and 34.2% (±14.6) of TDIC changes in live AG, VG and HN incubations respectively. Within control incubations, carbonate weathering accounted for an average of 82.2% (±22.9) of TDIC change within sterile controls. Additional contributions of TDIC in sterilised sediment could be explained by weathering of carbonate containing minerals other than calcium carbonate or dolomite, or from respiration by fungi that was observed to survive sterilisation by dry heat (see Section 5.2.2.1).

Rates of respiration, shown in Fig. 4.3.7a, were calculated by integrating TDIC between day 39 and 40 of the experiment. Differences between treatments followed a similar, though less pronounced, trend to the changes observed in Fig.

4.3.6. Excluding VG incubations, respiration was lowest in unamended microcosms, with rates of 0.0038 $\mu gCg^{-1}h^{-1}$ ($\pm$0.0002), 0.036 $\mu gCg^{-1}h^{-1}$ ($\pm$0.001) and 0.0014 $\mu gCg^{-1}h^{-1}$ ($\pm$0.004) observed for MK, AG and HN sediments respectively. It then increased with algal DOC, and glucose amendment, though differences between mean values were only significant in the case of AG ($p_{G>U}$ = 0.02; $p_{G>A}$ = 0.04), and HN ($p_{G>U}$ = 0.05) incubations. Respiration was significantly greater in VG incubations relative to the other sediments ($p <$ 0.01), and rates here did not follow the same pattern between treatment. As indicated by TDIC evolution in Fig. 4.3.6, respiration in unamended VG sediment was greatest, with rates of 0.080 $\mu gCg^{-1}h^{-1}$ ($\pm$ 0.004). Respiration in the glucose-amended VG microcosms was not significantly lower than unamended incubations, and all carbon-amended VG incubations had similar respiration rates after 40 days of incubation.

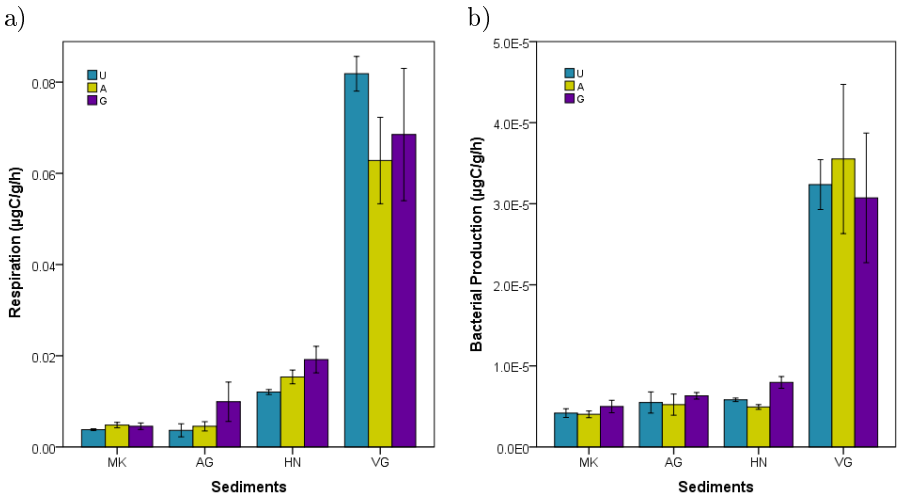

Figure 4.3.7: a) Rates of respiration, calculated from the TDIC change between day 39 and 40, and b), rates of bacterial production, determined by L-[4, 5-^{3}H(N)]leucine incorporation into nucleic acid after 40 days incubation. Sediment from: MK, AG, HN and VG glaciers; incubated in: unamended subglacial outflow (U), glucose-amended subglacial outflow (G) and algal DOC-amended subglacial outflow (A). Error bars show one standard deviation; n = 3.

Rates of bacterial production, shown in Fig. 4.3.7, were typically four orders of magnitude lower, and only weakly related to measured respiration rates; except in the case of HN sediment, which saw moderate correlation between respiration and production (r = 0.7, p = 0.03). As with respiration rates, mean

rates of bacterial production were greatest in glucose-amended microcosms for MK, AG and HN sediments, though this difference was only significant in HN incubations ($p_{G>U}$ =0.04; $p_{G>A}$= 0.01). VG sediments, again, had significantly greater rates of production than observed for MK, AG and HN incubations ($p < 0.01$), with mean production rates being broadly similar across treatments.

BGE values (Fig. 4.3.8) were low in all cases, with a range from 0.032% (±0.02) in unamended HN microcosms to 0.17% (±0.06) in glucose-amended HN sediment. For all microcosms except VG, BGE decreased in the order glucose-amended > algal DOC-amended > unamended, though the only significant difference between treatments was observed between glucose-amended and unamended HN sediment ($p_{G>P}$ = 0.03).

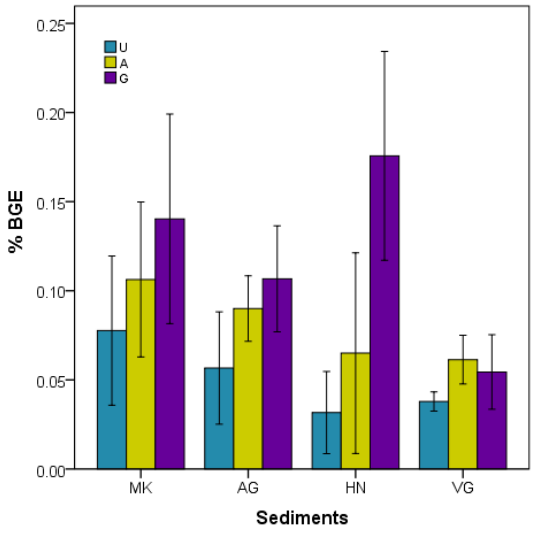

Figure 4.3.8: Bacterial growth efficiency (BGE), following 40 days incubation of sediment in: unamended subglacial outflow (U), glucose-amended subglacial outflow (G) and algal DOC-amended subglacial outflow (A). Error bars show one standard deviation; $n = 3$.

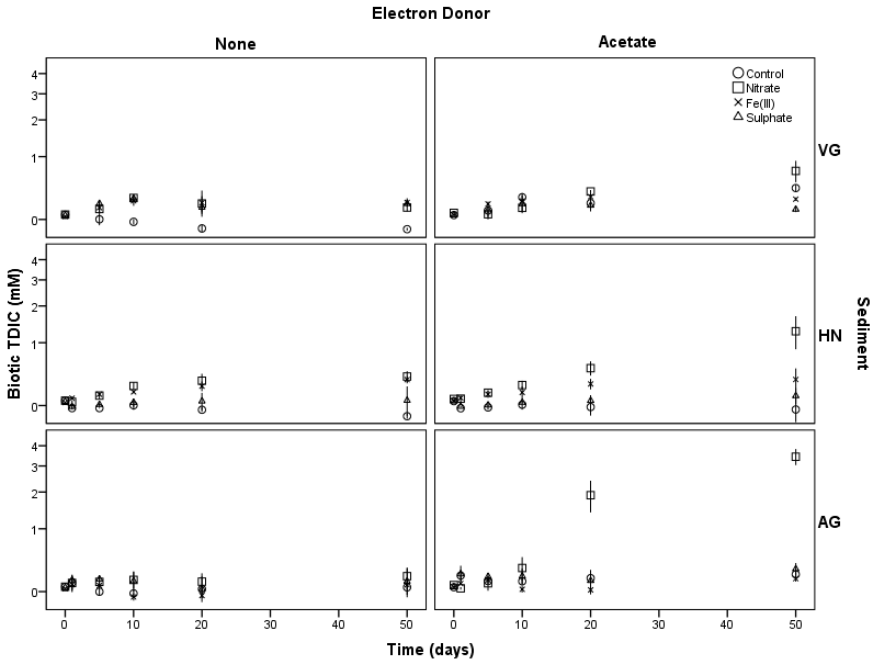

Figure 4.3.9: Biotic TDIC evolution in anaerobic microcosms containing sediments from VG, HN and AG, circle markers show control incubations in which no electron acceptor amendment was made, square markers show nitrate amended incubations, cross markers show ferric iron amended incubations and triangle markers show sulphate amended incubations. Left hand plots show TDIC change in incubations with no electron donor addition, right hand plots show change in microcosms amended with 5 mM sodium acetate.

4.3.6 Terminal Electron Accepting Processes

Figure 4.3.9 shows TDIC change as a result of biotic processes within anaerobic microcosms that contained different electron acceptor, and donor treatments. In control incubations: with no electron acceptor treatment, and without addition of sodium acetate, TDIC was below the detection limit of this methodology, with negative or *c.* zero TDIC concentrations returned as biotic values. Differences in TDIC between electron acceptor treatments for non acetate-amended incubations, then proceeded according to the energetics of each TEAP. NO_3^--amended incubations, the most energetically favourable electron acceptor, saw significantly more TDIC relative to control incubations in all sediments ($p < 0.05$). Fe^{3+}-amended incubations had significantly higher ($p < 0.01$) TDIC

concentrations compared to controls within VG and HN incubations, whereas SO_4^{2-}-amended incubations saw the lowest TDIC response, only being significantly higher ($p < 0.01$) than control values within VG incubations.

Initially, the evolution of TDIC within acetate-amended incubations did not vary significantly by electron acceptor treatment. After 50 days of incubation, however, TDIC within NO_3^- and acetate-amended incubations, it had significantly ($p < 0.05$) exceeded that of other treatments. By this point, it was *c.* 2×, 10× and 17× greater than respective, control and acetate-amended VG, HN and AG incubations, and *c.* 5×, 3× and 19× greater than NO_3^--amended incubations without acetate. Differences in TDIC between other electron acceptor amendments were not significant from control values at the 95% confidence interval. Average coefficient of variation between TDIC replicates was 37%.

No biotic decreases in SO_4^{2-} were observed within SO_4^{2-}-amended incubations, whilst biotic SO_4^{2-} production was observed within control incubations. Dissolved sulphide species, intermediates of sulphate reduction, remained below detection throughout the incubation period, both in control, and SO_4^{2-}-amended incubations. Though abiotic increases in Fe^{2+} were noted within all Fe^{3+}-amended samples, this was not significantly different between live and sterile incubations. Fe^{2+} was below detection within control samples, except in the case of HN sediment, and so the observed increase in Fe^{2+} within Fe^{3+}-amended incubations probably related to reduction of the added Fe_2O_3, rather than sediment iron oxyhydroxides. Increases in Fe^{2+} within HN incubations were strongly coupled to biotic SO_4^{2-} concentrations ($R^2 = 0.68$), whilst being weakly related to TDIC ($R^2 = 0.37$), suggesting that it was predominantly derived from pyrite oxidation.

Shown in Figure 4.3.10, biotic decreases in NO_3^- were observed within all NO_3^--amended incubations. Decreases were greatest within AG incubations, where a 2.3 (±0.4) mM decrease was observed over the course of the incubation (compared to 0.7 (±0.3) mM for VG, and 0.8 (±0.4) mM for HN). NO_2^- (also shown in Figure 4.3.10) was only detected within incubations that had been amended with both NO_3^- and acetate, though this was the case for all sediments. The magnitude of NO_2^- produced in these incubations was less than NO_3^- decreases, being 0.03 (± 0.01) mM in VG, 0.03 (± 0.02) mM in HN, and 0.09 (±0.06) mM in AG.

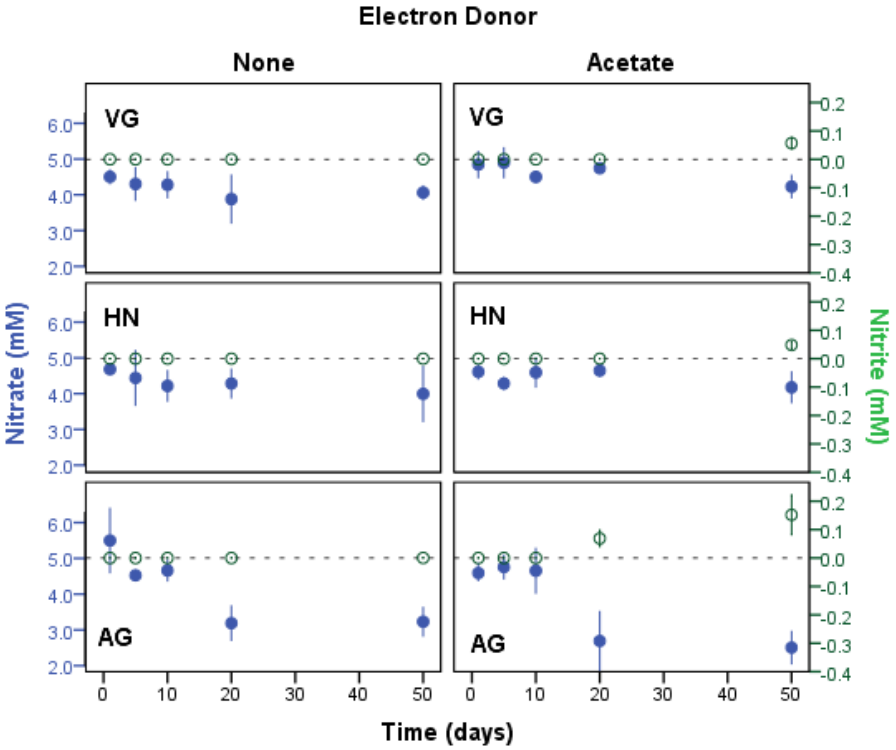

Figure 4.3.10: Evolution of nitrate (left axis, solid blue markers) and nitrite (right axis, hollow green markers) as a result of biotic processes within anaerobic incubations amended with 5 mM nitrate. Sediments incubated were VG (top row), HN (middle row) and AG (bottom row). Error bars show 1 standard deviation, $n = 3$.

4.4 Discussion

The work carried out in this Chapter, sought to address Objective 2, to assess carbon cycling within subglacial microbial ecosystems, and to determine the factors, which may influence productivity. Microcosms containing sediment sampled from glaciers in Svalbard, Greenland and the Maritime Antarctic were used to measure bacterial production, respiration and chemoautotrophic production. Reported here are estimates of bacterial production, respiration and primary production for subglacial sediment communities from a range of glaciers, and with a range of organic carbon conditions.

Carbon characterisation of subglacial sediments

Carbon concentrations within the sediments varied considerably between glaciers. Svalbard's organic-rich geology (Vorren et al., 2013) was evident, with sediment from VG, HB and TB glaciers containing significantly more organic carbon ($p < 0.01$) relative to HN, AG and MK averages. C/N was also higher in Svalbard sediments ($p < 0.002$), indicative of sediment-derived organic material in samples from these glaciers. This was further supported by FTIR analysis, which identified the highest intensity of aliphatic peaks within VG extracts, followed by TB and HB. Present only in Svalbard sediment, aliphatic compounds are typical of insoluble, sedimentary organic matter (Stankiewicz et al., 2000). Lower SOC in MK, AG and HN sediments, combined with the presence of proteinaceous organic matter, and C/N values close to Redfield stoichiometry, suggest that microbial organic matter was present within these sediments.

Though C/N values implied nitrogen limitation within Svalbard subglacial sediments, this result may be misleading. Amide groups and polysaccharides peaks were evident within all sediment extracts analysed; the relative intensity of amide I and II peaks decreasing in the order: VG, MK, HN, HB, TB and AG. High concentrations of low-nitrogen, fossilised SOC in Svalbard sediments may, therefore, not reflect the C/N of the carbon fraction actually utilised for microbial growth (Touratier et al., 1999). This also suggests that the fossilised SOC fraction in Svalbard sediments may be too nitrogen limited to support growth without an additional inputs, such as from precipitation (e.g. Hodson et al. (2010b)).

Microbial Activity

Significant ($p_{Live>Control} \leq 0.05$) levels of bacterial production were observed in all samples, one day subsequent to transferral from -20°C storage into 4°C cooled incubators. Rapid recovery from storage conditions suggests that the production rates reported in Fig. 4.3.2, was from communities that were active *in situ*, rather than communities acclimated to laboratory conditions. It is also possible that bacteria were active during storage, with other reports having measured macromolecular synthesis in subzero conditions (-39°C within permafrost (Panikov et al., 2006), -17°C within snow (Carpenter et al., 2000), and -15°C within subglacial lake ice (Amato et al., 2010)).

At the time of writing, the only other published account of subglacial bacterial production comes from subglacial lake Whillans, Antarctica, where rates of 3.75x10^{-5} $\mu gCg^{-1}h^{-1}$ were reported within sediment (Christner et al., 2014). Forefield bacterial production rates have been observed at Damma Glacier, in the Swiss Alps, with near-glacier production being similar to that of the Whillans observation (*c.* 4x10^{-5} $\mu gCg^{-1}h^{-1}$) (Göransson et al., 2011). In this study, median bacterial production rates were lower, in the order of 10^{-6} μgCg^{-1}h^{-1} for all sediments except VG (1.95x10^{-5} μgCg^{-1}h^{-1}). Distinct lag phases were observed within HB2 and VG2 sediment incubations, and slight lag was evident within HB1 and VG1 incubations also (Fig. 4.3.3). Bacterial production rates, reported in Fig. 4.3.2 should, therefore, be taken as a conservative estimate for *in situ* activity, rather then an assessment of potential ecosystem productivity.

Bacterial productivity was significantly greater in VG sediment relative to the other Svalbard glaciers ($p_{VG>HB} = 0.004$; $p_{VG>TB} = 0.002$), though not relative to HN ($p = 0.16$), AG ($p = 0.064$) or MK ($p = 0.32$) sediments. Variation in production rates between sediments was not explained by relative total or live cell concentrations (see Table 3.3, Chapter 3), organic carbon concentration or C/N values. It is perhaps of note, however that VG sediment contained the highest intensity peaks of labile proteinaceous organic matter. Though not significantly lower, productivity within TB sediment was less than in other sediments, probably due to the spring sampling conditions, where cells were more likely to be dormant due to colder conditions. This finding supports the seasonal carbon dynamics in Wadham et al. (2004) where subglacial respiration products were found to be several orders of magnitude less in winter relative to summer.

Acclimation to experimental conditions, showed the potential of subglacial

communities to adapt to warmer (4°C) conditions. Indeed, after 100 days of incubation, production rates in HB1 sediment had exceeded that of VG1 sediment, despite initially being an order of magnitude lower. Fig. 4.3.3 also indicates the lack of spatial homogeneity between sample sites at VG or HB. Initial rates of bacterial production were significantly greater ($p = 0.03$) in VG1, relative to VG2 sediment, with this difference increasing after 100 days. Growth limitation was evident in VG2 sediment, with production rates reaching a plateau by 30 days, compared to VG1, which was still increasing after 100 days incubation. With stationary growth phases often a response to resource limitation (Mehrotra and Sumbali, 2009), it is suggested that the spatial distribution of nutrient and/or substrate concentrations, likely resulted in heterogeneous bacterial production under VG. In HB incubations, initial differences between HB1 and HB2 were not so pronounced. By 100 days of incubation, however, HB1 production was significantly greater then that of HB2 ($p = 0.01$), with production in live HB2 sediments never significantly greater ($p_{t_{100}} = 0.2$) than control leucine uptake.

Inorganic carbon assimilation as a result of chemoautotrophic activity, was two to three orders of magnitude greater then recorded rates of heterotrophic organic carbon assimilation. Rates observed in VG2, HB1 and HB2 sediment were similar to those of subglacial primary production recorded in Boyd et al. (2014) (*c.* 5x10^{-4} $\mu gCg^{-1}h^{-1}$), with production in VG1 sediments being an order of magnitude higher. No significant change in primary production rates for any sediment was observed over the 100 day incubation period, shown in Fig. 4.3.5, suggesting a community well adapted and active under *in situ* conditions (Madigan, 2009).

High pCO_2 values in subglacial outflow have previously been attributed to microbial respiration (Hodgkins et al., 1998; Wynn et al., 2006; Nowak and Hodson, 2013; Andrews, 2015), and so it was somewhat expected that respiration would exceed primary productivity in these sediments. This result is further supported by the relative rates of chemoautotrophy (Boyd et al., 2014; Christner et al., 2014) and respiration (Mikucki et al., 2004; Gaidos et al., 2004; Mikucki and Priscu, 2007; Lawson, 2012) reported from other subglacial systems. Since the TDIC changes observed here encompassed both chemoautotrophic and respiratory carbon fluxes, they were representative of net ecosystem productivity (NEP), where: *NEP* ($\mu gCg^{-1}h^{-1}$) = *primary production - respiration.* Net respiration, or a negative NEP, was observed within all sediment (VG, HN, AG and MK), suggesting that the subglacial microbial community was a net

source of CO_2 to the subglacial environment. NEP was several orders of magnitude lower than rates reported for cryoconite hole granules in Hodson et al. (2010a) and Cook et al. (2010), with rates of *c.* -10^{-2} µgCg^{-1}h^{-1} within VG and HN sediments. NEP was lower, at *c.* -10^{-3} µgCg^{-1}h^{-1}, within AG and MK incubations, possibly as a result of lower organic carbon concentrations within these sediments. Within VG sediments, where measurements of both chemoautotrophic and net respiration were made, chemoautotrophic activity was approximately one order of magnitude less than net respiration, suggesting that rates of respiration within this sediment were similar to those of measured net respiration (0.089 (±0.005) µgCg^{-1}h^{-1}).

Net respiration rates in unamended microcosms (Fig. 4.3.7a), were similar to rates reported in Gaidos et al. (2004) and Mikucki and Priscu (2007), and were several orders of magnitude greater than rates reported in Lawson (2012). Respirative carbon fluxes reported here, exceed those of published methanogenic fluxes by factors ranging from *c.* 6×10^2 (Lower Wright glacier, Antarctica (Stibal et al., 2012c)) to 1×10^6 (Robertson glacier, Canada (Boyd et al., 2010)). Methane produced at the rates reported in Boyd et al. (2010) and Stibal et al. (2012c) would, regardless of the greater radiative forcing of methane (Shine et al., 1990), constitute a lower greenhouse gas potential than biologically produced carbon dioxide at the rates herein reported.

Carbon Cycling and Limitation

In the case of MK, AG and HN sediments, where SOC concentrations were relatively low, and C/N was below Redfield stoichiometry, increases in respiration were observed in carbon-amended microcosms relative to unamended microcosms (Fig. 4.3.7a). Increases with glucose amendment were more pronounced in measurements of bacterial production (Fig. 4.3.7b), though leucine uptake was similar within unamended and algal DOC-amended microcosms. Conversely, with VG sediment, which had higher SOC concentrations, and relatively high intensity FTIR peaks corresponding to proteinaceous organic matter, respiration and bacterial production were both significantly higher than in other sediments. Moreover, increases were not observed as a result of carbon addition to VG incubations, and, in the case of respiration, the highest rates were observed in unamended samples.

Bacterial growth efficiency was low in all incubations (Fig. 4.3.8), being of the same order of magnitude as calculated from data reported in Mikucki et al.

(2004), two to three orders of magnitude smaller than rates reported for Subglacial Lake Whillans bacteria (Vick-majors et al., 2013; Christner et al., 2014), and three orders of magnitude less than reported for cryoconite (Laybourn-Parry et al., 2012). Low BGE could, in part, have been attributed to fungal activity within the sediment. Bacteria have been shown to out-compete eukarya with respect to leucine uptake over short time periods (Buesing and Gessner, 2003), whereas, measures of respiration took account of the entire sediment community. Significant carbon dioxide derived from fungal activity would, therefore, result in the underestimation of BGE. When modelled, however, fungal activity could account for up to 90% ($\pm$0.06) of total respiration rates before BGE values increased by more than one order of magnitude. Viable bacterial cells were an order of magnitude more abundant than eukaryotic cells within Svalbard sediments (Table 3.6, Chapter 3) though, making this scenario unlikely.

Low BGE within all sediments, suggested that energy derived from catabolism was primarily utilised for cell maintenance rather than growth. Furthermore, relatively high bacterial production and BGE within glucose-amended MK, AG and HN microcosms, suggested some linkage between the quality of carbon available and bacterial growth; a preference for easily metabolisable carbon forms over alga-derived polysaccharides in this case. Regulation of growth efficiency to available nutrient or organic carbon supplies has been well documented empirically (Russell and Cook, 1995; Harder, 1997; Hall and Cotner, 2007), and within oligotrophic environments (Apple et al., 2006; Berggren and del Giorgio, 2015). And, is further supported for subglacial systems by the behaviour of VG microbes, the growth of which were seemingly not limited by either substrate quantity or quality. That BGE was still low in VG sediments instead implies that other factors such as temperature, or mineral nutrient availability were ultimately responsible for low growth efficiency within these sediments.

With suggestions of carbon limitation within MK, AG and HN sediments, this experiment raises questions as to the origin of carbon likely utilised *in situ*. In the case of MK sediment, where granitic mineralogy provides little in the way of organic carbon, respiration and bacterial growth were maintained at rates comparable to AG and HN sediments, which contained *c.* 20 times MK's organic carbon content. Continuing at the reported, unamended rates, catabolic processes would, theoretically, be capable of exhausting the measured masses of SOC within *c.* 5 (MK) to 30 (VG) years. It is suggested, therefore, that resupply of organic carbon, either from englacial ice and supraglacial meltwater, or from chemoautotrophic activity, would be crucial to maintaining active metabolism

underneath the glaciers herein examined.

TEAP in Subglacial Sediments

Within anaerobic incubations, rates of TDIC production where no electron acceptor or electron donor amendment had been made, were near or below the detection limit of this methodology. This compared to TDIC production under aerobic conditions, in which *c.* 0.9 mM, 0.2 mM and 0.4 mM of TDIC were produced within VG, HN and AG incubations respectively, over the same time period and using the same methodology to measure TDIC (see Section 4.3.5). These low values, which were slightly negative in the case of VG and HN sediments, could also suggest that chemoautotrophic activity exceeded that of anaerobic heterotrophic metabolism, suggesting a shift in net carbon flux throughout the redox scale. Within VG and AG incubations, increases in TDIC production upon addition of Fe^{3+} or SO_4^{2-} with acetate were small, alongside which no reaction products: enhanced Fe^{2+} production, or hydrogen sulphide (g), were noted throughout amended incubations. This suggested that the communities within these sediments were not adapted to utilising Fe^{3+} or SO_4^{2-} as electron acceptors. Within HN incubations, however, acetate amendment gave rise to significantly elevated TDIC within Fe^{3+}-amended incubations, relative to Control or SO_4^{2-}-amended values, suggesting the potential for Fe^{3+} reducing communities to be active within HN sediment.

More obvious within these anaerobic microcosms, was the TDIC change relating to NO_3^- amendment. This was greater relative to other electron acceptor treatments, and was especially pronounced within acetate amended incubations. Though biotic NO_3^- removal was observed in all NO_3^--amended incubations, concurrent production of NO_2^-, an intermediate product of denitrification, was only observed within acetate amended incubations (Chapelle, 2001). Plotting biotic NO_3^- changes against biotic TDIC changes (Figure 4.4.1), revealed that stoichiometry within acetate-amended incubations was similar to that of respiratory denitrification (C_{106}:$N_{94.4}$) (Torgersen and Branco, 2007) (127:94.4 (VG), 113:94.4 (HN) and 107:94.4 (AG)). No significant ($p < 0.05$) covariation was observed, however, between TDIC and NO_3^- within non acetate amended incubations. So whereas there was strong evidence showing denitrification within acetate-amended sediments, it is suggested that the majority of nitrate reduction observed in the absence of a suitable electron donor was assimilatory nitrate reduction, rather than respiratory denitrification.

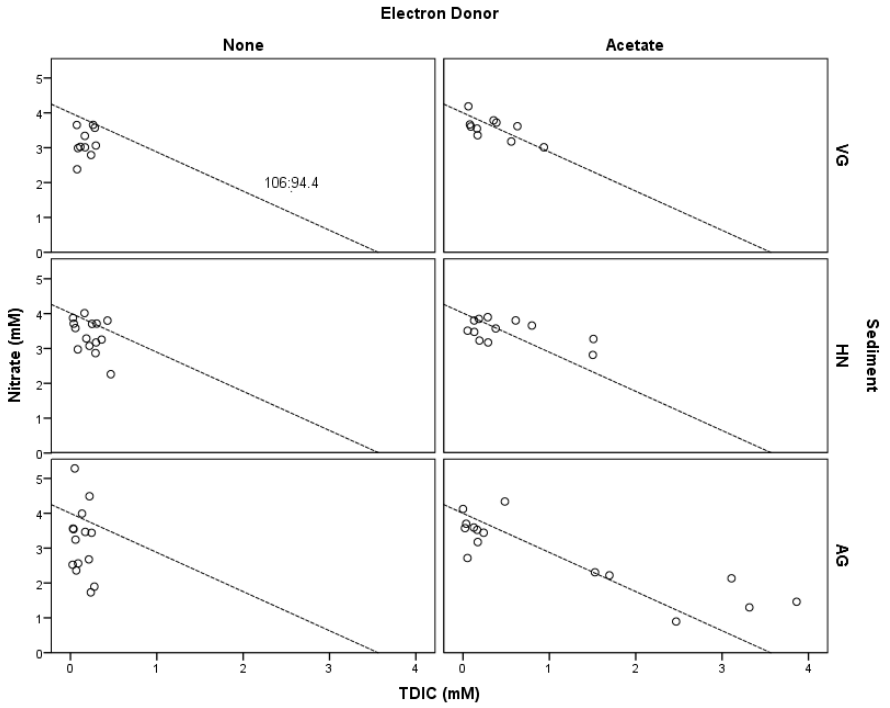

Figure 4.4.1: Association of biotic NO_3^- and TDIC concentration within anaerobic incubations of NO_3^- amended subglacial sediment. Dashed line is a reference showing 106:94.4 stoichiometry of microbial oxidation of organic matter by nitrate (Torgersen and Branco, 2007).

It is perhaps surprising that this experiment points to denitrification being the dominant TEAP within these sediments, with respect to the supply of SO_4^{2-} and $Fe(OH)_3$ groups from pyrite oxidation (see Chapter 5), and previous observations of SO_4^{2-} reduction in Svalbard sediments by Wadham et al. (2004). Previous studies, however, have described viable sources of NO_3^- to subglacial sediments, linking NO_3^- within subglacial outflow to nitrified snowpack ammonium (Wynn et al., 2007; Hodson et al., 2009; Ansari et al., 2013), or episodic, direct inputs of NO_3^- through precipitation (Hodson et al., 2010b). So too, studies have noted NO_3^- removal within subglacial channels (Tranter et al., 1994, 2002; Hodson et al., 2004, 2010a). Combined with observations of nitrate reducing bacteria within samples from subglacial sediments (Boyd et al., 2011), and isotopic evidence for denitrification (Wynn et al., 2006; Yde et al., 2010b), there is a strong case for denitrification to be an important process within these

sediments also. Anaerobic respiration relies on simple organic compounds or H_2 to serve as electron donors (Lovley and Chapelle, 1995), and since denitrification rates spiked upon acetate addition, it is probable that the supply of such compounds limits denitrification within these glacial samples. Under *in situ* conditions, electron donors are likely to be acetates, supplied from snowmelt (eg. Legrand et al. (2013)), fermentation of sediment organic matter to acetate (Gaidos et al., 2009; Thór Marteinsson et al., 2012), or H_2, derived from rock comminution (Thór Marteinsson et al., 2012; Telling et al., 2015).

Evidence of respiration under both aerobic and anaerobic conditions within the same sample, was suggestive of facultative anaerobic metabolisms, and/or, sediment with distinct aerobic/anaerobic zones with separate communities able to respire under each condition. This is consistent with our understanding of conditions under glaciers, where channelised drainage brings oxygen to discreet sections of the glacier bed, whilst chemical and biological oxygen demand create strong redox gradients within the sediment (Tranter and Skidmore, 2005; Knight, 2008). Though no measurements of methane were taken for this study, others have shown that it can take upwards of 200 days before methanogenesis develops as a dominant TEAP within laboratory incubations of subglacial sediment (Stibal et al., 2012c). This study, especially HN incubations in which both NO_3^- reduction and Fe^{3+} reduction were observed, suggests the importance of a range of TEAP. It is hypothesised that the reason Fe^{3+} reduction was only observed within HN incubations, was because of its greater relative concentrations of bioavailable Fe^{3+} phases (see Chapter 5, Section 5.3.4), pointing towards geological controls upon microbial diversity and metabolism (Mitchell et al., 2013). Since the sediments used within this investigation are from point sources, they cannot be used to define redox conditions under the entirety of their respective glaciers. Though denitrification was observed to be geographically widespread, occurring within samples from Svalbard, and from South Georgia and Livingstone Islands in the Maritime Antarctic.

4.5 Conclusion

This study quantified microbial carbon cycling processes within subglacial sediments. All of the sediments, taken from six glaciers and being of contrasting geology and nutrient status, were found to contain actively metabolising microbial ecosystems. Aerobic and anaerobic heterotrophic production was observed, as

was chemoautotrophic activity, implying the importance of multiple metabolic pathways. Conservative estimates of net respiration, bacterial production and chemoautotrophic activity suggested a system that was net heterotrophic under aerobic conditions. Under anaerobic conditions this appeared to shift towards net autotrophy, though the observed potential of denitrifying communities in these sediments suggests that net CO_2 production is possible where nitrate and a suitable electron donor are available. Though denitrification was determined to be the dominant electron accepting process within these sediments, active Fe^{3+} reducing populations were also observed within HN sediment.

Carbon availability was observed to be the primary control on bacterial production rates, with no differences noted based on glacier location. Lower rates or production within the channelised TB sediment could be explained through bedform morphology, but more likely related to the timing of TB sampling, as it was conducted early in the season when productivity is typically lower. The linkage between carbon and activity did not seem to be strictly linked to sedimentary organic carbon. Though catabolism was lower in sediments with lower organic carbon contents, it was the quality of available carbon, that appeared to limit anabolic processes. Indeed rates of bacterial production in the granitic MK sediment were in excess of rates in sediments with far greater organic carbon contents. Moreover, the rates of carbon turnover measured within these microcosms studies, could not have been sustained for extended time periods without renewal of the organic carbon pool, even in sediments with high sediment organic matter contents. This suggests the need for a source of organic carbon other than sediment derived organics to drive subglacial metabolisms. With chemoautotrophic rates of production being in excess of bacterial production, it may be that biomass produced through chemoautotrophy serves as an important, autochthonous source of bioavailable carbon to organotrophic subglacial microorganisms.

Anaerobic metabolism was only detectable with the addition of electron acceptors or donors, though the microbial communities in each sediment (VG, HN and AG) were shown to contain active denitrifiers. This supports the occurrence of *in situ* respiratory denitrification, whilst underlining the importance of electron donor availability as a control on this TEAP. Interestingly, the potential for anaerobic metabolism did not seem to be less within HN sediment, which was removed from channelised rather then distributed morphology. This suggested either an adaptable and/or facultative ecosystem, or perhaps highlighted the importance of small scale redox gradients in providing ecological niches for

anaerobic metabolisms. The methodology used to investigate TEAP in this study could have been improved through the use of a more sensitive method (such as the use of radio-labelled acetate) of assessing electron donor removal. Moreover, the assessment of H_2 concentrations has also been shown to separate TEAP within groundwater systems (Chapelle, 2001), and so its study within subglacial systems may provide a further methodology through which denitrification, and other TEAP can be assessed *in situ*. Culturing techniques could have also be used to further investigate the potential for different TEAP within subglacial communities here, and to isolate species active in under electron acceptor conditions. Time limitations prevented this angle of study during this project.

All sediments contained compounds thought to be microbial in origin, and there was some evidence to suggest that this fraction was more readily utilised for metabolism than fossilised organic matter. For this reason, it is suggested that sediment C/N is not a useful nutrient status indicator when SOC is high. Rather, selective methods, such as FTIR or chromatography (such as utilised in Lawson et al. (2015)), that allow the identification of lower molecular weight compounds, will provide better insight into the presence of bioavailable carbon. Whereas this study identifies the type of biomolecule present, chemical mapping techniques would provide substantially more information as to how certain compounds are utilised by sediment organisms. Moreover, with active chemoautotrophic communities within the Svalbard sediments, the importance of carbon fixation within subglacial communities should be further explored with respect to chemoautotrophy. The resources to do this were only available prior to sampling sediment at MK, HN and AG glaciers, and so rates of chemoautotrophic carbon fixation were not made for these samples.

These conclusions further our understanding of biological carbon cycling within the subglacial system, though they are presented with caveat. As with all current subglacial studies, sampling access was severely limited. As subglacial conditions are influenced by hydrology and the thermal state of the overlying glacier, it is difficult to suggest how representative these activity measurements are within the context of *in situ* heterogeneity. Moreover, though freezing and physical disturbance are commonplace to subglacial sediments, there is little understanding as to the impact of sampling, transport and ex situ experimentation upon the sediment community. Either novel *in situ* methods should be adopted for future investigation, or more should be done to constrain community shifts from bottle effects in laboratory incubations.

The research included in this Chapter only hints at the potential of the subglacial ecosystem. The identification of active eukaryotic cells (Chapter 3), as well as low values of bacterial growth efficiency, alludes to fungal activity within these sediments. Further to this point, no attempt has been made to integrate bacteriophage into this investigation, though they may reduce the transfer of nutrients and energy through lysis. Full complexity of *in situ* conditions were also not realised in laboratory microcosms, and though aerobic, anaerobic and chemoautotrophic metabolisms were recorded within these sediments, there is still uncertainty with respect to their relative importance across the glacier bed. Future work should seek to investigate the controlling influence of redox conditions, carbon and nutrient supply upon the full spectrum of microbial activity, in order to better integrate spatial factors within subglacial carbon cycling.

Chapter 5

Microbial Geochemistry Under Glaciers

5.1 Introduction

Since the identification of microbes within subglacial sediments (Sharp et al., 1999; Skidmore et al., 2000), attention has been turned to the interactions of these microbial communities with their environment. The inclusion of microbes in a system once considered devoid of life, though complicating subglacial outflow geochemistry, also provided a mechanism through which gaps in its interpretation could be addressed. Foremost amongst these gaps, related to the weathering of pyrite. Pyrite is a common metal sulphide mineral, whose importance in glacial hydrochemistry derives from the abundance of its weathering product, SO_4^{2-}, within glacial outflow (Tranter et al., 1996; Bottrell and Tranter, 2002; Tranter et al., 2002; Wadham et al., 2010a). In most natural systems, the oxidation of pyrite occurs through Equations 5.1.1 and 5.1.2, with dissolved O_2 or Fe $^{3+}$ acting as an electron acceptor. Previous studies had noted that SO_4^{2-} concentrations in glacial waters were in excess of that which could be supplied through pyrite oxidation by Equation 5.1.1, based upon the available concentrations of O_2 (Lamb et al., 1995; Irvine-Fynn and Hodson, 2010). Significant oxidation of pyrite by Equation 5.1.2 requires a mobile Fe^{3+} phase, and at the circumneutral pH values observed in glacial systems, the dissolution of Fe^{3+} is unlikely without microbial catalysis (Moses and Herman, 1991; Tranter et al., 2002; Ehrlich and Newman, 2009). Hence, microbes are thought to be active in

promoting pyrite dissolution under glaciers, by reoxidising ferrous iron to ferric iron (Equation 5.1.3) at the pyrite surface (Tranter et al., 2002).

$$FeS_2 + 3.5O_2 + H_2O \rightleftharpoons 2SO_4^{2-} + 2Fe^{2+} + 2H^+ \tag{5.1.1}$$

$$FeS_2 + Fe^{3+} + 8H_2O \rightleftharpoons 2SO_4^{2-} + 2Fe^{2+} + 16H^+ \tag{5.1.2}$$

$$Fe^{2+} + 0.25O_2 + H^+ \rightleftharpoons Fe^{3+} + 0.5H_2O \tag{5.1.3}$$

This observation led to several studies that tried to capture the signal of microbial sulphide oxidation by analysing the stable isotope composition of SO_4^{2-} within glacial outflow (Bottrell and Tranter, 2002; Wynn et al., 2006; Hodson et al., 2009; Wadham et al., 2010a). These were performed under the premise that isotopically distinct oxygen from either O_2 or H_2O would become incorporated into the resultant SO_4^{2-} molecule in different ratios, depending upon whether pyrite was oxidised by Equation 5.1.1 or 5.1.2, and that pyrite oxidised by Equation 5.1.2 was microbially mediated. In other circumneutral pH systems, however, it has been found that microbial pyrite oxidation occurred through the microbial reoxidation of ferrous iron to ferric iron at the pyrite mineral surface (Equation 5.1.3), a process that may utilise O_2, MnO_2 or NO_3^- as an electron acceptor (Singer and Stumm, 1970; Moses and Herman, 1991; Hall et al., 2012; Schippers and Jorgensen, 2001). Should this be the case within subglacial sediments, then the isotopic signature of oxygen in SO_4^{2-}, may suggest oxidation by Fe^{3+} when conditions are aerobic, or may be influenced by oxygen incorporation from NO_3^- or MnO_2, depending upon their role as an electron acceptor in Fe^{2+} reoxidation, or direct pyrite oxidation.

Laboratory incubations and community analysis have been used to investigate microbial mineral weathering processes in sediments from a handful of subglacial systems, and have provided direct evidence of microbially enhanced pyrite oxidation (Sharp et al., 1999; Montross et al., 2012; Boyd et al., 2014). Interactions between pyrite oxidation and the weathering of carbonates or silicates under glaciers, have been well defined by Tranter et al. (2002). These were compiled from a borehole survey of waters under the Haut Glacier D'Arolla, Switzerland, and, summarised by Equations 5.1.4 to 5.1.6, primarily relate to the hydrolysis of carbonate and silicate minerals by acid generated through Equations 5.1.1 and 5.1.2. It follows, therefore, that microbes are indirectly

involved in a range of other weathering processes aside from pyrite oxidation, though direct evidence of these linkages are not prominent in the literature, with the exception of Montross et al. (2012).

Equation 5.1.4: Pyrite oxidation by O_2 coupled to carbonate dissolution (Tranter et al., 2002):

$$\begin{aligned} &4FeS_2(s) + 16Ca_{1-x}(Mg_x)CO_3^-(s) + 15O_2(aq) + 14H_2O(l) \\ &\rightleftharpoons \\ &16(1-x)Ca^{2+}(aq) + 16xMg^{2+}(aq) + 16HCO_3^-(aq) + 8SO_4^{2-}(aq) + 4Fe(OH)_3(s) \end{aligned} \tag{5.1.4}$$

Equation 5.1.5: Pyrite oxidation by Fe^{3+} coupled to carbonate dissolution (Tranter et al., 2002):

$$\begin{aligned} &FeS_2(s) + 14Fe^{3+}(aq) + 8H_2O(l) + 16CaCO_3(s) \\ &\rightleftharpoons \\ &15Fe^{2+}(aq) + 16Ca^{2+}(aq) + 16HCO_3^-(aq) + 2SO_4^{2-}(aq) \end{aligned} \tag{5.1.5}$$

Equation 5.1.6: Pyrite oxidation by oxygen coupled to feldspar dissolution (Tranter et al., 2002):

$$\begin{aligned} &4FeS_2(s) + 16Na_{1-x}K_xAlSi_3O_8(s) + 15O_2(aq) + 86H_2O(l) \\ &\rightleftharpoons \\ &16(1-x)Na^+(aq) + 16xK^+(aq) + 8SO_4^{2-}(aq) + 4Al_4Si_4O_{10}(OH)_8(s) \\ &\qquad + 32H_4SiO_4(aq) + 4Fe(OH)_3(s) \end{aligned} \tag{5.1.6}$$

A fuller understanding of the geochemical processes in which subglacial microbes are involved, will lead to a better interpretation of outflow hydrogeochemistry, and hence glacial hydrology. Moreover, metal sulphides appear to be a major energy source for chemolithotrophic organisms in subglacial environments, yet

there is no real understanding of how this occurs. Investigating the pyrite oxidation mechanism will increase our knowledge of this microbial process that is so dominant a feature in outflow geochemistry, and increase our understanding of microbial adaptation and survival in subglacial systems. Also implicit in the oxidation of pyrite is the generation of reactive iron phases (Raiswell and Canfield, 2012). With a substantial research initiative investigating the transfer of potentially bioavailable iron from glaciers to marine systems (Raiswell et al., 2010; Hawkings et al., 2014; Raiswell et al., 2008b), exploring how microbial processes within sediments affects this, may suggest important linkages between subglacial and marine ecosystems.

The majority of subglacial biogeochemical studies make use of field surveys, which, whilst providing insight into *in situ* processes, rely on inference to separate microbial processes from bulk geochemistry. This is a problem in subglacial environments as glacial comminution creates a highly reactive sediment which, when mixed with water, is subject to a variety of abiotic chemical weathering processes, potentially masking microbial processes (Tranter et al., 2002). This study will utilise batch microcosm which incorporate both live and sterilised experiments to address the 3rd Objective of this Thesis: to directly explore microbial mineral weathering processes, in a range of subglacial sediments. The following Chapter details the methods, results and interpretation of these batch microcosm experiments, exploring the separation of biotic and abiotic processes within the sediments, and so investigating the role of subglacial microbes in sulphur, carbonate, silicate and iron biogeochemistry.

5.2 Methodology

This Section describes the methodology used to assess the microbial contribution to mineral weathering process. The sediments included in this study were sampled from: Vestre Grønfjordbreen (VG), Tellbreen (TB) and Hørbyebreen (HB), Svalbard; Mittivakkat Gletscher (MK), Southeast Greenland; Argentina Glacier (AG), Livingstone Island, Antarctica; and Heaney Glacier (HN), South Georgia, Antarctica.

5.2.1 Initial Characterisation of the Sediment

To better understand outcomes of the laboratory experiments performed using the sediments, a number of analyses were conducted upon them to characterise

their geology and organic carbon content.

5.2.1.1 Mineral Composition

The major element composition of each sediment was examined using X-Ray Fluorescence (XRF). To do this, portions of each sediment were air-dried and powdered before being analysed using an Olympus Delta DS2000 handheld XRF device. Samples were analysed in soil mode for 180 seconds at 50 kV, 30 kV and then 10 kV. Analysis was performed for Si, Al, S, Cl, K, Ca, Ti, V, Cr, Mn, Fe, Co, Ni, Cu, Zn, As, Se, Rb, Sr, Y, Zr, Nb, Mo, Ag, Cd, Sn, Sb, Ba, La, Ce, Pr, Nd, Hf, Hg, Pb, Bi, Th and U.

The calcium carbonate-equivalent content of each sediment was measured using a Bascomb Calcimeter. For this method the CO_2 gas evolved following the mixing of dried, powder-ground sediment with 3 M HCl, was captured in a burette where its volume was determined. Coeval measurements of barometric pressure, and temperature were used to calculate the mass of this CO_2 using the ideal gas law. The CO_2 released during acidification of each sample is taken to be produced by the hydrolysis of any calcium carbonate present (Avery and Bascomb, 1974), and as such, was used to calculate calcium carbonate concentration.

5.2.1.2 Particle Size Analysis

Particle size distribution was performed by dry sieving. Five randomly selected aliquots of each sediment were dried at 80°C after which the dry sediment was passed though ultrasound-cleaned 600 µm and 63 µm sieves. The resultant three size fractions of sediment were weighed on a Ohaus AS660D microbalance.

5.2.2 Measuring the Microbial Contribution to Weathering Processes

5.2.2.1 Batch mineral weathering microcosm experiments

The microbial contribution to solute concentrations as a result of mineral weathering was assessed using batch microcosms. Sterile centrifuge tubes (50 mL) were used as incubation vessels, enabling approximately 2 g (wet mass) of freshly defrosted sediment to be incubated in 45 mL, low nutrient media. Media was 0.2 μm, filter-sterilised, and consisted of 5 μM ammonium nitrate, 100 μm sodium carbonate and 1 μm potassium dihydrogen orthophosphate. Each incubation

vessel was capped and shaken to homogenise the sediment and media prior to incubation. Each microcosm was then placed into cooled incubators (Panasonic, MIR-254-PE), where dark, 4^{o}C conditions were maintained for the duration of the experiment. Anaerobic end member incubations were set up in the same manner as aerobic incubations, but were sealed inside autoclaved glass, crimp-top 60mL vials, after being sparged with N_2 gas for 3 minutes to remove oxygen. Caps for both types of incubation vessel were gas tight, to prevent evaporation of incubation media over the long incubation periods.

Nine "live" replicates and three sterile controls were incubated per sediment origin. Two controls were prepared using dry heat (150^{o}C for 72 hours) with the third being fixed, through the addition of 2% (v/v) (final concentration) formaldehyde (Fischer Scientific) to its incubation media, which was then buffered to a pH of 7 using analytical grade sodium hydroxide (Fischer Scientific). These methods of sterilisation were chosen based upon the work of Trevors (1996), which determined that dry heat methods did the least damage to sediment structure, and artificially enhancing weathering. Using an additional chemical sterilisation method provided some quality control when later interpreting the data from sterilised microcosms, whilst also being more reliable over the long incubation periods (Trevors, 1996). Sterilisation was verified by mixing aliquots of sterilised sediment with UHQ deionised water, agitating and then centrifuging them, at 4000 rpm for 10 minutes. A serial dilution of the supernatant was spread onto yeast extract agar and left to grow at room temperature with colony forming units being counted after two weeks of incubation. Sediment was resterilised if colony forming units exceeded 10 per 100 mL.

Aliquots of supernatant were removed for analysis at 5, 10, 20, 30, 50, 100 and 300 day intervals in the case of VG and HB sediment; 5, 10, 30, 40, 75, 105 and 210 day intervals in the case of MK and AG sediment; and 5, 10, 50, 100 and 300 day intervals in the case of TB and HN sediment. Microcosms were sampled using sterile, gas tight syringes and under N_2 atmosphere in the case of anaerobic incubations. The supernatant was filtered through a 0.2 μm, nylon filter membrane (Whatman), and analysed for SO_4^{2-}, NO_3^-, Cl^-, Mg^{2+}, Ca^{2+}, Na^+, K^+ and NH_4^+ ions using a Dionex ICS1500 ion chromatography system. Chromatography standards were prepared on the day of analysis from IonPac® 5-Anion and 6-Cation standard concentrates (Thermo Scientific). HCO_3^- concentrations were estimated for each incubation using the ionic charge balance of the supernatant. Dissolved O_2 and pH were measured initially, and at the end of the incubation period. This was done using a calibrated, ELE Interna-

tional, Clark electrode-type dissolved oxygen sensor, and a calibrated Jenway 3505 pH meter. Ion concentrations were normalised against the dry mass of sediment within their respective incubation vessel, and values reported in μeq g^{-1}. Normalising by mass factors out variance associated with sediment density, and allowed a better comparison of sediment processes between the different samples analysed relative to volume normalised concentrations. Saturation indexes, based upon supernatant ion concentrations, were calculated for calcite using PHREEQC (Version 2.18) geochemical modelling software. Precision errors for all analytical methods were less than 5%.

Initial ion concentrations within the supernatant of batch microcosms, were largely present as a result of *in situ* weathering processes prior to incubation. Associations between initial concentrations, however, were likely to have been altered by freeze concentration, and evaporite precipitation during -20°C storage conditions. Cl^- ions were also present within all analysed microcosms, suggesting that a portion of initial ion concentrations were a result of marine aerosols. Of note, initial [Cl^-] was two orders of magnitude greater within AG supernatant, relative to other sediments, and continued to increase in contrast to the other sediments' values. This suggested that AG sample was comprised of overridden marine sediments, or received a significantly greater influx of Cl^- from snowpack elution.

To mitigate these factors, and to reduce complexity within the batch incubation data, initial ion concentrations, inclusive of marine aerosol contribution, were accounted for within each ion's time series. This was done by subtracting the linear intercept of ion concentration over the first three sampling intervals, from all corresponding ionic concentrations. Corrected data were reported with the notation: $*X$ (where "X" is the ionic species), a commonly used nomenclature for reporting crustal-derived ions within glacial hydrochemistry (Wadham et al., 2010b,a; Nowak and Hodson, 2013).

To enable comparisons of pyrite oxidation rates within the wider literature, SO_4^{2-} production rates were converted to pyrite oxidation rates using Equation 5.2.1 (Balci et al., 2007).

$$R_{Pyrite} = \frac{\int SO_4}{m \times p \times 0.147} \tag{5.2.1}$$

Where R_{Pyrite} was the rate of pyrite oxidation in (mol m^{-2} s^{-1}); $\int SO_4$ was the integral of SO_4^{2-} concentration (mol) across the incubation time period (in seconds); "m" was the mass of sediment incubated, "p" was the fraction of pyrite

within each sediment, estimated from the mean elemental sulphur concentration of each sediment (Table 5.1); and 0.147 is a factor based upon the mass-area relationship of pyrite calculated in Gleisner et al. (2006).

5.2.2.2 Microbial Weathering of Iron

Subglacial iron weathering was investigated in sediments from VG, AG, MK and HN glaciers. As with the mineral weathering experiments described in Section 5.2.2.1, this was done using batch microcosms, and under aerobic conditions. Iron produced as a weathering product in aerobic, circumneutral pH conditions, would precipitate as an oxide, hydroxide or oxyhydroxide (Ehrlich and Newman, 2009). For this reason, changes in solid phase iron were tracked over the course of the aerobic experiment. Use of the ascorbic acid method (Kostka and Luther, 1994; Raiswell et al., 2010) to extract ferrihydrite that was present as secondary weathering products, was adopted in this study. This allowed the results of these batch experiments to be compared with the majority of studies that investigate iron export by glaciers (see Section 1.3.5.2).

Batch incubations were set up as described in Section 5.2.2.1, with analysis performed at sampling intervals of 5, 10, 20, 50 and 80 days of incubation. Five live microcosms, and two sterilized microcosms per sediment, were terminated for analysis at each interval. For analysis, the incubation medium was removed and filtered through a 0.45 μm cellulose nitrate filter membrane (Whatman). The filter membrane was placed, with the sediment, in the 50 mL incubation vessel, to which 25 mL of pH 7.5, ascorbic acid solution (0.17 M sodium citrate, 0.6 M sodium bicarbonate, 0.057 M ascorbic acid) was added. The incubation vessels were placed on a rotary shaker for 24 hours before a 25 mL aliquot was extracted, 0.45 μm filtered through cellulose nitrate membranes, and analysed for total iron using the Ferrozine^{TM} (Sigma Aldrich) assay (Viollier et al., 2000). Analysis was conducted using a Shimadzu UV-1800 UV-VIS Spectrometer, with calibrations performed immediately prior and subsequent to analysis. Dilutions were performed using UHQ deionised water where concentrations exceeded the upper limits of detection for the Ferrozine method. A 1.5 mL aliquot of media was additionally reserved at each sample interval, 0.45 μm filtered through a cellulose nitrate membrane (Whatman), and analysed for sulphate using ion chromatography (Dionex ICS1500). Control analyses were performed, testing for iron contamination within the incubations vessels, filter membranes and ascorbic acid solution. Precision error for the Ferrozine assay was less than 5%.

5.3 Results

5.3.1 Sediment Characteristics

Physical and major elemental characteristics of each sediment are displayed in Table 5.1. Calcium carbonate was present within all sediments, though comparing its concentration to that of elemental calcium (derived from XRF data), suggested the presence of Ca-silicates within TB, HN and MK sediments also. Sulphur was an order of magnitude higher within HN, VG and TB sediments, relative to MK, AG and HB. Iron concentrations were similar within all sediments. Sieving indicated that TB and AG samples predominantly fell within the silt classification. MK and HN samples mostly medium to very fine sands, whereas HB and VG were comprised of very coarse to very fine sands.

Table 5.1: A summary of major elements, calculated from XRF analysis, $CaCO_3$, calculated by calcimitry, and size composition of subglacial sediments used within batch incubations. Mean values are percentages by mass.

	Sediments											
	MK		AG		HN		HB		TB		VG	
Element	*wt%*											
	μ	σ	μ	σ	μ	σ	μ	σ	μ	σ	μ	σ
Si	12	*0.2*	12	*0.2*	13	*0.2*	11	*0.2*	8.0	*0.2*	12	*0.2*
Fe	3.2	*0.01*	3.7	*0.02*	3.0	*0.01*	3.1	*0.01*	4.3	*0.02*	1.4	*0.006*
Al	24	*0.4*	2.4	*0.5*	28	*0.5*	4.4	*0.5*	2.6	*0.5*	1.6	*0.4*
Mn	0.049	$7E^{-4}$	0.080	$1E^{-4}$	0.061	$7E^{-4}$	0.054	$7E^{-4}$	0.036	$6E^{-4}$	0.072	$8E^{-4}$
S	0.062	*0.02*	0.060	*0.02*	0.36	*0.02*	0.065	*0.02*	0.13	*0.02*	0.14	*0.02*
K	1.0	*0.01*	2.5	*0.02*	1.8	*0.02*	1.7	*0.02*	2.3	*0.02*	1.1	*0.01*
Ca	0.4	*0.02*	1.35	*0.01*	0.87	*0.009*	2.9	*0.02*	0.44	*0.005*	6.8	*0.04*
$CaCO_3$	0.09	*0.01*	1.58	*0.7*	0.36	*0.07*	3.94	*0.5*	0.21	*0.5*	14	*0.6*
Size Fraction							*wt%*					
$>600\mu m$	41	*9*	28	*13*	19	*3*	37	*14*	9	*4*	43	*12*
600-$63\mu m$	56	*10*	35	*3*	77	*4*	34	*9*	29	*23*	43	*9*
$<63\mu m$	4	*2*	37	*10*	4	*1*	29	*13*	62	*21*	14	*3*

σ = one standard deviation

5.3.2 Microbial Mineral Weathering in Batch Microcosms

Figures 5.3.1, 5.3.2 and 5.3.3 show the respective temporal evolutions of $*K^+$, $*Ca^{2+} + *Mg^{2+}$ and $*SO_4^{2-}$ within aerobic batch incubations, giving insight

into the weathering dynamics of silicates, carbonates and pyrite within each sediment. Literature that considers the biogeochemistry of glacial outflow typically considers both Na^+ and K^+ cations as proxy to silicate weathering processes (Tranter et al., 2002; Wadham et al., 2010a,b). With high Na^+ intercepts, and high error between replicate $*Na^+$ values, evaporite dissolution was determined to be driving Na^+ dynamics within some incubations, obscuring trends set by silicate weathering in these sediments. Intercept values of K^+ were small relative to those of Na^+, and, except for AG incubations, were two orders of magnitude less than Cl^-:K^+ values for seawater (Ehrlich and Newman, 2009). This suggests a crustal origin to initial $K^+_{(aq)}$, with the principal source being from the hydrolysis of K-feldspar and mica (Tranter et al., 2002). For this reason, only $*K^+$ was employed as a measure of silicate weathering.

Temporal changes in $[*K^+]$, Figure 5.3.1, were lower than increases of carbonate or metal sulphide-derived ions, with final $[*K^+]$:$[*Ca^{2+} + *Mg^{2+}]$ ranging from 1:11 in MK incubations, to 1:593 in HN incubations, and final $[*K^+]$:$[*SO_4^{2-}]$ ranging from 1:0.9 in AG incubations, to 1:419 in HN incubations. AG sediments saw the largest increase, though the slope of association between $[*K^+]$ and $[Cl^-]$ measurements, suggested that approximately 10% of this increase related to further sea salt inputs within the first 10 days of incubation. No significant differences between live or sterilised silicate weathering rates were observed for any sediment. Error was low, however, with the average coefficients of variation being 26.3% between live replicates, and 9.9% between sterile replicates.

Temporal increases in $*Ca^{2+}$+$*Mg^{2+}$ concentration are shown in Fig. 5.3.2. Values of $[*Ca^{2+} + *Mg^{2+}]$ within HN and AG supernatant, were almost entirely derived from calcium carbonate, with $*Mg^{2+}$ concentrations close to detection limit for these incubations. Mg^{2+} within HB incubations evolved more slowly than Ca^{2+} ions, with concentrations that were below detection up until *c.* 100 days of incubation, suggesting that it was derived from silicate rather than carbonate weathering. Strong initial (first 20 days of incubation) associations between $*Ca^{2+}$ and $*Mg^{2+}$ within VG ($R^2 = 0.94$), TB ($R^2 = 0.75$) and MK ($R^2 = 0.93$) sediments, suggested that Mg^{2+} and Ca^{2+} were predominantly derived from the same carbonate source, and were consistent with observations of dolomite close to VG and TB glaciers (Semevskij and Škatov, 1965) and supracrustal marble near the margin of MK (Escher, 1990).

For VG, HB, TB and HN sediments, carbonate weathering rates were initially highest, reaching a plateau after *c.* 100 days of incubation. Svalbard

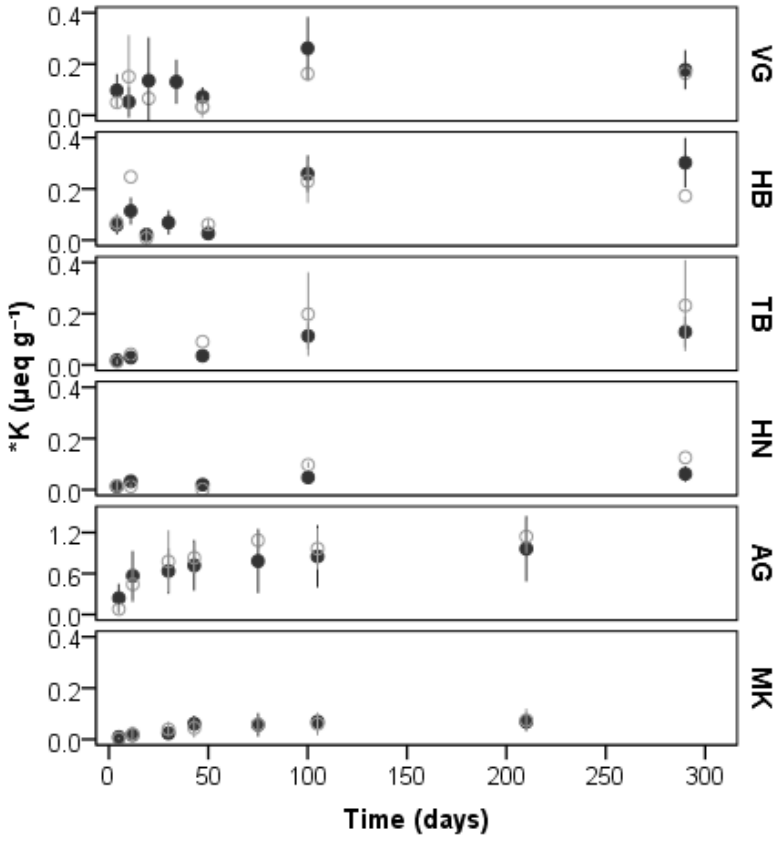

Figure 5.3.1: Temporal evolution of dissolved $^*K^+$ ions within the supernatant of aerobic microcosms containing subglacial sediments (dark grey, solid markers), and corresponding sediments that had undergone sterilisation (light grey, hollow markers). Markers represent mean values, $n = 9$ for live sediments, and $n = 3$ for sterilised sediment. Error bars show one standard deviation. Sediments incubated were VG, HB, TB, HN, AG and MK. Note different scales on y-axes.

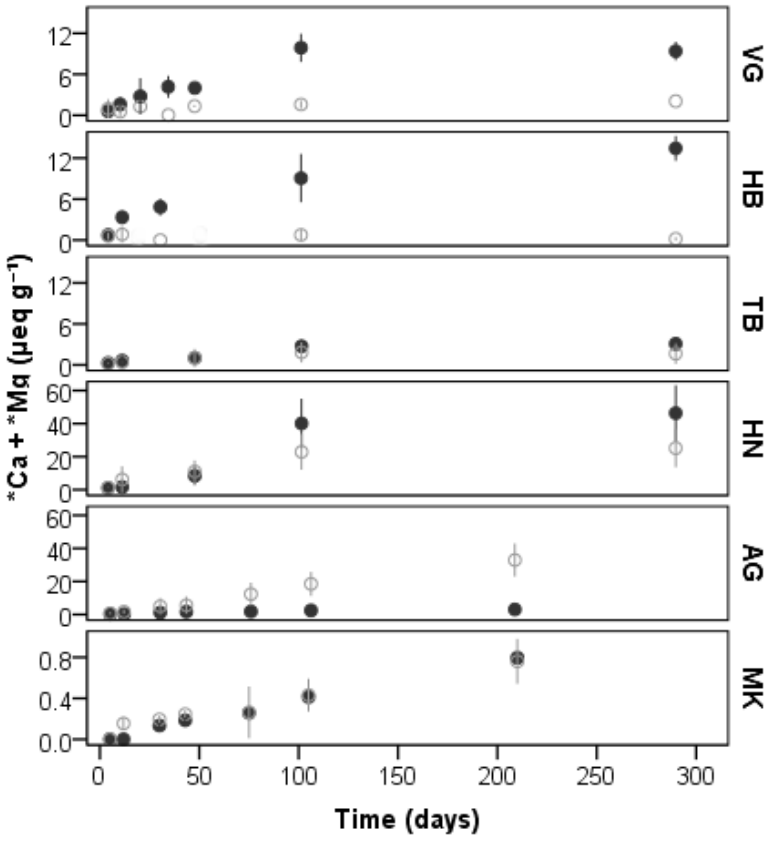

Figure 5.3.2: Temporal evolution of dissolved $*Ca^{2+}$ and $*Mg^{2+}$ ions within the supernatant of aerobic microcosms containing subglacial sediments (dark grey, solid markers), and corresponding sediments that had undergone sterilisation (light grey, hollow markers). Markers represent mean values, $n = 9$ for live sediments, and $n = 3$ for sterilised sediment. Error bars show one standard deviation. Sediments incubated were VG, HB, TB, HN, AG and MK. Note different scales on y-axes.

Table 5.2: Saturation with respect to calcite, based upon final average supernatant conditions in aerobic batch incubations.

Sediments	$SI_{CALCITE}$
VG	-2.08
HB	-2.62
TB	-4.51
HN	-3.81
AG	-2.22
MK	-6.48

sediments reached similar concentrations, with VG and HB incubations plateauing at *c.* 10 μeq g^{-1}, and TB at *c.* 3 μeq g^{-1}, HN sediment, despite having the third lowest $CaCO_3$ concentration, reached the highest concentration, plateauing at *c.* 40 μeq g^{-1}. AG and MK sediments saw lower, linear increases in [$*Ca^{2+}$+$*Mg^{2+}$], with no indication of plateau by 210 days of incubation. Incubations remained undersaturated with respect to calcite throughout the experiment (Table 5.2), suggesting that the slow down in weathering observed for VG, HB, TB and HN sediments probably related to the formation of a weathering crust (Dobrovolsky, 1987). Error was generally higher than for SO_4^{2-} or K^+, with average coefficients of variation being 37.1% between live replicates, and 24% between sterile replicates.

Total $*Ca^{2+}$+ $*Mg^{2+}$ concentration changes were significantly greater within live VG, HB, HN (all $p < 0.01$) and TB ($p < 0.05$) incubations, compared to changes in sterilised incubations, with concentrations upon termination being 7.4×, 4.5×, 5.0× and 2.0× greater than sterile incubations respectively. MK live and sterile incubations saw similar $*Ca^{2+}$+ $*Mg^{2+}$ evolution over time, and both variables had similar average concentrations after 210 days of incubation. AG sterilised sediment saw a significantly ($p < 0.01$) greater magnitude change compared to its unsterilised counterparts. This occurred within all replicate sterilised controls, albeit to a greater extent within dry heat-sterilised samples, suggesting significant carbonate precipitation within AG sediment upon sterilisation.

The evolution of SO_4^{2-} within live and sterile batch incubations is shown in Figure 5.3.3. Within live incubations, concentration increases of SO_4^{2-} were similar, but typically of lesser magnitude, than those of $*Ca^{2+}$+ $*Mg^{2+}$ (Fig. 5.3.2). SO_4^{2-} changes within sterile incubations were significantly lower ($p <$

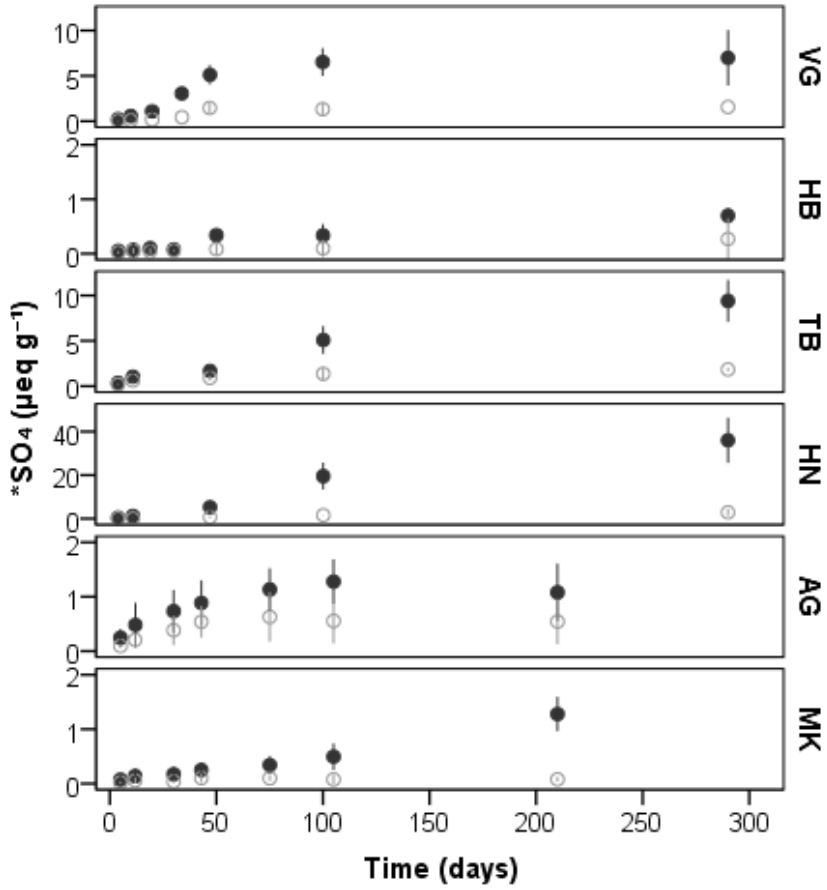

Figure 5.3.3: Temporal evolution of dissolved $*SO_4^{2-}$ ions within the supernatant of aerobic microcosms containing subglacial sediments (dark grey, solid markers), and corresponding sediments that had undergone sterilisation (light grey, hollow markers). Markers represent mean values, $n = 9$ for live sediments, and $n = 3$ for sterilised sediment. Error bars show one standard deviation. Sediments incubated were VG, HB, TB, HN, AG and MK. Note different scales on y-axes.

0.01, except for HB incubations, where $p = 0.02$) relative to live sediments, though increases were observed in all cases. Error between live replicates was low, with average coefficients of variation being 17.1%. Good agreement between the different sterile controls, with a coefficient of variation of 7.7% between methods, indicated that the sterilisation methods did not artificially alter weathering, and that the observed differences between live and sterile sediments were due to biological processes (Trevors, 1996). Regression models comparing mean $[SO_4^{2-}]$ at each time interval, revealed strong, linear relationships between live and sterile sulphate production within all sediments except TB. This allowed the slope of each regression model to be used as a measure of the relative contributions of abiotic and biotic sulphide oxidation processes over the course of the incubation period. Biotic processes contributed 48% ($R^2 = 0.9$) of SO_4^{2-} in AG; 66% ($R^2 = 0.9$) of SO_4^{2-} in HB; 68% ($R^2 = 0.8$) of SO_4^{2-} in MK, 78% ($R^2 = 0.8$) of SO_4^{2-} in VG and 93% ($R^2 = 0.9$) of SO_4^{2-} in HN incubations. Within TB sediment, biotic processes accounted for 46% of total SO_4^{2-} in solution over the first 47 days of incubation, after which this increased to 88%.

Rates of pyrite oxidation, converted from SO_4^{2-} production rates (using Equation 5.2.1), are listed in Table 5.3. It is probable that the rates reported here underestimate actual rates, as the comminuted glacial sediments incubated here would likely have a greater surface area to volume ratios than the pyrite grains upon which the empirical mass-area relationship (Gleisner et al., 2006) (used in Equation 5.2.1) was derived. Uncertainty in the pyrite surface area was reflected by a relatively high error, with the average coefficient of variation between live replicates being 66%, and being 75% between sterile replicates. Despite this limitation, differences between live and sterile sediments were sufficient to allow a stochastic comparison of rates. Pyrite oxidation rates within live, aerobic incubations were typically lower than those within live, anaerobic sediments, though not significantly, with both typically occurring at *c.* 10^{-10} (mol m^{-2} s^{-1}). Abiotic, aerobic rates were higher than abiotic rates in anaerobic incubations, but lower than live aerobic rates (*c.* 2× lower within AG, HB, TB and VG incubations, and 7× and 12× lower within live MK and HN incubations respectively). Abiotic rates of oxidation in anaerobic incubations, *c.* 10^{-11} (mol m^{-2} s^{-1}), were an order of magnitude lower than all live rates, and most sterile aerobic rates.

The concentration change in ascorbic acid-extractable iron, using a method developed to be highly selective for ferrihydrite (Raiswell et al., 2010), is shown over its 80 day incubation period in Figure 5.3.4. Ferrihydrite increased within

Table 5.3: Pyrite Oxidation Rates within aerobic and anaerobic incubations of subglacial sediment.

		Pyrite Oxidation Rate $\times 10^{-10}$ (mol m^{-2} s^{-1})			
		Live		Sterile	
Sediment		μ	σ	μ	σ
VG	Aerobic	7.7	*3.8*	2.2	*1.3*
	Anaerobic	8.8	*5.4*	0.1	*0.05*
HB	Aerobic	1.8	*1.9*	0.8	*0.9*
	Anaerobic	3.6	*2.4*	0.1	*0.2*
TB	Aerobic	6.8	*4.3*	3.8	*2.7*
	Anaerobic	9.3	*5.4*	0.7	0.6
HN	Aerobic	5.5	*5.6*	0.4	*0.3*
	Anaerobic	8.1	*2.3*	0.1	*0.3*
AG	Aerobic	8.2	*4.7*	4.8	*2.3*
	Anaerobic	8.4	*6.3*	0.6	*0.5*
MK	Aerobic	1.7	*1.3*	0.3	*0.2*
	Anaerobic	3.5	*2.8*	0.2	*0.2*

each sediment during aerobic incubations, though no significant differences were observed between live and sterilised sediments by 80 days. Large differences between sediment were evident, however, with concentrations in HN sediment reaching 84.7 ($\pm$ 10) μm g^{-1}, compared to concentrations of 24.8 ($\pm$ 2.2), 23.9 ($\pm$ 3.1) and 19.1 ($\pm$ 2.6) μm g^{-1} for VG, AG and MK respectively. Error between replicates was good, with coefficient of variation averaging at 15.9% for live incubations, and 10.5% for sterile incubations.

5.4 Discussion

The experiments detailed in this Chapter, sought to address this thesis' 3rd Objective: to investigate the influence of microbes upon mineral weathering processes in subglacial sediments. Live and sterile microcosms were used to separate biotic and abiotic weathering processes within a range of subglacial sediments with contrasting geologies. Microbes were found to significantly en-

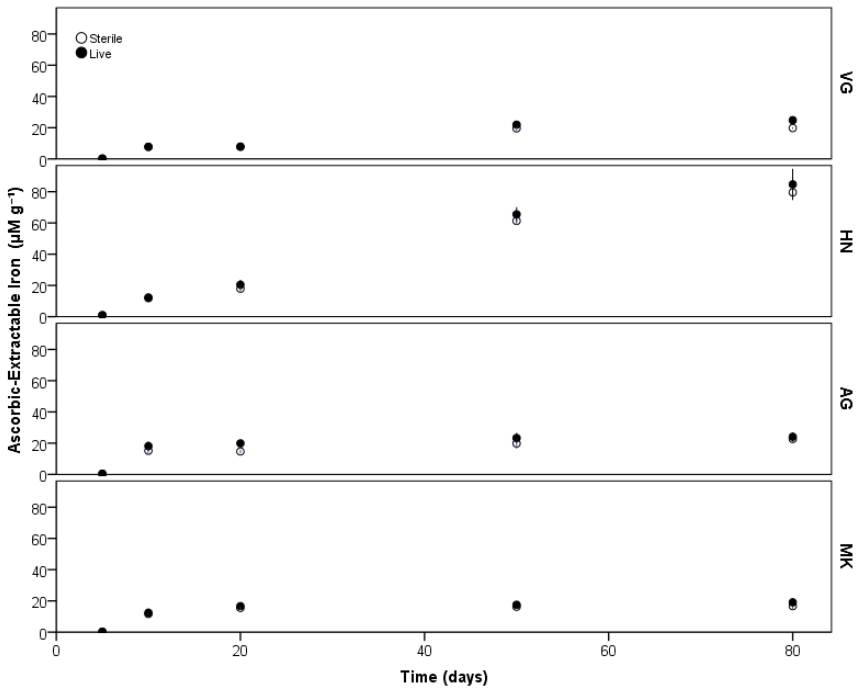

Figure 5.3.4: Temporal evolution of ascorbic acid-extractable iron within VG, HN, AG and MK sediments. Aerobic microcosms containing live sediments (black, solid markers), and corresponding sediments that had undergone sterilisation (black, hollow markers). Markers represent mean values, $n = 5$ for live sediments, and $n = 2$ for sterilised sediment. Error bars show one standard deviation.

hance pyrite weathering within all the sediments analysed, whilst carbonate weathering was also seen to be enhanced. The linkages between these processes, and the likely mechanism through which pyrite oxidation was occurring were explored.

Microbial enhancement of pyrite weathering was observed within all sediments. Enhanced carbonate weathering was also noted in all sediments, with the exception of AG and MK, whereas evidence for microbially enhanced silicate weathering was only observed in VG sediment. Similar to results from batch incubations by Montross et al. (2012), solute yields were dominated by Ca^{2+} and SO_4^{2-} ions. These ions also typically dominate the chemistry of glacial outflow, though were present here in smaller concentrations than observed by

the field analyses in Tranter et al. (2002); Wadham et al. (2010a) or Nowak and Hodson (2013). It was considered, therefore, that these microcosm experiments provided a fair, scaled down representation of *in situ* processes.

Coupling of Weathering Processes

With microbially enhanced weathering noted within batch incubations, correlation matrices were used to explore the associations between major ions, and hence weathering processes within the subglacial sediments. Figures 5.4.1 and 5.4.2, and the accompanying correlation matrices within the Appendix (Table 7.2), show the respective associations between ions in live and sterile sediment incubations. These show significant relationships (at the 99% confidence interval) between $*Ca^{2+}$ and $*SO_4^{2-}$ within all live sediments except HB ($R^2 = 0.2$). Within sterilised sediments, however, covariation between $*Ca^{2+}$ and $*SO_4^{2-}$ at the 99% confidence level was only observed within VG and HN incubations. Indicating that for most sediments, abiotic levels of sulphide oxidation did not influence carbonate weathering over the *c.* 300 day incubation period. The relationship between pyrite oxidation and carbonate dissolution in live sediments was explored further by examining $*Ca^{2+}$ and $*SO_4^{2-}$ associations between replicates at different time intervals. This allowed the timing of co-evolution to be considered, and suggested that coupling between weathering processes, as indicated by significant ($p < 0.01$) covariation between the $*Ca^{2+}$ and $*SO_4^{2-}$ concentrations of replicates, were not observed until *c.* 100 days within VG and HN incubations, *c.* 50 days within TB and AG incubations, and *c.* 210 days within MK incubations.

In analysis of glacial waters, Tranter et al. (2002) and Wadham et al. (2010a) both note high intercept concentrations with respect to Ca^{2+}+Mg^{2+}, in plots of Ca^{2+}+Mg^{2+} against SO_4^{2-}, attributing this intercept value to carbonate hydrolysis or carbonation in the early stages of weathering. Since all incubations remained undersaturated with respect to calcite (Table 5.4), hydrolysis of carbonates (Equation 5.4.1) would have been kinetically favourable throughout the incubation period (Wigley and Plummer, 1976). The initial weathering period observed in most live incubations, prior to covariation between $*Ca^{2+}$ and $*SO_4^{2-}$, was, therefore, most likely dominated by carbonate hydrolysis or carbonation, with proton activity from sulphide oxidation still too low to influence bulk carbonate chemistry. This supports the interpretation of Tranter

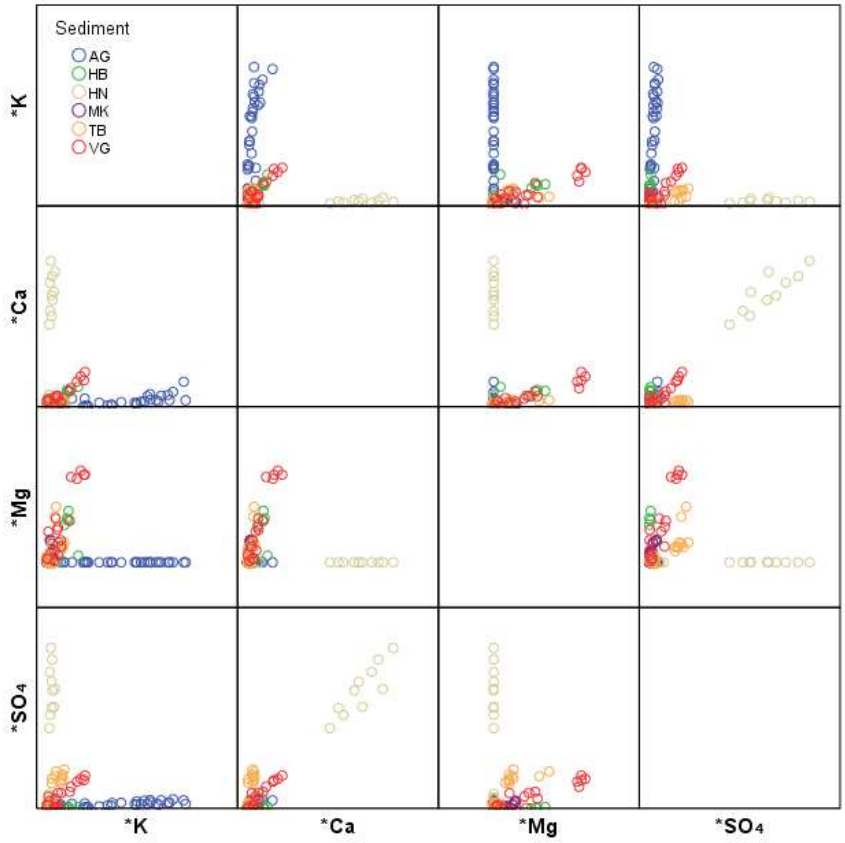

Figure 5.4.1: Live sediment correlation matrix, showing the relative associations of $*Ca^{2+}$,$*Mg^{2+}$, $*SO_4^{2-}$ and $*K^+$ over the course of the incubation experiment. Accompanying table showing Pearson rank correlation coefficients is in the Appendix: Table 7.2. Units are μeq g^{-1}.

et al. (2002) and Wadham et al. (2010a), and suggests that microbial processes may be required to supply sufficient SO_4^{2-} to drive carbonate weathering beyond its initial hydrolysis phase, since covariation of $*Ca^{2+}$ and $*SO_4^{2-}$ did not occur within most sterilised incubations.

$$CaCO_3(s) + 2H_2O(l) \rightleftharpoons Ca^{2+} + HCO_3^- + OH^- \tag{5.4.1}$$

Association between $*K^+$ and $*SO_4^{2-}$ are also shown in Figures 5.4.1. Though significant covariation in the temporal evolution of $*K^+$ and $*SO_4^{2-}$ ions was observed within most incubations, correlation between replicates at different time intervals was not, except in the case of VG sediment. As with replicate associations of $*Ca^{2+}$ and $*SO_4^{2-}$, covariation between $*K^+$ and $*SO_4^{2-}$ in VG sediment did not occur until *c.* 100 days of incubation. Low associations between sulphide oxidation and silicate weathering have also been noted in glacial outflow analyses (Tranter et al., 2002; Wadham et al., 2010a; Skidmore et al., 2010). Where, if water residence time is relatively short, and hence waters are not saturated with respect to carbonate, then coupled pyrite and carbonate weathering is kinetically more favourable than coupled pyrite and silicate weathering (Laybourn-Parry and Hodson, 2012). Though carbonate weathering rates here, were observed to slow down within some incubations, calcite saturation had not yet been reached, and so ion yields within all incubations except AG, which saw very low Ca^{2+} inputs, were dominated by cations from carbonate dissolution, rather than silicate weathering.

To further investigate coupling between sulphide oxidation and carbonate dissolution, the stoichiometry of observed carbonate and pyrite weathering products was considered. Implied by Equations 5.1.4 and 5.1.6, total coupling of pyrite oxidation by O_2, and carbonate or silicate dissolution, should produce equivalent stoichiometries of 2:1 between $*Ca^{2+} + *Mg^{2+}$ and $*SO_4^{2-}$, and 1:1 between $*K^+$ and $*SO_4^{2-}$. Whereas, coupling to abiotic pyrite oxidation by Fe^{3+}, or indirect microbial pyrite oxidation, would produce a $*Ca^{2+} + *Mg^{2+}$:$*SO_4^{2-}$ of 8:1, and a $*K^+$:$*SO_4^{2-}$ of 4:1, according to the stoichiometry of Equation 5.1.5 (Tranter et al., 2002).

Since the hydrolysis reaction shown in Equation 5.4.1 doesn't require a proton source, rates of hydrolysis should be the same between live and sterile sediments, if one assumes that the saturation of Ca^{2+} containing minerals was the same. Average concentrations of $*Ca^{2+} + *Mg^{2+}$ or $*SO_4^{2-}$ within sterile incubations were, therefore, subtracted from concentrations in live incubations, so

that biotic weathering processes could be considered in isolation. Associations in biotic [$*Ca^{2+}{}_{bio}$ + $*Mg^{2+}{}_{bio}$] versus [$*SO_4^{2-}{}_{bio}$] are shown in Figure 5.4.3, with the stoichiometry and correlation coefficients of these relationships listed in Table 5.4. For AG sediments, since Ca^{2+} was so much higher within its sterile incubations, the relationship shown in Figure 5.4.3 and Table 5.4, relates to uncorrected live sediments.

Shown in Table 5.4, VG and HN sediments were the only incubations in which significant covariation between $*Ca^{2+}{}_{bio}$ + $*Mg^{2+}{}_{bio}$ and $*SO_4^{2-}{}_{bio}$ was observed. The stoichiometry of $*Ca^{2+}{}_{bio}$ + $*Mg^{2+}{}_{bio}$:$*SO_4^{2-}{}_{bio}$ within these incubations, however, were lower than those defined by Equations 5.1.4 or 5.1.5, indicating that coupling between processes could have been as low as 10%, assuming pyrite oxidation through Fe^{3+}. Tranter et al. (2002); Wadham et al. (2010a) and Nowak and Hodson (2013) all observed $*Ca^{2+}$ + $*Mg^{2+}$:$*SO_4^{2-}$ within glacial waters, that had stoichiometries lower than would be observed through complete coupling of carbonate and sulphide weathering. Tranter et al. (2002) attributes some of the $*Ca^{2+}$ + $*Mg^{2+}$ deficit to coupled pyrite/silicate weathering. This was partially the case within VG incubations, with the observed stoichiometry between $*SO_4^{2-}{}_{bio}$ and $*K^{+}{}_{bio}$ accounting for a further 1.4% of the protons released from the observed SO_4^{2-} yields. Very low $*K^{+}{}_{bio}$ concentrations produced by HN sediments, however, did not help to explain its low $*Ca^{2+}$ + $*Mg^{2+}$:$*SO_4^{2-}$ stoichiometry, though it was unlikely to be a result of anhydrite or gypsum dissolution, as Ca^{2+} and SO_4^{2-} association was low within the first *c.* 100 days of incubation.

Poor coupling of $*Ca^{2+}{}_{bio}$ + $*Mg^{2+}{}_{bio}$ and $*SO_4^{2-}{}_{bio}$ within TB and MK sediments, was thought to relate to their relatively low calcium carbonate to pyrite concentrations (Table 5.1). Instead, pH decreases were observed during incubation (decreasing by 1.4 (± 0.8) in TB, 0.8 (±0.19) in MK, and 1.3 (±0.3) in HN incubations), and so it is suggested that the available carbonate was unable to buffer the acid generated through pyrite oxidation within these sediments. Low correlation coefficients, and low levels of SO_4^{2-} production within HB and AG incubations, suggested that carbonate weathering was principally driven by processes other than coupled pyrite oxidation within these sediments.

Table 5.4: Stoichiometries of [*Ca_{bio}+*Mg_{bio}]:[*SO_{4bio}] within different sediments, based upon linear regression models.

Sediments		[*Ca+*Mg]:[*SO_4] Live	R^2
VG	Aerobic	1.1:1	0.91**
HB[h]	Aerobic	18.9:1	0.11
TB	Aerobic	0.2:1	0.63
HN	Aerobic	0.9:1	0.97**
AG	Aerobic	2.2:1	0.57
MK	Aerobic	0.1:1	0.46

** indicates that the relationships is significant at the 99% confidence limit (2 Tailed Pearson).
[h] Mg^{2+} was excluded from ratios in HB incubations due to probable silicate source.

Table 5.5: Average rates of sulphate production within aerobic microcosms containing glacial sediments.

	SO_4^{2-} Production Rate (neq $g^{-1}day^{-1}$)			
	Live		Sterile	
Sample	μ	σ	μ	σ
VG	23.6	*10.3*	5.2	*2.3*
HB	2.3	*0.2*	0.8	*1.2*
TB	31.6	*7.4*	5.7	*4.1*
HN	124.5	*35.5*	9.6	*5.5*
AG	4.1	*1.7*	2.2	*1.9*
MK	5.9	*1.2*	0.3	*0.1*

Pyrite Oxidation in Glacial Sediments

Rates of SO_4^{2-} production within the aerobic batch incubations (reported in Table 5.5), compared well to those in Montross et al. (2012) and Boyd et al. (2014). The lowest observed rates occurred in HB, AG and MK microcosms, which, at between 2 and 6 neq $g^{-1}day^{-1}$, were similar to rates of 3 and 1.4 neq $g^{-1}day^{-1}$ rates reported for Robertson Glacier and Haut Glacier D'Arolla respectively (Boyd et al., 2014; Montross et al., 2012). VG and TB rates were an order of magnitude greater, similar to those reported for Bodalsbreen sediment (Montross et al., 2012). Sulphate production in HN sediment was an order of magnitude greater again, attributed to far greater concentrations of elemental sulphur within HN sediment (Table 5.1).

Exploring the differences in sulphate production between sediments, and that factors that influence this, yielded a strong correlation between the SO_4^{2-} production, and sediment sulphur concentration (Table 5.1) ($R^2 = 0.9$). No significant correlations were observed between SO_4^{2-} production and live cell concentration, average primary productivity, average bacterial production, or relative grain size fractions; though a sample size of six was too small to fully explore the influence of these factors. To better explore the impact of microbial activity on pyrite oxidation, the analysis was broadened to encompass rates of bacterial production and chemoautotrophic activity made concurrent to major ion analyses over the first 100 days of VG and HB incubations. This analysis included incubations of secondary sample from each glacier, that were incubated for this period also, giving measurements of microbial activity alongside SO_4^{2-} production for VG1, VG2, HB1 and HB2 sediments (see Chapter 2 for descriptions of VG2 and HB2, and Chapter 4, Section 4.2.4 for the analysis of chemoautotrophy within these sediments). Within this subset of incubations, microbial production of sulphate was only observed within VG1 microcosms. Moreover, in this case, greater pyrite content did not correspond with enhanced microbial oxidation of pyrite. Instead, microbially enhanced pyrite oxidation within VG1 sediment was best explained by order of magnitude greater rates of chemoautotrophy, relative to VG2, HB1 and HB2 sediments. This finding, is supported by observations in Boyd et al. (2014), which observed correlation between chemoautotrophy and sulphate production in subglacial sediments.

Pyrite Oxidation Kinetics

The rate-determining step in pyrite oxidation, relates to electron transfer from the pyrite surface to the electron acceptor, with the overall oxidation rate faster with Fe^{3+} as an electron acceptor relative to O_2 (Rimstidt, 2003). Empirical evidence has also shown that microbial processes can cause a significant increase in weathering rates with O_2 as an electron acceptor, but that there is there is little microbial rate enhancement when oxidation occurs through Fe^{3+} (Williamson and Rimstidt, 1994; Gleisner et al., 2006; Balci et al., 2007). This is thought to be because microbial enhancement utilises the O_2 present to re-oxidise Fe^{2+} to Fe^{3+} at the mineral surface, with pyrite oxidation rates then being determined by the rate of microbial Fe^{3+} supply (Gleisner et al., 2006; Balci et al., 2007). Hence the use here, of anaerobic incubations alongside aerobic incubations, provided rate information relating to the biotic and abiotic

oxidation of pyrite in the absence of oxygen as an electron acceptor, allowing a better understanding of the kinetics of subglacial pyrite oxidation.

The findings of Williamson and Rimstidt (1994); Gleisner et al. (2006), or Balci et al. (2007), in which experiments were mostly performed at *c.* 25°C, and at low pH, differed to the results of this low temperature experiment with glacial sediments. In the absence of oxygen, or microbial life, oxidation rates were very low (*c.* 10^{-11} mol m^{-2}), an order of magnitude lower than rates reported for abiotic oxidation by O_2 in Williamson and Rimstidt (1994) and Gleisner et al. (2006) (*c.* 10^{-10}). Oxidation rates were highest within anaerobic incubations of live sediments, with rates similar in magnitude to values reported for microbial oxidation by Fe^{3+} in Gleisner et al. (2006). Live anaerobic rates exceeded those observed within sterilised sediments by factors ranging from 10 to 50×.

Final supernatant pH values were between 4 and 7. The solubility of iron is very low at this pH range (Ehrlich and Newman, 2009), with Fe^{3+} typically present as solid oxy(hyd)roxides. In the absence of O_2 as an electron acceptor, therefore, pyrite oxidation can only be sustained by Fe^{3+} that is adsorbed to the pyrite mineral (Moses and Herman, 1991; Nordstrom et al., 2008), or by utilising NO_3^- (Vaclavkova et al., 2015) or MnO_2 (Schippers and Jorgensen, 2001) to oxidise Fe^{2+} at the pyrite surface. The significant ($p < 0.01$) difference in rates between live and sterile anaerobic incubations suggests, therefore, that subglacial microbes are implicit in mediating one, or more, of these reactions. With denitrification observed within these sediments, it is possible that anaerobic pyrite oxidation could be partially coupled to denitrification through Equations 5.4.2 or 5.4.3 (Bosch and Meckenstock, 2012). However, the NO_3^- concentrations within these incubations were insufficient to produce the observed concentrations of SO_4^{2-} through these reaction couplings, making this unlikely to be the dominant oxidation mechanism within these incubations. Moreover, similar kinetics within both aerobic and anaerobic incubations, suggests that an alternative electron acceptor to oxygen or nitrate, may be utilised for pyrite oxidation under aerobic conditions. This supports the hypothesis that biological pyrite oxidation within these sediments occurred through an indirect weathering mechanism, being mediated through the microbial re-oxidation of reduced iron species at the mineral interface. This finding recommends caution in the use of stable isotopes, specifically in the interpretation of $\delta^{18}O_{SO_4^{2-}}$ data, for inferring subglacial redox conditions.

$$FeS_2(s) + 3NO_3^-(aq) + 2H_2O \rightarrow Fe(OH)_3(s) + 2SO_4^{2-}(aq) + 1.5N_2(g) + H^+ \quad (5.4.2)$$

$$FeS_2(s) + 7.5NO_3^-(aq) + 3.5H_2O \rightarrow Fe(OH)_3(s) + 2SO_4^{2-}(aq) + 7.5NO_2^-(aq) + 4H^+ \quad (5.4.3)$$

This idea is further supported by the results of the iron weathering experiment (Fig. 5.3.4), as no significant differences were observed in ferrihydrite concentrations between live and sterilised incubations, despite significantly ($p < 0.01$) greater SO_4^{2-} concentrations within live incubations of all sediments (data not shown). A possible explanation for this absent Fe phase, is that it becomes incorporated within a microbially mediated electron shuttle. Here, Fe^{2+} produced by pyrite weathering is re-oxidised by Equation 5.1.3, with the resultant Fe^{3+} being used to further oxidise pyrite through Equation 5.1.2, rather than precipitating as ferrihydrite (Singer and Stumm, 1970; Moses and Herman, 1991; Schippers and Jorgensen, 2001). In this scenario, the observed increases of sediment-ferrihydrite concentration would have been derived from pyrite that had been oxidised abiotically, through Equation 5.1.1 (Raiswell et al., 2009).

5.5 Conclusions

Batch microcosm experiments were used to assess microbial mineral weathering processes within subglacial sediments. Significant microbial enhancement of pyrite weathering was observed within subglacial sediments of contrasting geology, and originating from glaciers in Svalbard, Greenland and the Maritime Antarctic. This finding supports the contention that sulphide redox processes are a dominant microbial energy cycle within the subglacial environment. New data presented here, suggested that the microbial oxidation mechanism of pyrite was indirect, with oxidation occurring with Fe^{3+} as an electron acceptor in aerobic conditions, as well as in the absence of O_2. This has important implications for the use of stable isotopes to infer subglacial oxygen conditions, and hence drainage pathways, suggesting that it might not be able to reliably differentiate between biotic sulphide oxidation mechanisms.

Microbial processes were also shown to influence carbonate weathering through the generation of protons from sulphide oxidation. The results shown

here suggest that for some glaciers, where reactive pyrite phases are limited, microbial processes may be important in the generation of sufficient protons to weather carbonates beyond levels determined by hydrolysis equilibria. Coupling of microbial pyrite oxidation and silicate weathering in VG sediment, lent further support to the importance of sulphur-cycling microbes to other weathering processes. Elemental sulphur content of the sediment was determined to be the dominant factor influencing SO_4^{2-} production, however, chemoautotrophic activity also appeared to influence the proportion of SO_4^{2-} produced by microbial processes in some cases. Glacier location, sediment morphology, bacterial production, cell or organic carbon concentration, all had no discernible impact upon rates of SO_4^{2-} production, or the proportion of SO_4^{2-} that was produced through biotically enhanced weathering.

Several limitations and directions for further research were put forward for consideration by these microcosm experiments. Future microcosm studies should employ genetic techniques such as denaturing gradient gel electrophoresis (DGGE), to monitor succession and bottle effects upon community diversity during the incubation period. Improved methods to sterilise sediment should be employed in future studies also. This study utilised a combination of chemical and dry heat approaches to produce control microcosms, allowing some assessment of the impact of these methods upon inorganic sediment chemistry. Future studies may increase the accuracy of abiotic assessment through the use of gamma sterilisation, a method that was cost prohibitive in this study.

A stable isotope survey is necessary to confirm and strengthen the conclusions derived from pyrite oxidation kinetics. Whilst kinetic data reported here could be improved if normalised against measured pyrite grain size. This could be achieved through experiments similar to that of Mitchell et al. (2013), where sterile mineral phases were implanted into a subglacial till. Moreover, more needs to be done to assess the mechanism behind pyrite oxidation, perhaps using stable isotope tracers to determine whether NO_3^- or MnO_2 are important here. Furthermore, the data reported here hinted at a relationship between chemoautotrophy in microbially mediated sulphate. Future experiments should focus on this linkage, to investigate whether this relationship is a widespread within subglacial sediments.

Whilst this experiment allowed comparison between weathering at different glaciers, the samples used probably did not entirely represent their respective subglacial systems. Further attempts are required to identify spatial variation in redox conditions and microbial processes under glaciers, and future studies

should incorporate both laboratory and field techniques when assessing subglacial processes. This experiment, however, benefited from its laboratory approach, as it allowed a wider geographical range of sediments to be considered concurrently, whilst also allowing the constraint of microbial processes. Adopting a lab approach in this study, has more than doubled the number of existing direct observations of subglacial microbial-mineral interactions available within the wider literature.

Whilst geology was certainly still the dominant control on bulk weathering chemistry, microbes significantly increased solute yields within these microcosms. Differences in the level of microbial enhancement varied by sediment geology, with greater microbial pyrite oxidation in sediments containing more elemental sulphur. The work carried out in this Chapter, furthers our understanding of the adaptations and activity of microbial life under glaciers, as well as improving our interpretation of microbial signatures within outflow geochemistry. Without direct, easy access to the subglacial environment, it is clear that our understanding of the small scale processes needs to be further improved before stronger, more general conclusions about subglacial biogeochemistry can be drawn.

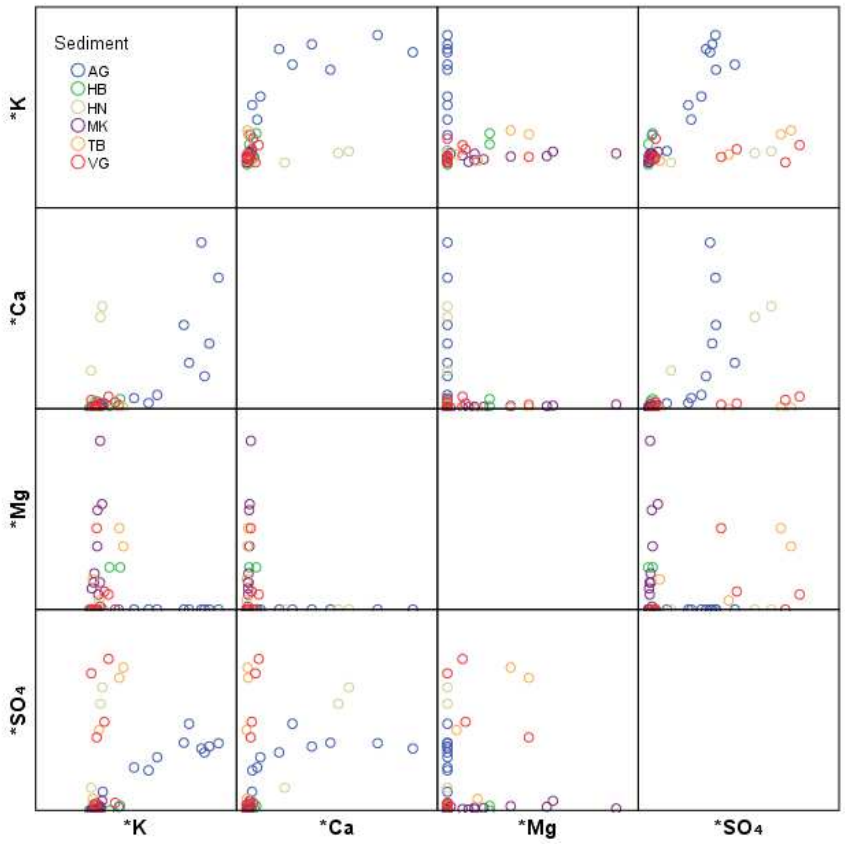

Figure 5.4.2: Sterile sediment correlation matrix, showing the relative associations of $*Ca^{2+}$,$*Mg^{2+}$, $*SO_4^{2-}$ and $*K^{+}$ over the course of the incubation experiment. Accompanying table showing Pearson rank correlation coefficients is in the Appendix: Table 7.2. Units are μeq g^{-1}.

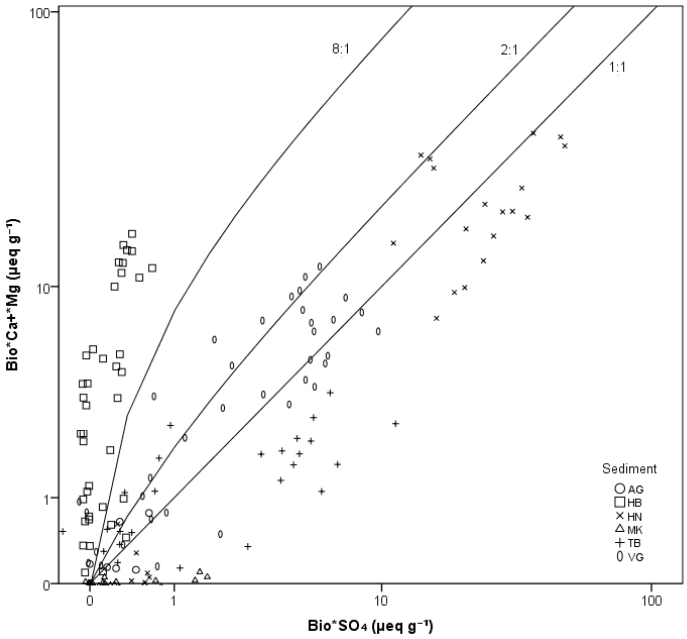

Figure 5.4.3: A log-log scatterplot showing association of $[*Ca^{2+}{}_{bio} + *Mg^{2+}{}_{bio}]$ and $[*SO_4^{2-}{}_{bio}]$ ions between 40 and 300 days incubations for different sediments. Lines show reference 1:1, 2:1, and 8:1 stoichiometries.

Chapter 6

Summary of Results and Conclusions

6.1 Introduction

This study set out to empirically assess the role of microbial life within the geochemical cycles that characterise the sediment-rich environment beneath glaciers and ice sheets. The subglacial environment was first characterised as an ecosystem when the work of Sharp et al. (1999) identified active bacterial communities inhabiting the basal sediments of Glacier de Tsanfleuron, and Haut Glacier d'Arolla in Switzerland. It was the work carried out by Tranter et al. (2002), however, that really hinted at the widespread importance of this microbial ecosystem within glacial biogeochemical cycles. Since these studies, there has been a considerable research effort directed at the importance of subglacial microbes within glacial biogeochemistry. This has mostly been approached through assessing the presence of known geochemically important microbes, or by inferring a biological signal within the chemistry of subglacial meltwaters. The relative inaccessibility of sediments, however, has prevented a widespread, representative study of processes within sediments themselves, with direct measurements of microbial activity, or of microbial contribution to meltwater chemistry, limited to a handful of studies, investigating point samples, from few glaciers.

This study, therefore, set out to make direct measurements of these processes, in a manner that would investigate some of the factors which influence geomicrobiology in context of differing subglacial conditions. This was approached

with three interrelated topics which formed the basis for Chapters 3, 4 and 5, and which related to the objectives of this thesis. Respectively investigating:

Objective 1: The influence of factors such as geology, organic matter content, glacier hydrology and geographic location, upon the microbial ecology of subglacial sediments.

Objective 2: The importance of aerobic and anaerobic heterotrophic metabolisms, chemoautotrophy, and the conditions within sediments which affect the rate and pathway of carbon turnover.

Objective 3: The influence of subglacial microorganisms upon major rock weathering chemistries within subglacial sediments and the mechanisms through which this weathering occurs.

To compensate for poor access to any one subglacial bed, the sediment analysed for this study originated from the immediate forefield of retreating glaciers across Svalbard, Greenland and the maritime Antarctic. Aside from providing sample replication, this strategy enabled geomicrobiology to be considered in context of a range of subglacial conditions. In this case allowing comparison of geomicrobiology between differing sediment geologies, channelised and distributed sediments, and between glaciers from different locations in the Arctic and maritime Antarctic. Microcosm studies were then used under laboratory conditions to enable direct measurements of microbial processes within sediment carbon cycling, and mineral geochemistry.

6.2 Synthesis

This thesis arrived at the following major conclusions:

1. Live microbial populations within the sediments underneath polar glaciers are geographically widespread, in this case being observed within subglacial sediments from across Svalbard, Greenland, South Georgia (South Atlantic) and Livingston Island (maritime Antarctic). Moreover, live population densities were similar in magnitude between sediments of differing geology, or of differing glacial drainage bedform, suggesting an ecosystem independent of the inputs of cells, nutrients and oxygen associated with channelised transport of seasonal snow melt. Instead, large spatial variation in cell concentrations within the c. 1kg of sample taken from each

glacier, suggested that small scale changes in sediment conditions had a great influence over life here. The live cells inhabiting subglacial sediment were predominantly bacteria, though archaea and eukaryotes, probably fungi, were also suggested as important within the subglacial ecosystem.

2. Chemoautotrophy was shown to be an important metabolism within subglacial sediments, and likely underpins heterotrophic activity under glaciers where no other sources of organic carbon are available. Carbon fixation by chemoautotrophy exceeded that of inputs of supraglacial algal biomass, and so is suggested as the dominant source of the proteinaceous organic carbon within these samples. Heterotrophy was found to be the dominant metabolism within subglacial sediments, each of the samples analysed in this study being a net source of CO_2. Anabolic processes were not affected by the concentration of sediment organic matter, and instead were limited by the quality of the organic carbon pool. It is suggested, therefore, that the labile organic carbon fraction produced by chemoautotrophy was the predominant source of organic carbon for heterotrophic organisms within these subglacial systems. Oxygen and nitrate were found to be the dominant electron acceptors during subglacial heterotrophy, the use of less energetically favourable electron acceptors was only noted within Heaney (HN) sediment, where ferric iron was also utilised.

3. Microbial mediation of pyrite oxidation within subglacial sediment was found to be widespread, occurring within all sediments analysed for this project. Moreover, microbial mediation of this process was significant, contributing to between 48% and 93% of total sulphate produced during incubation. Through pyrite oxidation, microbes were found to greatly influence the bulk chemistry of glacial waters, with acid generated during this process contributing to elevated carbonate concentrations in some cases. The dominant reaction mechanisms through which microbial oxidation of metal sulphide minerals occurred was determined to be indirect, probably involving the re-oxidation of ferrous iron at the mineral surface as a means to supply ferric iron as an electron donor for pyrite oxidation.

In addition to these conclusions, which address the overarching aim of this study, the use of a multi-glacier sampling strategy allowed geomicrobial processes to be compared between glaciers. From this, it was concluded that despite bac-

terial production being maintained at low levels in sediments with little or no sediment-derived organic material, heterotrophic metabolisms in these subglacial sediments were limited by the availability of labile forms of organic carbon. As such, it is suggested that under polar glaciers, the linkage between organic carbon and heterotrophy, is based upon supply from chemoautotrophic primary production, or from supraglacial and englacial transport of cellular material. The observations here suggested that geology containing lithified organic material did not to increase bacterial production relative to metamorphic sediments. Instead, other factors which influence the delivery of low molecular weight carbon to subglacial sediments were shown to be more important in affecting an increase in production. For example, Vestre Grønfjordbreen (VG) sediments, which contained higher proportions of proteinaceous organic material, had significantly higher rates of bacterial production and respiration compared to other sediments of similar geology.

Chemoautotrophy was also suggested as important in affecting microbial pyrite oxidation rates in subglacial sediments, though too few measurements of chemoautotrophy were made in this study to determine whether this relationship is likely to be widespread. Instead, the biggest factor affecting total sulphate production, as well as the proportion of sulphate produced as a result of microbial processes, was the sulphide content within the sediment itself. This supports the findings of transplant studies, which have shown that sediment mineralogy selects for species best able to geochemically exploit their environment (Mitchell et al., 2013). Moreover, it suggests that mineralogy may well be an important factor which influences the activity of a subset of subglacial microbes, rather than the community as a whole.

6.3 Theoretical Implications

This study provides empirical evidence of the microbial enhancement of pyrite weathering under glaciers. Moreover, it is suggested that microbially enhanced weathering is common under glaciers, with observations from Svalbard, Greenland, South Georgia and Livingston Island, in this study, adding to the findings of other studies in the Canadian Arctic (Boyd et al., 2014), the Swiss Alps (Sharp et al., 1999; Montross et al., 2012), and Norway (Montross et al., 2012). The direct observations of sediment processes within this study, provide an evidence base for earlier inverse-modelling approaches that have been used to constrain

subglacial biogeochemistry. The results of microcosm experiments here, largely support the inferred conclusions of Tranter et al. (2002) and Wadham et al. (2010a) with respect to microbial catalysis of sulphide oxidation, and coupling between sulphate and carbonate chemistries. However, the kinetics of sulphide oxidation indicated that microbial oxidation of pyrite was indirect, cautioning the use of stable isotope approaches, such as those used in Wadham et al. (2004) and Wynn et al. (2006), when interpreting a "microbial" signature, or inferring subglacial redox conditions from sulphate ions in glacial outflow.

The conclusions of the carbon cycling experiments, were set within context of studies that have mostly investigated down-stream impacts of carbon export from glaciers. Should widespread chemoautotrophy underpin heterotrophy beneath glaciers, then it may also provide a potential source of proteinaceous organic carbon to connected ecosystems. Analysis of the quality of organic matter, through FTIR in this study, and through other methods within the wider literature (Lafrenière and Sharp, 2004; Barker et al., 2009; Lawson et al., 2015), suggests that subglacial sediments are reservoirs, if not producers, of low molecular weight organic carbon. With the export of such organic phases noted by Fellman et al. (2014), Hood et al. (2015) and Lawson et al. (2014), this highlights the need to better understand autochthonous production of organic carbon within the subglacial system, and how it fits within wider glacial transport of supraglacial biomass.

With respect to heterotrophic activity, the results here suggest an ecosystem in which facultative species are present, adapting to changing redox conditions, and/or one characterised by suboxic conditions, where strong redox gradients within the sediment provide conditions for both aerobic and anaerobic metabolisms. This conclusion provides an interesting basis upon which to explore controls upon subglacial ecology, and perhaps suggests why distinct differences in cell concentrations or carbon cycling were not apparent when comparing channelised and distributed sediments. Moreover, it suggests that redox is an important control upon ecology and metabolism under glaciers, and whilst conditions for methanogenesis clearly do manifest underneath glaciers (Wadham et al., 2008; Boyd et al., 2010; Stibal et al., 2012c), processes lower down the redox scale are likely to be of greater significance.

6.4 Limitations

Adequate sampling of the subglacial environment is a difficult task, and poor access to sediments has limited the scope of past studies investigating subglacial ecology. This project sought to address the problem of access to a representative sample set, by combining analysis of sediments from multiple glaciers. This approach provided a broad assessment of subglacial sediments as ecosystems, as well as offering a means to investigate variation in geomicrobial processes as a result of differing physico-chemical conditions. A multi-glacier approach was not without its own limitations, however, as it added complexity when comparing differences between samples. For example, whilst comparisons between sediments have been made throughout this thesis, using parameters such as mineralogy, grain size, location, glacial hydrology etc., the complexity of subglacial conditions posed additional parameters that were more difficult to factor in. These include glacial and sediment history, which may impact the maturity and stability of the ecosystem, and the extent to which species selection influences microbial diversity. Further, necessity dictated that sediments removed from meltwater channels were sampled in spring, whilst sediment from underneath retreating frontal margins were taken in summer. Ecological selection may well affect sediment microbial diversity during the seasonal evolution of the subglacial system. Without seasonal and long term monitoring of the changes in sediment microbial diversity, it is difficult to assess whether sampling at different points in the melt season has influenced the microbial community, and hence carbon dynamics or the rates and mechanisms of sulphide oxidation within these sediments.

The relative inaccessibility of subglacial sediments, in addition to limiting sample availability, made *in situ* measurements and experiments difficult also. For this reason, and to enable a controlled comparison between the different sediments, lab-based microcosms were used to investigate geomicrobiology, under simulated subglacial conditions. A lab-based approach, whilst deemed appropriate for this study into sediment processes, imposed limitations upon the scope of the results with respect to quantifying biogeochemical fluxes. Generally, as long term microcosm experiments can suffer from ecological selection, they may introduce bias in favour of species better adapted for conditions in the lab. Combined with non-perfect simulation of subglacial temperatures and pressure, this had the potential to influence the magnitude of biogeochemical fluxes. Where possible, this has been mitigated against. For example, reported bacterial pro-

duction rates were made before ecosystem acclimation to lab conditions. The impact of community changes over the duration of the mineral weathering experiments was unknown, however, and so comparison of the reported fluxes with glacial outflow chemistry should be made with caution. Moreover, since subglacial sediments undergo significant changes throughout the melt season, whereas the microcosms used were static batch incubations, the results reported here perhaps best correspond to conditions within distributed drainage, with slow flow and limited recharge of nutrients or carbon.

The subglacial environment is a complex and dynamic place, with seasonally driven changes in hydrology, and physical disturbances from overlying ice. The challenge to fully assess ecology within subglacial sediments is of such magnitude that it remains unlikely to be characterised to the same degree as supraglacial ecosystems. Instead, studies such as this one, which seek a greater understanding of important sediment processes, are crucial to interpreting seasonal outflow chemistry, and hence improve spatial and temporal understanding of sediment geomicrobiology.

6.5 Future Work

The insight gained through direct measurements of microbial processes in subglacial sediments, suggests several directions for further study. These primarily involve refining direct observations of subglacial geomicrobiology, as well as further assessing the importance of subglacial ecosystems in glacial scale biogeochemical fluxes.

This study would have been greatly improved with integration of a metagenomic assessment of the microbial communities present within the analysed sediments. Future microcosm experiments should include a broad characterisation of the sediment community, encompassing of bacteria, archaea and eukaryotes, and focussing upon cell function. Moreover, quantitative assessment of community changes throughout microcosm experiments, such as those utilised within this study, may give insight into which species are responsible for observed geomicrobial processes, as well as providing an assessment of bottle effects. Metagenomic techniques not only have application in assessing ecosystem function, but should also be used to better understand microbial diversity within the subglacial ecosystem. This should take a small focus, and attempt to constrain community changes with respect to different environmental gradi-

ents within the subglacial system, whether comparing between channelised and distributed sediment, across redox gradients, seasonal evolution, or the impact of freezing, thawing or even deglaciation.

By focussing future investigation at such a scale, the microbial community can be better linked within subglacial carbon and geochemical cycles. For example, function-specific staining techniques such as FISH, could be utilised in combination with microautoradiography techniques, which would pinpoint metabolically active communities within the subglacial sediments. Or techniques like secondary ion mass spectrometry could be used to directly observe cellular transformations of different substrates, or reduced mineral species. This integrated and technological approach could be used to great effect in establishing the functional roles of different parts of the subglacial community, in turn increasing the insight gained from functional metagenomic studies. Another objective for future genetic assessment, is to investigate the biogeography of subglacial communities. Several studies have investigated the ecology of subglacial sediments, yet there is a need to integrate these in an attempt to better define the spatial scale of subglacial ecosystems, their common constituents and ecosystem function.

The investigation into the role of microbes within mineral geochemistry could have been improved through the incorporation of a stable isotope study to directly investigate differences in isotopic composition between biotic and abiotic pyrite oxidation, and to determine whether ferric iron is commonly utilised as an electron acceptor during microbial oxidation. Improvements could also have been made through better assessment of the linkages between activity and geochemistry. For example, the data reported here hinted at a relationship between chemoautotrophy and pyrite oxidation within the sediments from Svalbard. Future microcosms experiments should address this shortcoming, making measurements of chemoautotrophy alongside major ion analysis.

The nature of subglacial systems means that any practicable sampling strategy will, in some aspect, limit the scope of the inquiry. Future studies should, therefore, use an integrated approach to assess *in situ* microbial processes under glaciers, at least until a means of conducting replicable, representative, *in situ* experiments is determined. This can be approached by combining a laboratory assessments of sediment geomicrobial processes with seasonal hydro-biogeochemical datasets, to more accurately determine the microbial role within glacial solute and nutrient fluxes. Moreover, the integration of organic and inorganic chemical assessment of outflow, may also provide informative links

between biology and geochemistry.

Finally, the study of this cold, dark, inaccessible, geomicrobiological haven, is often considered in isolation. Future research should ensure that the subglacial ecosystem is given meaning within the wider context of life within the cryosphere. As shown here and elsewhere, microbial life within subglacial sediments is metabolically active. With glaciers covering approximately 10% of the earth's surface (Boetius et al., 2014), more needs to be done to assess the role of glaciers within global carbon cycles, and the complexities of subglacial carbon cycling factored into this model. It is notable that this study focuses upon glaciers in the Polar regions, glaciers in lower latitude mountainous regions may have greater potential to support subglacial life, and so a better understanding of how carbon cycling varies under world's glaciers is necessary to fully understand its potential in global carbon budgets.

6.6 Conclusions

The sediments underneath glaciers contain surprisingly diverse communities of prokaryotic life. This study is currently the most widespread investigation into microbial geochemistry within subglacial sediments, and provides direct evidence of the importance of these microbes within the mineral weathering processes that so characterise the chemistry of glacial waters. This empirical evidence largely supports the findings of past studies, which have identified geochemically active species, or inferred microbial processes from bulk meltwater chemistry. The oxidation of pyrite was found to be the most significant weathering process in which microbes were active, and it was common, occurring in sediments from the Arctic and Antarctic, as well as in range of base geologies. This research also makes the first assessment of net carbon cycling by subglacial sediments, finding that subglacial sediments are net heterotrophic. Of note, however, significant primary productivity from chemoautotrophs was also apparent, as were linkages between chemoautotrophy and mineral weathering processes. In conducting a laboratory study of subglacial sediments, this research has provided an important empirical basis to support and guide future studies investigating life within the cryosphere. Moreover, it further adds to the evidence which presents subglacial systems, not as a sterile conduit for snow melt, but as characterised with life; widespread, diverse and active within globally relevant biogeochemical cycles.

Chapter 7

Appendix

7.1 Cell mineral separation results

Innoculum concentration	*100mM EDTA*	*100mM EDTA and ultrasound*	*Methanol*	*Methanol and ultrasound*	*Triton X-100*	*Triton X-100 and ultrasound*
	Percentage recovery of inoculated cells					
1 in 1	*71.2*	*93.8*	*43.2*	*38.4*	*10.0*	*9.2*
1 in 10	*83.9*	*90.0*	*38.8*	*37.9*	*16.3*	*na*
1 in 100	*20.0*	*67.1*	*29.2*	*32.5*	*na*	*na*
1 in 1000	*na*	*na*	*na*	*na*	*na*	*na*

Table 7.1: Percentage recovery of inoculated cells for different methodologies of cell extraction and different concentrations of inoculum. Where value is *na*, extracted inoculae are indistinguishable from error associated with uninoculated sediment enumeration.

7.2 Correlation Matrix of Geochemistry

Table 7.2: Correlation matrices exploring the co-evolution of Mg^{2+}, Ca^{2+}, SO_4^{2-} and K^+ ions in aerobic and anaerobic batch incubations.

Correlations

	Aerobic Anaerobic	L/D			*Mg	*Ca	*SO4	*K
VG	Aerobic	Live	*Mg	Pearson Correlation	1	.943**	.913**	.898**
				Sig. (2-tailed)		.000	.000	.000
				N	20	20	18	19
			*Ca	Pearson Correlation	.943**	1	.907**	.896**
				Sig. (2-tailed)	.000		.000	.000
				N	20	20	18	19
			*SO4 uEq/g	Pearson Correlation	.913**	.907**	1	.869**
				Sig. (2-tailed)	.000	.000		.000
				N	18	18	18	17
			*K	Pearson Correlation	.898**	.896**	.869**	1
				Sig. (2-tailed)	.000	.000	.000	
				N	19	19	17	19
		Sterile	*Mg	Pearson Correlation	1	.065	.249	-.069
				Sig. (2-tailed)		.878	.551	.871
				N	8	8	8	8
			*Ca	Pearson Correlation	.065	1	.849**	.449
				Sig. (2-tailed)	.878		.008	.264
				N	8	8	8	8
			*SO4 uEq/g	Pearson Correlation	.249	.849**	1	.022
				Sig. (2-tailed)	.551	.008		.958
				N	8	8	8	8
			*K	Pearson Correlation	-.069	.449	.022	1
				Sig. (2-tailed)	.871	.264	.958	
				N	8	8	8	8
	Anaerobic	Live	*Mg	Pearson Correlation	1	.149	-.092	.859**
				Sig. (2-tailed)		.479	.662	.000
				N	25	25	25	25
			*Ca	Pearson Correlation	.149	1	.853**	.426*
				Sig. (2-tailed)	.479		.000	.034
				N	25	25	25	25
			*SO4 uEq/g	Pearson Correlation	-.092	.853**	1	.198
				Sig. (2-tailed)	.662	.000		.342
				N	25	25	25	25
			*K	Pearson Correlation	.859**	.426*	.198	1
				Sig. (2-tailed)	.000	.034	.342	
				N	25	25	25	25
		Sterile	*Mg	Pearson Correlation	1	.188	-.418	-.321
				Sig. (2-tailed)		.762	.484	.598
				N	5	5	5	5
			*Ca	Pearson Correlation	.188	1	.703	.844
				Sig. (2-tailed)	.762		.185	.072
				N	5	5	5	5
			*SO4 uEq/g	Pearson Correlation	-.418	.703	1	.843
				Sig. (2-tailed)	.484	.185		.073
				N	5	5	5	5
			*K	Pearson Correlation	-.321	.844	.843	1
				Sig. (2-tailed)	.598	.072	.073	
				N	5	5	5	5

**. Correlation is significant at the 0.01 level (2-tailed).

*. Correlation is significant at the 0.05 level (2-tailed).

a. Cannot be computed because at least one of the variables is constant.

Correlations

Sediment	Aerobic Anaerobic	L/D			*Mg	*Ca	*SO4	*K
HB	Aerobic	Live	*Mg	Pearson Correlation	1	.782**	.016	.691**
				Sig. (2-tailed)		.000	.952	.004
				N	19	19	16	15
			*Ca	Pearson Correlation	.782**	1	.252	.910**
				Sig. (2-tailed)	.000		.347	.000
				N	19	19	16	15
			*SO4 uEq/g	Pearson Correlation	.016	.252	1	.157
				Sig. (2-tailed)	.952	.347		.591
				N	16	16	16	14
			*K	Pearson Correlation	.691**	.910**	.157	1
				Sig. (2-tailed)	.004	.000	.591	
				N	15	15	14	15
		Sterile	*Mg	Pearson Correlation	1	.457	-.252	.936**
				Sig. (2-tailed)		.255	.548	.001
				N	8	8	8	8
			*Ca	Pearson Correlation	.457	1	.150	.674
				Sig. (2-tailed)	.255		.723	.067
				N	8	8	8	8
			*SO4 uEq/g	Pearson Correlation	-.252	.150	1	.021
				Sig. (2-tailed)	.548	.723		.961
				N	8	8	8	8
			*K	Pearson Correlation	.936**	.674	.021	1
				Sig. (2-tailed)	.001	.067	.961	
				N	8	8	8	8
	Anaerobic	Live	*Mg	Pearson Correlation	1	-.321	-.259	-.090
				Sig. (2-tailed)		.118	.211	.675
				N	25	25	25	24
			*Ca	Pearson Correlation	-.321	1	.888**	.891**
				Sig. (2-tailed)	.118		.000	.000
				N	25	25	25	24
			*SO4 uEq/g	Pearson Correlation	-.259	.888**	1	.809**
				Sig. (2-tailed)	.211	.000		.000
				N	25	25	25	24
			*K	Pearson Correlation	-.090	.891**	.809**	1
				Sig. (2-tailed)	.675	.000	.000	
				N	24	24	24	24
		Sterile	*Mg	Pearson Correlation	1	.302	-.181	.453
				Sig. (2-tailed)		.396	.642	.444
				N	10	10	9	5
			*Ca	Pearson Correlation	.302	1	.308	.136
				Sig. (2-tailed)	.396		.420	.827
				N	10	10	9	5
			*SO4 uEq/g	Pearson Correlation	-.181	.308	1	.159
				Sig. (2-tailed)	.642	.420		.799
				N	9	9	9	5
			*K	Pearson Correlation	.453	.136	.159	1
				Sig. (2-tailed)	.444	.827	.799	
				N	5	5	5	5

**. Correlation is significant at the 0.01 level (2-tailed).

*. Correlation is significant at the 0.05 level (2-tailed).

a. Cannot be computed because at least one of the variables is constant.

Correlations

Sediment	Aerobic Anaerobic	L/D			*Mg	*Ca	*SO4	*K
TB	Aerobic	Live	*Mg	Pearson Correlation	1	.749**	.795**	.489*
				Sig. (2-tailed)		.000	.000	.018
				N	25	25	25	23
			*Ca	Pearson Correlation	.749**	1	.827**	.615**
				Sig. (2-tailed)	.000		.000	.002
				N	25	25	25	23
			*SO4 uEq/g	Pearson Correlation	.795**	.827**	1	.865**
				Sig. (2-tailed)	.000	.000		.000
				N	25	25	25	23
			*K	Pearson Correlation	.489*	.615**	.865**	1
				Sig. (2-tailed)	.018	.002	.000	
				N	23	23	23	23
		Sterile	*Mg	Pearson Correlation	1	.653	.717	.846
				Sig. (2-tailed)		.232	.173	.154
				N	5	5	5	4
			*Ca	Pearson Correlation	.653	1	.427	.892
				Sig. (2-tailed)	.232		.473	.108
				N	5	5	5	4
			*SO4 uEq/g	Pearson Correlation	.717	.427	1	.951*
				Sig. (2-tailed)	.173	.473		.049
				N	5	5	5	4
			*K	Pearson Correlation	.846	.892	.951*	1
				Sig. (2-tailed)	.154	.108	.049	
				N	4	4	4	4
	Anaerobic	Live	*Mg	Pearson Correlation	1	.556**	.480*	.702**
				Sig. (2-tailed)		.004	.015	.000
				N	25	25	25	23
			*Ca	Pearson Correlation	.556**	1	.707**	.676**
				Sig. (2-tailed)	.004		.000	.000
				N	25	25	25	23
			*SO4 uEq/g	Pearson Correlation	.480*	.707**	1	.653**
				Sig. (2-tailed)	.015	.000		.001
				N	25	25	25	23
			*K	Pearson Correlation	.702**	.676**	.653**	1
				Sig. (2-tailed)	.000	.000	.001	
				N	23	23	23	23
		Sterile	*Mg	Pearson Correlation	1	.774	.929*	.871
				Sig. (2-tailed)		.124	.023	.129
				N	5	5	5	4
			*Ca	Pearson Correlation	.774	1	.894*	.965*
				Sig. (2-tailed)	.124		.041	.035
				N	5	5	5	4
			*SO4 uEq/g	Pearson Correlation	.929*	.894*	1	.944
				Sig. (2-tailed)	.023	.041		.056
				N	5	5	5	4
			*K	Pearson Correlation	.871	.965*	.944	1
				Sig. (2-tailed)	.129	.035	.056	
				N	4	4	4	4

**. Correlation is significant at the 0.01 level (2-tailed).

*. Correlation is significant at the 0.05 level (2-tailed).

a. Cannot be computed because at least one of the variables is constant.

Correlations

Sediment	Aerobic Anaerobic	L/D			*Mg	*Ca	*SO4	*K
HN	Aerobic	Live	*Mg	Pearson Correlation	.[a]	.[a]	.[a]	.[a]
				Sig. (2-tailed)		.	.	.
				N	25	25	25	22
			*Ca	Pearson Correlation	.[a]	1	.992**	.762**
				Sig. (2-tailed)	.		.000	.000
				N	25	25	25	22
			*SO4 uEq/g	Pearson Correlation	.[a]	.992**	1	.724**
				Sig. (2-tailed)	.	.000		.000
				N	25	25	25	22
			*K	Pearson Correlation	.[a]	.762**	.724**	1
				Sig. (2-tailed)	.	.000	.000	
				N	22	22	22	22
		Sterile	*Mg	Pearson Correlation	.[a]	.[a]	.[a]	.[a]
				Sig. (2-tailed)		.	.	.
				N	5	5	5	5
			*Ca	Pearson Correlation	.[a]	1	.988**	.910*
				Sig. (2-tailed)	.		.002	.032
				N	5	5	5	5
			*SO4 uEq/g	Pearson Correlation	.[a]	.988**	1	.960**
				Sig. (2-tailed)	.	.002		.010
				N	5	5	5	5
			*K	Pearson Correlation	.[a]	.910*	.960**	1
				Sig. (2-tailed)	.	.032	.010	
				N	5	5	5	5
	Anaerobic	Live	*Mg	Pearson Correlation	.[a]	.[a]	.[a]	.[a]
				Sig. (2-tailed)		.	.	.
				N	25	25	25	18
			*Ca	Pearson Correlation	.[a]	1	.857**	.587*
				Sig. (2-tailed)	.		.000	.010
				N	25	25	25	18
			*SO4 uEq/g	Pearson Correlation	.[a]	.857**	1	.571*
				Sig. (2-tailed)	.	.000		.013
				N	25	25	25	18
			*K	Pearson Correlation	.[a]	.587*	.571*	1
				Sig. (2-tailed)	.	.010	.013	
				N	18	18	18	18
		Sterile	*Mg	Pearson Correlation	.[a]	.[a]	.[a]	.[a]
				Sig. (2-tailed)		.	.	.
				N	5	5	5	4
			*Ca	Pearson Correlation	.[a]	1	.968**	.983*
				Sig. (2-tailed)	.		.007	.017
				N	5	5	5	4
			*SO4 uEq/g	Pearson Correlation	.[a]	.968**	1	.978*
				Sig. (2-tailed)	.	.007		.022
				N	5	5	5	4
			*K	Pearson Correlation	.[a]	.983*	.978*	1
				Sig. (2-tailed)	.	.017	.022	
				N	4	4	4	4

**. Correlation is significant at the 0.01 level (2-tailed).

*. Correlation is significant at the 0.05 level (2-tailed).

a. Cannot be computed because at least one of the variables is constant.

Correlations

Sediment	Aerobic Anaerobic	L/D			*Mg	*Ca	*SO4	*K
AG	Aerobic	Live	*Mg	Pearson Correlation	.[a]	.[a]	.[a]	.[a]
				Sig. (2-tailed)		.	.	.
				N	35	35	35	34
			*Ca	Pearson Correlation	.[a]	1	.760**	.640**
				Sig. (2-tailed)	.		.000	.000
				N	35	35	35	34
			*SO4 uEq/g	Pearson Correlation	.[a]	.760**	1	.731**
				Sig. (2-tailed)	.	.000		.000
				N	35	35	35	34
			*K	Pearson Correlation	.[a]	.640**	.731**	1
				Sig. (2-tailed)	.	.000	.000	
				N	34	34	34	34
		Sterile	*Mg	Pearson Correlation	.[a]	.[a]	.[a]	.[a]
				Sig. (2-tailed)		.	.	.
				N	14	14	14	13
			*Ca	Pearson Correlation	.[a]	1	.565*	.756**
				Sig. (2-tailed)	.		.035	.003
				N	14	14	14	13
			*SO4 uEq/g	Pearson Correlation	.[a]	.565*	1	.899**
				Sig. (2-tailed)	.	.035		.000
				N	14	14	14	13
			*K	Pearson Correlation	.[a]	.756**	.899**	1
				Sig. (2-tailed)	.	.003	.000	
				N	13	13	13	13
	Anaerobic	Live	*Mg	Pearson Correlation	.[a]	.[a]	.[a]	.[a]
				Sig. (2-tailed)		.	.	.
				N	35	35	31	31
			*Ca	Pearson Correlation	.[a]	1	.540**	.145
				Sig. (2-tailed)	.		.002	.437
				N	35	35	31	31
			*SO4 uEq/g	Pearson Correlation	.[a]	.540**	1	-.344
				Sig. (2-tailed)	.	.002		.073
				N	31	31	31	28
			*K	Pearson Correlation	.[a]	.145	-.344	1
				Sig. (2-tailed)	.	.437	.073	
				N	31	31	28	31
		Sterile	*Mg	Pearson Correlation	.[a]	.[a]	.[a]	.[a]
				Sig. (2-tailed)		.	.	.
				N	14	14	14	14
			*Ca	Pearson Correlation	.[a]	1	-.001	.458
				Sig. (2-tailed)	.		.998	.099
				N	14	14	14	14
			*SO4 uEq/g	Pearson Correlation	.[a]	-.001	1	-.107
				Sig. (2-tailed)	.	.998		.717
				N	14	14	14	14
			*K	Pearson Correlation	.[a]	.458	-.107	1
				Sig. (2-tailed)	.	.099	.717	
				N	14	14	14	14

**. Correlation is significant at the 0.01 level (2-tailed).

*. Correlation is significant at the 0.05 level (2-tailed).

a. Cannot be computed because at least one of the variables is constant.

Correlations

Sediment	Aerobic Anaerobic	L/D			*Mg	*Ca	*SO4	*K
MK	Aerobic	Live	*Mg	Pearson Correlation	1	.929**	.900**	.559**
				Sig. (2-tailed)		.000	.000	.000
				N	35	35	35	35
			*Ca	Pearson Correlation	.929**	1	.815**	.662**
				Sig. (2-tailed)	.000		.000	.000
				N	35	35	35	35
			*SO4 uEq/g	Pearson Correlation	.900**	.815**	1	.319
				Sig. (2-tailed)	.000	.000		.062
				N	35	35	35	35
			*K	Pearson Correlation	.559**	.662**	.319	1
				Sig. (2-tailed)	.000	.000	.062	
				N	35	35	35	35
		Sterile	*Mg	Pearson Correlation	1	.903**	.446	.532
				Sig. (2-tailed)		.000	.110	.061
				N	14	14	14	13
			*Ca	Pearson Correlation	.903**	1	.533*	.640*
				Sig. (2-tailed)	.000		.050	.019
				N	14	14	14	13
			*SO4 uEq/g	Pearson Correlation	.446	.533*	1	.678*
				Sig. (2-tailed)	.110	.050		.011
				N	14	14	14	13
			*K	Pearson Correlation	.532	.640*	.678*	1
				Sig. (2-tailed)	.061	.019	.011	
				N	13	13	13	13
	Anaerobic	Live	*Mg	Pearson Correlation	.[a]	.[a]	.[a]	.[a]
				Sig. (2-tailed)		.	.	.
				N	35	35	35	31
			*Ca	Pearson Correlation	.[a]	.[a]	.[a]	.[a]
				Sig. (2-tailed)	.		.	.
				N	35	35	35	31
			*SO4 uEq/g	Pearson Correlation	.[a]	.[a]	1	.473**
				Sig. (2-tailed)	.	.		.007
				N	35	35	35	31
			*K	Pearson Correlation	.[a]	.[a]	.473**	1
				Sig. (2-tailed)	.	.	.007	
				N	31	31	31	31
		Sterile	*Mg	Pearson Correlation	.[a]	.[a]	.[a]	.[a]
				Sig. (2-tailed)		.	.	.
				N	14	14	14	14
			*Ca	Pearson Correlation	.[a]	.[a]	.[a]	.[a]
				Sig. (2-tailed)	.		.	.
				N	14	14	14	14
			*SO4 uEq/g	Pearson Correlation	.[a]	.[a]	1	.559*
				Sig. (2-tailed)	.	.		.038
				N	14	14	14	14
			*K	Pearson Correlation	.[a]	.[a]	.559*	1
				Sig. (2-tailed)	.	.	.038	
				N	14	14	14	14

**. Correlation is significant at the 0.01 level (2-tailed).

*. Correlation is significant at the 0.05 level (2-tailed).

a. Cannot be computed because at least one of the variables is constant.

References

Alley, R., Cuffey, K., Evenson, E., Strasser, J., Lawson, D., and Larson, G. (1997). How glaciers entrain and transport basal sediment: Physical constraints. *Quaternary Science Reviews*, 16(9):1017–1038.

Amato, P., Doyle, S. M., Battista, J. R., and Christner, B. C. (2010). Implications of subzero metabolic activity on long-term microbial survival in terrestrial and extraterrestrial permafrost. *Astrobiology*, 10(8):789–798.

Andrews, G. (2015). Seasonal Variation and Controls on Subglacial Riverine CO2 Concentrations From a Small Catchment, West Greenland Ice Sheet. In *Advances in our understanding of processes at the beds of glaciers and ice sheets; AGU Fall Meeting*, San Francisco.

Anesio, A. M., Sattler, B., Foreman, C., Telling, J., Hodson, A., Tranter, M., and Psenner, R. (2010). Carbon fluxes through bacterial communities on glacier surfaces. *Annals of Glaciology*, 51(56):32–40.

Ansari, a. H., Hodson, a. J., Heaton, T. H. E., Kaiser, J., and Marca-Bell, A. (2013). Stable isotopic evidence for nitrification and denitrification in a High Arctic glacial ecosystem. *Biogeochemistry*, 113:341–357.

Apple, J. K., Del Giorgio, P. a., and Kemp, W. M. (2006). Temperature regulation of bacterial production, respiration, and growth efficiency in a temperate salt-marsh estuary. *Aquatic Microbial Ecology*, 43(3):243–254.

Assmy, P., Cisewski, B., Henjes, J., Assmy, P., Cisewski, B., and Henjes, J. (2006). Plankton rain in the Southern Ocean: The European Iron Fertilization Experiment EIFEX. Technical Report Das AWI in den Jahren 2004 und 2005, Norwegian Polar Institute.

Avery, B. and Bascomb, C. (1974). *Soil survey laboratory methods.* Harpenden: Soil survey of England and Wales.

Bælum, K. and Benn, D. I. (2011). Thermal structure and drainage system of a small valley glacier (Tellbreen, Svalbard), investigated by ground penetrating radar. *Cryosphere*, 5(1):139–149.

Balci, N., Shanksiii, W., Mayer, B., and Mandernack, K. (2007). Oxygen and sulfur isotope systematics of sulfate produced by bacterial and abiotic oxidation of pyrite. *Geochimica et Cosmochimica Acta*, 71(15):3796–3811.

Bárcena, T. G., Finster, K. W., and Yde, J. C. (2011). Spatial Patterns of Soil Development, Methane Oxidation, and Methanotrophic Diversity along a Receding Glacier Forefield, Southeast Greenland. *Arctic, Antarctic, and Alpine Research*, 43(2):178–188.

Barker, J., Klassen, J., Sharp, M., Foght, J., Fitzsimons, S., and Turner, R. (2010). Detecting biogeochemical activity in basal ice using fluorescence spectroscopy. *Annals of Glaciology*, 51(56):47–55.

Barker, J. D., Sharp, M. J., and Fitzsimonst, S. J. (2006). Abundance and Dynamics of Dissolved Organic Carbon in Glacier Systems. *Arctic, Antarctic and Alpine Research*, 38(2):163–172.

Barker, J. D., Sharp, M. J., and Turner, R. J. (2009). Using synchronous fluorescence spectroscopy and principal components analysis to monitor dissolved organic matter dynamics in a glacier system. *Hydrological Processes*, 1500(April):1487–1500.

Bartholomew, I., Nienow, P., Sole, A., Mair, D., Cowton, T., Palmer, S., and Wadham, J. (2011). Supraglacial forcing of subglacial drainage in the ablation zone of the Greenland ice sheet. *Geophysical Research Letters*, 38(8):1–5.

Behrenfeld, M. J., Bale, A. J., Kolber, Z. S., Aiken, J., and Falkowski, P. G. (1996). Confirmation of iron limitation of phytoplankton photosynthesis in the equatorial Pacific Ocean. *Nature*, 383(6600):508–511.

Berggren, M. and del Giorgio, P. a. (2015). Distinct patterns of microbial metabolism associated to riverine dissolved organic carbon of different source and quality. *Journal of Geophysical Research: Biogeosciences*, 120(JUNE):989–999.

Bhatia, M., Sharp, M., and Foght, J. (2006). Distinct bacterial communities exist beneath a high arctic polythermal Glacier. *Applied and Environmental Microbiology*, 72(9):5838–5845.

Bhatia, M. P., Kujawinski, E. B., Das, S. B., Breier, C. F., Henderson, P. B., and Charette, M. a. (2013). Greenland meltwater as a significant and potentially bioavailable source of iron to the ocean. *Nature Geoscience*, 6(4):274–278.

Bingham, R. G., Nienow, P. W., Sharp, M. J., and Boon, S. (2005). Subglacial drainage processes at a High Arctic polythermal valley glacier. *Journal of Glaciology*, 51(172):15–24.

Blomeier, D., Dustira, A., Forke, H., and Scheibner, C. (2011). Environmental change in the Early Permian of NE Svalbard: From a warm-water carbonate platform (Gipshuken Formation) to a temperate, mixed siliciclastic-carbonate ramp (Kapp Starostin Formation). *Facies*, 57(3):493–523.

Boetius, A., Anesio, A. M., Deming, J. W., Mikucki, J., and Rapp, J. Z. (2014). Microbial ecology of the cryosphere : sea ice and glacial habitats. *Nature Reviews Microbiology*, (September):1–14.

Bonkowski, M. (2004). Protozoa and plant growth: The microbial loop in soil revisited. *New Phytologist*, 162(3):617–631.

Bosch, J. and Meckenstock, R. U. (2012). Rates and potential mechanism of anaerobic nitrate-dependent microbial pyrite oxidation. *Biochemical Society transactions*, 40(6):1280–3.

Boschker, H. T. S., Vasquez-Cardenas, D., Bolhuis, H., Moerdijk-Poortvliet, T. W. C., and Moodley, L. (2014). Chemoautotrophic carbon fixation rates and active bacterial communities in intertidal marine sediments. *PLoS ONE*, 9(7):e101443.

Bothe, H., Newton, W. E., and Ferguson, S. (2007). *Biology of the Nitrogen Cycle*. Elsevier.

Bottrell, S. H. and Tranter, M. (2002). Sulphide oxidation under partially anoxic conditions at the bed of the Haut Glacier d'Arolla, Switzerland. *Hydrological Processes*, 16(12):2363–2368.

Boyd, E. S., Hamilton, T. L., Havig, J. R., Skidmore, M. L., and Shock, E. L. (2014). Chemolithotrophic primary production in a subglacial ecosystem. *Applied and Environmental Microbiology*, 80(19):6146–6153.

Boyd, E. S., Lange, R. K., Mitchell, A. C., Havig, J. R., Hamilton, T. L., Lafreni??re, M. J., Shock, E. L., Peters, J. W., and Skidmore, M. (2011). Diversity, abundance, and potential activity of nitrifying and nitrate-reducing microbial assemblages in a subglacial ecosystem. *Applied and Environmental Microbiology*, 77(14):4778–4787.

Boyd, E. S., Skidmore, M., Mitchell, A. C., Bakermans, C., and Peters, J. W. (2010). Methanogenesis in subglacial sediments. *Environmental Microbiology Reports*, 2(5):685–692.

Brown, G. H. (2002). Glacier meltwater hydrochemistry. *Applied Geochemistry*, 17:855–883.

Buesing, N. and Gessner, M. O. (2003). Incorporation of radiolabeled leucine into protein to estimate bacterial production in plant litter, sediment, epiphytic biofilms, and water samples. *Microbial Ecology*, 45(3):291–301.

Carpenter, E. J., Lin, S., and Capone, D. G. (2000). Bacterial Activity in South Pole Snow Bacterial Activity in South Pole Snow. *Applied and Environmental Microbiology*, 66(10):4514–4517.

Castello, J. D. and Rogers, S. O. (2005). *Life in Ancient Ice*. Princeton University Press.

Castello, J. D., Rogers, S. O., Starmer, W. T., Catranis, C. M., Ma, L., Bachand, G. D., Zhao, Y., and Smith, J. E. (1999). Detection of tomato mosaic tobamovirus RNA in ancient glacial ice. *Polar Biology*, 22(3):207–212.

Chapelle, F. (2001). *Ground-Water Microbiology and Geochemistry*. Wiley.

Chapelle, F. H., Bradley, P. M., Lovley, D. R., and Vroblesky, D. A. (1996). Measuring Rates of Biodegradation in a Contaminated Aquifer Using Field and Laboratory Methods. *Ground Water*, 34(4):691–698.

Cheng, S. M. and Foght, J. M. (2007). Cultivation-independent and -dependent characterization of Bacteria resident beneath John Evans Glacier. *FEMS Microbiology Ecology*, 59(2):318–30.

Chillrud, S. N., Pedrozo, F. L., Temporetti, P. F., Planas, H. F., and Froelich, P. N. (1994). Chemical weathering of phosphate and germanium in glacial meltwater streams : Effects of subglacial pyrite oxidation. *Limnology and Oceanography*, 39(5):1130–1140.

Christner, B. C., Priscu, J. C., Achberger, A. M., Barbante, C., Carter, S. P., Christianson, K., Michaud, A. B., Mikucki, J. a., Mitchell, A. C., Skidmore, M. L., Vick-Majors, T. J., Adkins, W. P., Anandakrishnan, S., Barcheck, G., Beem, L., Behar, a., Beitch, M., Bolsey, R., Branecky, C., Edwards, R., Fisher, a., Fricker, H. a., Foley, N., Guthrie, B., Hodson, T., Jacobel, R., Kelley, S., Mankoff, K. D., McBryan, E., Powell, R., Purcell, a., Sampson, D., Scherer, R., Sherve, J., Siegfried, M., and Tulaczyk, S. (2014). A microbial ecosystem beneath the West Antarctic ice sheet. *Nature*, 512(7514):310–313.

Coale, K. H., Johnson, K. S., Chavez, F. P., Buesseler, K. O., Barber, R. T., Brzezinski, M. A., Cochlan, W. P., Millero, F. J., Falkowski, P. G., Bauer, J. E., Wanninkhof, R. H., Kudela, R. M., Altabet, M. A., Hales, B. E., Takahashi, T., Landry, M. R., Bidigare, R. R., Wang, X., Chase, Z., Strutton, P. G., Friederich, G. E., Gorbunov, M. Y., Lance, V. P., Hilting, A. K., Hiscock, M. R., Demarest, M., Hiscock, W. T., Sullivan, K. F., Tanner, S. J., Gordon, R. M., Hunter, C. N., Elrod, V. A., Fitzwater, S. E., Jones, J. L., Tozzi, S., Koblizek, M., Roberts, A. E., Herndon, J., Brewster, J., Ladizinsky, N., Smith, G., Cooper, D., Timothy, D., Brown, S. L., Selph, K. E., Sheridan, C. C., Twining, B. S., and Johnson, Z. I. (2004). Southern Ocean iron enrichment experiment: carbon cycling in high- and low-Si waters. *Science (New York, N.Y.)*, 304(5669):408–414.

Cook, J., Hodson, A., Telling, J., Anesio, A., Irvine-Fynn, T., and Bellas, C. (2010). The mass-area relationship within cryoconite holes and its implications for primary production. *Annals of Glaciology*, 51(56):106–110.

Cuffey, K. and Paterson, W. S. B. (2010). *The Physics of Glaciers*. Academic Press. Butterworth-Heinemann/Elsevier, 4th edition.

Dallmann, W, K., Piepjohn, K., and Blomeier, D. (2004). Geological map of Billefjorden, Central Spitsbergen, Svalbard with geological excursion guide. *Norsk Polarinstitutt*.

Dattagupta, S., Schaperdoth, I., Montanari, A., Mariani, S., Kita, N., Valley, J. W., and Macalady, J. L. (2009). A novel symbiosis between chemoauto-

trophic bacteria and a freshwater cave amphipod. *The ISME journal*, 3(8):935–943.

de Baar, H., Buma, A., Nolting, R. F., Cadee, G. C., Jacques, G., and Treguer, P. J. (1990). On iron limitation of the Southern Ocean : experimental observations in the Weddell and Scotia Seas. *Marine Ecology Progress Series*, 65:105–122.

Death, R., Wadham, J. L., Monteiro, F., Le Brocq, a. M., Tranter, M., Ridgwell, A., Dutkiewicz, S., and Raiswell, R. (2014). Antarctic ice sheet fertilises the Southern Ocean. *Biogeosciences*, 11(10):2635–2643.

D'Elia, T., Veerapaneni, R., and Rogers, S. O. (2008). Isolation of microbes from Lake Vostok accretion ice. *Applied and Environmental Microbiology*, 74(15):4962–4965.

Dhungana, S. and Crumbliss, A. L. (2005). Coordination Chemistry and Redox Processes in Siderophore-Mediated Iron Transport. *Geomicrobiology Journal*, 22(3-4):87–98.

Dix, N. J. (2012). *Fungal Ecology*. Springer Netherlands.

Dobrovolsky, E. V. (1987). Physico-chemical mechanisms of weathering processes and corresponding models of dynamics of mineral zonality evolution. *Chemical Geology*, 60:89–94.

dos Santos Furtado, A. and Casper, P. (2000). Different methods for extracting bacteria from freshwater sediment and a simple method to measure bacterial production in sediment samples. *Journal of Microbiological Methods*, 41(3):249–57.

Dowdeswell, J. a., Hodgkins, R., Nuttall, a. M., Hagen, J. O., and Hamilton, G. S. (1995). Mass balance changes as a control on the frequency and occurrence of glacier surges in Svalbard, Norwegian High Arctic. *Geophysical Research Letters*, 22(21):2909–2912.

Doyle, S. (2015). *Diversity and Activity of Bacteral in Basal Ice Environments*. PhD thesis, Louisiana State University.

Dubelman, S., Fischer, J., Zapata, F., Huizinga, K., Jiang, C., Uffman, J., Levine, S., and Carson, D. (2014). Environmental fate of double-stranded RNA in agricultural soils. *PLoS ONE*, 9(3).

Dubnick, A., Barker, J., Sharp, M., Wadham, J., Lis, G., Telling, J., Fitzsimons, S., and Jackson, M. (2010). Characterization of dissolved organic matter (DOM) from glacial environments using total fluorescence spectroscopy and parallel factor analysis. *Annals of Glaciology*, 51(56):111–122.

Ehrlich, H. L. and Newman, D. K. (2009). *Geomicrobiology*. CRC Press, London.

Escher, J. (1990). Geological map of Greenland 1 : 500 000. Technical report, Skjoldungen. Geol. Sure., Copenhagen, Denmark.

Evans, D. J., Strzelecki, M., Milledge, D. G., and Orton, C. (2012). Hørbyebreen polythermal glacial landsystem, Svalbard. *Journal of Maps*, 8(2):146–156.

Fellman, J. B., Hood, E., Spencer, R. G. M., Stubbins, A., and Raymond, P. a. (2014). Watershed Glacier Coverage Influences Dissolved Organic Matter Biogeochemistry in Coastal Watersheds of Southeast Alaska. *Ecosystems*, 17(6):1014–1025.

Fogg, G. E. (1967). Observations on the Snow Algae of the South Orkney Islands. *Philosophical Transactions of the Royal Society B: Biological Sciences*, 252(777):279–287.

Foght, J., Aislabie, J., Turner, S., Brown, C. E., Ryburn, J., Saul, D. J., and Lawson, W. (2004). Culturable Bacteria in Subglacial Sediments and Ice from Two Southern Hemisphere Glaciers. *Microbial Ecology*, 47(4):329–340.

Fordyce, S. L., Kampmann, M.-L., van Doorn, N. L., and Gilbert, M. T. P. (2013). Long-term RNA persistence in postmortem contexts. *Investigative Genetics*, 4(1):7.

Fountain, A. G. and Walder, J. S. (1998). Water flow through temperate glaciers. *Reviews of Geophysics*, 36(97):299–328.

Fukuda, R., Ogawa, H., Nagata, T., and Koike, I. (1998). Direct determination of carbon and nitrogen contents of natural bacterial assemblages in marine environments. *Applied and Environmental Microbiology*, 64(9):3352–8.

Gaidos, E., Lanoil, B., Thorsteinsson, T., Graham, A., Skidmore, M., Han, S.-k., Rust, T., and Popp, B. (2004). A viable microbial community in a subglacial volcanic crater lake, Iceland. *Astrobiology*, 4(3):327–344.

Gaidos, E., Marteinsson, V., Thorsteinsson, T., Jóhannesson, T., Rúnarsson, A. R., Stefansson, A., Glazer, B., Lanoil, B., Skidmore, M., Han, S., Miller, M., Rusch, A., and Foo, W. (2009). An oligarchic microbial assemblage in the anoxic bottom waters of a volcanic subglacial lake. *The ISME journal*, 3(4):486–97.

Gardner, A. S., Moholdt, G., Wouters, B., Wolken, G. J., Burgess, D. O., Sharp, M. J., Cogley, J. G., Braun, C., and Labine, C. (2011). Sharply increased mass loss from glaciers and ice caps in the Canadian Arctic Archipelago. *Nature*, 473(7347):357–360.

Gasol, J. M., Giorgio, P. A. D. E. L., and del Giorgio, P. a. (2000). Using flow cytometry for counting natural planktonic bacteria and understanding the structure of planktonic bacterial communities. *Scientia Marina*, 64(2):197–224.

Geelhoed, J. S., Sorokin, D. Y., Epping, E., Tourova, T. P., Banciu, H. L., Muyzer, G., Stams, A. J. M., and van Loosdrecht, M. C. M. (2009). Microbial sulfide oxidation in the oxic-anoxic transition zone of freshwater sediment: involvement of lithoautotrophic Magnetospirillum strain J10. *FEMS Microbiology Ecology*, 70(1):54–65.

Geider, R. J. and La Roche, J. (1994). The role of iron in phytoplankton photosynthesis, and the potential for iron-limitation of primary productivity in the sea. *Photosynthesis Research*, 39(3):275–301.

Giovanela, M., Crespo, J. S., Antunes, M., Adamatti, D. S., Fernandes, A. N., Barison, A., Da Silva, C. W. P., Guégan, R., Motelica-Heino, M., and Sierra, M. M. D. (2010). Chemical and spectroscopic characterization of humic acids extracted from the bottom sediments of a Brazilian subtropical microbasin. *Journal of Molecular Structure*, 981(1-3):111–119.

Gleisner, M., Herbert, R. B., and Frogner Kockum, P. C. (2006). Pyrite oxidation by Acidithiobacillus ferrooxidans at various concentrations of dissolved oxygen. *Chemical Geology*, 225(1-2):16–29.

Goldstein, J. I., Newbury, D. E., Echlin, P., David C, J., Lyman, C. E., Lifshin, E., Sawyer, L., and Michael, J. R. (2003). *Scanning Electron Microscopy and X-Ray Microanalysis. A text for Biologists, Material Scientists and Geologists.* Plenum Press, London, 2nd edition.

Göransson, H., Olde Venterink, H., and Bååth, E. (2011). Soil bacterial growth and nutrient limitation along a chronosequence from a glacier forefield. *Soil Biology and Biochemistry*, 43(6):1333–1340.

Gordon, J. E. and Timmis, R. J. (1992). Glacier fluctuations on South Georgia during the 1970s and early 1980s. *Antarctic Science*, 4(02):215–226.

Griebler, C., Mindl, B., and Slezak, D. (2001). Combining DAPI and SYBR Green II for the enumeration of total bacterial numbers in aquatic sediments. *International Review of Hydrobiology*, 86(4-5):453–465.

Griffiths, P. R. (1992). The Handbook of Infrared and Raman Characteristic Frequencies of Organic Molecules. *Vibrational Spectroscopy*, 4(1):121.

Hagen, J. O., Liestøl, O., Roland, E., and Jørgensen, T. (1993). *Glacier Atlas of Svalbard and Jan Mayen*. Meddelelser (Norsk polarinstitutt). Norsk polarinstitutt.

Hagen, J. O., Melvold, K., Pinglot, F., and Dowdeswell, J. a. (2003). On the Net Mass Balance of the Glaciers and Ice Caps in Svalbard, Norwegian Arctic. *Arctic, Antarctic, and Alpine Research*, 35(2):264–270.

Hall, C. R., Behe, B. K., Campbell, B. L., Dennis, J. H., Lopez, R. G., and Yue, C. (2012). The appeal of biodegradable packaging to US floral consumers. *Acta Horticulturae*, 930(4):121–126.

Hall, E. K. and Cotner, J. B. (2007). Interactive effect of temperature and resources on carbon cycling by freshwater bacterioplankton communities. *Aquatic Microbial Ecology*, 49(1):35–45.

Harder, J. (1997). Species-independent maintenance energy and natural population sizes. *FEMS Microbiology Ecology*, 23(1):39–44.

Hawkings, J., Wadham, J., Tranter, M., Lawson, E., Sole, A., Cowton, T., Tedstone, A., Bartholomew, I., Nienow, P., Chandler, D., and Telling, J. (2015). The effect of warming climate on nutrient and solute export from the Greenland Ice Sheet. *Geochemical Perspectives Letters*, pages 94–104.

Hawkings, J. R., Wadham, J. L., Tranter, M., Raiswell, R., Benning, L. G., Statham, P. J., Tedstone, A., Nienow, P., Lee, K., and Telling, J. (2014). Ice sheets as a significant source of highly reactive nanoparticulate iron to the oceans. *Nature communications*, 5(May):3929.

Heidel, C. and Tichomirowa, M. (2011). The isotopic composition of sulfate from anaerobic and low oxygen pyrite oxidation experiments with ferric iron - New insights into oxidation mechanisms. *Chemical Geology*, 281(3-4):305–316.

Hobbs, G. J. (1968). The geology of the South Shetland Islands - IV - the geology of Livingston Island. Technical report, BAS Scientific Report 47, London.

Hodgkins, R., Hagen, J. O., and Hamran, S. E. (1999). Twentieth-century mass balance and thermal regime change at an Arctic glacier. *Annals Of Glaciology*, 28:216–220.

Hodgkins, R., Tranter, M., and Dowdeswell, J. a. (1998). The hydrochemistry of runoff from a 'cold-based' glacier in the High Artic (Scott Turnerbreen, Svalbard). *Hydrological Processes*, 12(January 1997):87–103.

Hodson, A., Anesio, A. M., Ng, F., Watson, R., Quirk, J., Irvine-Fynn, T., Dye, A., Clark, C., Mccloy, P., Kohler, J., and Sattler, B. (2007). A glacier respires: Quantifying the distribution and respiration CO2 flux of cryoconite across an entire arctic supraglacial ecosystem. *Journal of Geophysical Research: Biogeosciences*, 112(4):1–9.

Hodson, A., Cameron, K., Bøggild, C., Irvine-fynn, T., Langford, H., Pearce, D., and Banwart, S. (2010a). The structure, biological activity and biogeochemistry of cryoconite aggregates upon an Arctic valley glacier: Longyearbreen, Svalbard. *Journal of Glaciology*, 56(196):349–362.

Hodson, A., Heaton, T., Langford, H., and Newsham, K. (2009). Chemical weathering and solute export by meltwater in a maritime Antarctic glacier basin. *Biogeochemistry*, 98(1-3):9–27.

Hodson, A., Mumford, P., and Lister, D. (2004). Suspended sediment and phosphorus in proglacial rivers: bioavailability and potential impacts upon the P status of ice-marginal receiving waters. *Hydrological Processes*, 18(13):2409–2422.

Hodson, A., Roberts, T. J., Engvall, A. C., Holmén, K., and Mumford, P. (2010b). Glacier ecosystem response to episodic nitrogen enrichment in Svalbard, European High Arctic. *Biogeochemistry*, 98(1-3):171–184.

Hodson, A. J., Anesio, A. M., Tranter, M., Fountain, A. G., Osborn, M., Priscu, J. C., Laybourn-Parry, J., and Sattler, B. (2008). Glacial Ecosystems. *Ecological Monographs*, 78(1):41–67.

Hofreiter, M., Jaenicke, V., Serre, D., Haeseler Av, a., and Pääbo, S. (2001). DNA sequences from multiple amplifications reveal artifacts induced by cytosine deamination in ancient DNA. *Nucleic acids research*, 29(23):4793–4799.

Hood, E., Battin, T. J., Fellman, J., Neel, S. O., and Spencer, R. G. M. (2015). Storage and release of organic carbon from glaciers and ice sheets. *Nature Publishing Group*, 8(2):91–96.

Hood, E., Fellman, J., Spencer, R. G. M., Hernes, P. J., Edwards, R., D'Amore, D., and Scott, D. (2009). Glaciers as a source of ancient and labile organic matter to the marine environment. *Nature*, 462(7276):1044–7.

Hopwood, M. J., Bacon, S., Arendt, K., Connelly, D. P., and Statham, P. J. (2015). Glacial meltwater from Greenland is not likely to be an important source of Fe to the North Atlantic. *Biogeochemistry*, 124(1):1–11.

Hurtgen, M. T., Arthur, M. A., Suits, N. S., and Kaufman, A. J. (2002). The sulfur isotopic composition of Neoproterozoic seawater sulfate: Implications for a snowball Earth? *Earth and Planetary Science Letters*, 203(1):413–429.

Irvine-Fynn, T. and Hodson, A. J. (2010). Biogeochemistry and dissolved oxygen dynamics at a subglacial upwelling Midtre Lovenbreen, Svalbard. *Annals of Glaciology*, 51(56):41–46.

Jania, J. A. and Navarro, F. (2010). Sensitivity of Svalbard glaciers to climate change (SvalGlac). Technical Report April, University of Silesia.

Kastovská, K., Elster, J., Stibal, M., and Santrucková, H. (2005). Microbial assemblages in soil microbial succession after glacial retreat in Svalbard (high arctic). *Microbial Ecology*, 50(3):396–407.

Kaštovská, K., Stibal, M., Šabacká, M., Černá, B., Šantručková, H., and Elster, J. (2006). Microbial community structure and ecology of subglacial sediments in two polythermal Svalbard glaciers characterized by epifluorescence microscopy and PLFA. *Polar Biology*, 30(3):277–287.

Keer, J. T. and Birch, L. (2003). Molecular methods for the assessment of bacterial viability. *Journal of Microbiological Methods*, 53(2):175–183.

Kehoe, M., Beavis, S., and Welch, S. (2004). Investigating the role of biotic versus abiotic processes in the generation of acid sulfate soils in coastal NSW. In I.C., R., editor, *Regolith*, pages 171–174. CRC Press.

Kepner, R. L. and Pratt, J. R. (1994). Use of fluorochromes for direct enumeration of total bacteria in environmental samples: past and present. *Microbiological Reviews*, 58(4):603–15.

Kirchman, D. (1993). Measuring Bacterial Biomass Production and Growth Rates from Leucine Incorporation in Natural Aquatic Environments. *Bacterial Biomass Production and Growth Rates*, 30:227–237.

Knight, P. G. (2008). *Glacier Science and Environmental Change*. Wiley.

Knudsen, N. T. and Hasholt, B. (1999). Radio-echo Sounding at the Mittvakkat Gletscher, Southeast Greenland. *Arctic, Antarctic, and Alpine Research*, 31(3):321–328.

Kostka, J. E. and Luther, G. W. (1994). Partitioning and speciation of solid phase iron in saltmarsh sediments. *Geochimica et Cosmochimica Acta*, 58(7):1701–1710.

Koziol, K., Moggridge, H. L., and Hodson, A. J. (2016). The organic carbon budget of a glacial system: can glaciers recycle organic matter?

Lafrenière, M. J. and Sharp, M. J. (2004). The Concentration and Fluorescence of Dissolved Organic Carbon (DOC) in Glacial and Nonglacial Catchments: Interpreting Hydrological Flow Routing and DOC Sources. *Arctic, Antarctic and Alpine Research*, 36(2):156–165.

Lafrenière, M. J. and Sharp, M. J. (2005). A comparison of solute fluxes and sources from glacial and non-glacial catchments over contrasting melt seasons. *Hydrological Processes*, 19(15):2991–3012.

Lam, P., Lavik, G., Jensen, M. M., van de Vossenberg, J., Schmid, M., Woebken, D., Gutiérrez, D., Amann, R., Jetten, M. S. M., and Kuypers, M. M. M. (2009). Revising the nitrogen cycle in the Peruvian oxygen minimum zone. *Proceedings of the National Academy of Sciences of the United States of America*, 106(12):4752–4757.

Lamb, H. R., Tranter, M., Brown, G. H., Hubbard, B. P., Sharp, M. J., Gordon, S., Smart, C. C., Willis, I. C., and Nielsen, M. K. (1995). The composition of subglacial meltwaters sampled from boreholes at the Haut Glacier d'Arolla, Switzerland. *IAHS Publications-Series of Proceedings and Reports-Intern Assoc Hydrological Sciences*, 228:395–404.

Langford, H., Hodson, A., Banwart, S., and Bøggild, C. (2010). The microstructure and biogeochemistry of Arctic cryoconite granules. *Annals of Glaciology*, 51(56):87–94.

Lanoil, B., Skidmore, M., Priscu, J. C., Han, S., Foo, W., Vogel, S. W., Tulaczyk, S., and Engelhardt, H. (2009). Bacteria beneath the West Antarctic ice sheet. *Environmental Microbiology*, 11(3):609–15.

Lawson, E. C. (2012). *Investigating Carbon Sourcing and Cycling in Subglacial Environments*. PhD thesis, University of Bristol.

Lawson, E. C., Wadham, J. L., Lis, G. P., Tranter, M., Pickard, a. E., Stibal, M., Dewsbury, P., and Fitzsimons, S. (2015). Identification and analysis of low molecular weight dissolved organic carbon in subglacial basal ice ecosystems by ion chromatography. *Biogeosciences Discussions*, 12(16):14139–14174.

Lawson, E. C., Wadham, J. L., Tranter, M., Stibal, M., Lis, G. P., Butler, C. E. H., Laybourn-Parry, J., Nienow, P., Chandler, D., and Dewsbury, P. (2014). Greenland Ice Sheet exports labile organic carbon to the Arctic oceans. *Biogeosciences*, 11:4015–4028.

Laybourn-Parry, J. and Hodson, A. (2012). Subglacial Environments. In *Subglacial Biogeochemistry Book Chapter*.

Laybourn-Parry, J., Hodson, A., Tranter, M., and Hodson, A. (2012). *The Ecology of Snow and Ice Environments*. Oxford University Press, Oxford.

Legrand, M., Preunkert, S., Jourdain, B., Guilhermet, J., Faïn, X., Alekhina, I., and Petit, J. R. (2013). Water-soluble organic carbon in snow and ice deposited at Alpine, Greenland, and Antarctic sites: A critical review of available data and their atmospheric relevance. *Climate of the Past*, 9:2195–2211.

Lim, E. L., Amaral, L. A., Caron, D. A., and DeLong, E. F. (1993). Application of rRNA-based probes for observing marine nanoplanktonic protists. *Applied and Environmental Microbiology*, 59(5):1647–1655.

Lin, X., Wakeham, S. G., Putnam, I. F., Astor, Y. M., Scranton, M. I., Chistoserdov, A. Y., and Taylor, G. T. (2006). Comparison of vertical distributions of prokaryotic assemblages in the anoxic cariaco basin and black sea by use of fluorescence in situ hybridization. *Applied and Environmental Microbiology*, 72(4):2679–2690.

Lis, G. P., Wadham, J. L., Lawson, E., Stibal, M., and Telling, J. (2010). Organic chemistry of basal ice - presence of labile , low molecular weight compounds available for microbial metabolism. *Geophysical Research Letters*, 12:EGU2010–9977.

Lovley, D. R. and Chapelle, F. H. (1995). Deep Subsurface Microbial Processes. *Reviews of Geophysics*, 33(3):365–381.

Luther, G. W., Findlay, A. J., MacDonald, D. J., Owings, S. M., Hanson, T. E., Beinart, R. a., and Girguis, P. R. (2011). Thermodynamics and Kinetics of Sulfide Oxidation by Oxygen: A Look at Inorganically Controlled Reactions and Biologically Mediated Processes in the Environment. *Frontiers in Microbiology*, 2(April):1–9.

Lutz, S., Anesio, A. M., Jorge Villar, S. E., and Benning, L. G. (2014). Variations of algal communities cause darkening of a Greenland glacier. *FEMS Microbiology Ecology*, 89(2):402–414.

Madigan, M. T. (2009). *Brock Biology of Microorganisms*. Pearson international edition. Pearson/Benjamin Cummings.

Madsen, E. L. (2011). *Environmental Microbiology: From Genomes to Biogeochemistry*. John Wiley and Sons.

Major, H. and Nagy, J. (1972). Geology of the Adventdalen map area : with a geological map, Svalbard C9G 1:100 000. Technical report, Norsk Polarinstitutt, Oslo.

Manz, W., Amann, R., Ludwig, W., Vancanneyt, M., and Schleifer, K. H. (1996). Application of a suite of 16S rRNA-specific oligonucleotide probes designed to investigate bacteria of the phylum cytophaga-flavobacter-bacteroides in the natural environment. *Microbiology (Reading, England)*, 142(5):1097–106.

Manz, W., Amann, R., Ludwig, W., Wagner, M., and Schleifer, K.-H. (1992). Phylogenetic Oligodeoxynucleotide Probes for the Major Subclasses of Proteobacteria: Problems and Solutions. *Systematic and Applied Microbiology*, 15(4):593–600.

Marie, D., Brussaard, C. P. D., Thyrhaug, R., Bratbak, G., and Vaulot, D. (1999). Enumeration of marine viruses in culture and natural samples by flow cytometry. *Applied and Environmental Microbiology*, 65(1):45–52.

Marie, D., Partensky, F., Vaulot, D., and Brussaard, C. (2001). Enumeration of Phytoplankton, Bacteria, and Viruses in Marine Samples. In *Current Protocols in Cytometry*, volume Chapter 11, page Unit 11.11.

Mazumdar, A., Goldberg, T., and Strauss, H. (2008). Abiotic oxidation of pyrite by Fe(III) in acidic media and its implications for sulfur isotope measurements of lattice-bound sulfate in sediments. *Chemical Geology*, 253(1-2):30–37.

Mehrotra, R. S. and Sumbali, M. A. (2009). *Principles Of Microbiology*. McGraw-Hill Education (India) Pvt Ltd.

Mernild, S. H., Knudsen, N. T., Hoffman, M. J., Yde, J. C., Lipscomb, W. H., Hanna, E., Malmros, J. K., and Fausto, R. S. (2012). Thinning and slowdown of Greenland's Mittivakkat Gletscher. *The Cryosphere Discussions*, 6(5):4387–4415.

Mernild, S. H., Knudsen, N. T., Lipscomb, W. H., Yde, J. C., Malmros, J. K., Hasholt, B., and Jakobsen, B. H. (2011). Increasing mass loss from Greenland's Mittivakkat Gletscher. *Cryosphere*, 5(2):341–348.

Meyers, P. a. and Ishiwatari, R. (1993). Lacustrine organic geochemistry-an overview of indicators of organic matter sources and diagenesis in lake sediments. *Organic Geochemistry*, 20(7):867–900.

Mikucki, J. A., Foreman, C. M., Sattler, B., Berry Lyons, W., and Priscu, J. C. (2004). Geomicrobiology of blood falls: An iron-rich saline discharge at the terminus of the Taylor Glacier, Antarctica. *Aquatic Geochemistry*, 10(3-4):199–220.

Mikucki, J. A., Pearson, A., Johnston, D. T., Turchyn, A. V., Farquhar, J., Schrag, D. P., Anbar, A. D., Priscu, J. C., and Lee, P. A. (2009). A contemporary microbially maintained subglacial ferrous "ocean". *Science (New York, N.Y.)*, 324(5925):397–400.

Mikucki, J. A. and Priscu, J. C. (2007). Bacterial diversity associated with blood falls, a subglacial outflow from the Taylor Glacier, Antarctica. *Applied and Environmental Microbiology*, 73(12):4029–4039.

Mitchell, A. C. and Brown, G. H. (2008). Modeling Geochemical and Biogeochemical Reactions in Subglacial Environments. *Arctic, Antarctic and Alpine Research*, 40(3):531–547.

Mitchell, A. C., Lafrenière, M. J., Lange, R. K., Pitts, B., Skidmore, M. L., and Boyd, E. S. (2009). Mineralogical controls on microbial communities in glacial environments. In *Goldschmidt Conference Abstracts*, number 2008.

Mitchell, a. C., Lafreniere, M. J., Skidmore, M. L., and Boyd, E. S. (2013). Influence of bedrock mineral composition on microbial diversity in a subglacial environment. *Geology*, 41(8):855–858.

Miteva, V. I., Sheridan, P. P., and Brenchley, J. E. (2004). Phylogenetic and Physiological Diversity of Microorganisms Isolated from a Deep Greenland Glacier Ice Core Phylogenetic and Physiological Diversity of Microorganisms Isolated from a Deep Greenland Glacier Ice Core. *Applied Environmental Microbiology*, 70(1):202–213.

Molina, C., Navarro, F. J., Calvet, J., García-Sellés, D., and Lapazaran, J. J. (2007). Hurd Peninsula glaciers, Livingston Island, Antarctica, as indicators of regional warming: Ice-volume changes during the period 1956-2000. In *Annals of Glaciology*, volume 46, pages 43–49.

Montross, S. N., Skidmore, M., Tranter, M., Kivimaki, A.-L., and Parkes, R. J. (2012). A microbial driver of chemical weathering in glaciated systems. *Geology*, 41(2):215–218.

Moses, C. O. and Herman, J. S. (1991). Pyrite oxidation at circumneutral pH. *Geochimica et Cosmochimica Acta*, 55(2):471–482.

Navarro, F. J., Otero, J., Macheret, Y. Y., Vasilenko, E. V., Lapazaran, J. J., Ahlstrøm, a. P., and MacHío, F. (2009). Radioglaciological studies on Hurd Peninsula glaciers, Livingston Island, Antarctica. *Annals of Glaciology*, 50(51):17–24.

Neilands, J. (1995). Siderophores: Structure and Function of Microbial Iron Transport Compounds. *The Journal of Biological Chemistry*, 270(45):26723–26726.

Ng, T. F. F., Chen, L.-F., Zhou, Y., Shapiro, B., Stiller, M., Heintzman, P. D., Varsani, A., Kondov, N. O., Wong, W., Deng, X., Andrews, T. D., Moorman, B. J., Meulendyk, T., MacKay, G., Gilbertson, R. L., and Delwart, E. (2014). Preservation of viral genomes in 700-y-old caribou feces from a subarctic ice patch. *Proceedings of the National Academy of Sciences*, 111(47):16842–16847.

Nienow, P. W., Sharp, M. J., and Willis, I. C. (1998). Seasonal changes in the morphology of the subglacial drainage system, Haut Glacier d'Arolla, Switzerland. *Earth Surface Processes and Landforms*, 23(9):825–843.

Nordstrom, B. D. K., Wright, W. G., Mast, M. A., Bove, D. J., and Rye, R. O. (2008). Aqueous-Sulfate Stable Isotopes - A Study of Mining-Affected and Undisturbed Acidic Drainage. In Church, S. E., von Guerard, P., and Finger, Susan, E., editors, *Integrated Investigations of Environmental Effects of Historical Mining in the Animas River Watershed, San Juan County, Colorado*, chapter 8, pages 391–416. U.S. Geological Survey.

Nowak, A. and Hodson, A. (2013). Changes in meltwater chemistry over a 20 year period following a thermal regime switch from polythermal to cold-based glaciation at Austre Brøggerbreen, Svalbard. *Polar Research*, 1:1–19.

Panikov, N. S., Flanagan, P. W., Oechel, W. C., Mastepanov, M. a., and Christensen, T. R. (2006). Microbial activity in soils frozen to below -39C. *Soil Biology and Biochemistry*, 38(4):785–794.

Parekh, P. (2004). Modeling the global ocean iron cycle. *Global Biogeochemical Cycles*, 18(1):1–16.

Parlanti, E. (2000). Dissolved organic matter fluorescence spectroscopy as a tool to estimate biological activity in a coastal zone submitted to anthropogenic inputs. *Organic Geochemistry*, 31(12):1765–1781.

Pavia, D. L., Lampman, G. M., and Kriz, G. S. (2001). *Introduction to Spectroscopy: A Guide for Students of Organic Chemistry*. Saunders Golden Sunburst Series. Harcourt College Publishers.

Pearce, D., Hodgson, D., Thorne, M., Burns, G., and Cockell, C. (2013). Preliminary Analysis of Life within a Former Subglacial Lake Sediment in Antarctica. *Diversity*, 5(3):680–702.

Peterson, B. J. (1980). Aquatic Primary Productivity and the 14C-CO2 Method: A History of the Productivity Problem. *Annual Review of Ecology and Systematics*, 11(1):359–385.

Petsch, S. T., Eglington, T. I., and Edwards, K. J. (2001). 14C-dead living biomass: evidence for microbial assimilation of ancient organic carbon during shale weathering. *Science (New York, N.Y.)*, 292(5519):1127–31.

Pisapia, C., Chaussidon, M., Mustin, C., and Humbert, B. (2007). O and S isotopic composition of dissolved and attached oxidation products of pyrite by Acidithiobacillus ferrooxidans: Comparison with abiotic oxidations. *Geochimica et Cosmochimica Acta*, 71(10):2474–2490.

Plassen, L., Vorren, T. O., and Forwick, M. (2004). Integrated acoustic and coring investigation of glacigenic deposits in Spitsbergen fjords. *Polar Research*, 23(1):89–110.

Priscu, J. C., Adams, E. E., Lyons, W. B., Voytek, M. a., Mogk, D. W., Brown, R. L., McKay, C. P., Takacs, C. D., Welch, K. a., Wolf, C. F., Kirshtein, J. D., and Avci, R. (1999). Geomicrobiology of subglacial ice above Lake Vostok, Antarctica. *Science (New York, N.Y.)*, 286(5447):2141–4.

Priscu, J. C., Christner, B. C., Foreman, C. M., and Royston-Bishop, G. (2007). Biological Material in Ice Cores. In *Encyclopedia of Quaternary Sciences*, number October.

Radojevic, M. and Bashkin, V. N. (1999). *Practical Environmental Analysis*. Royal Society of Chemistry, 2nd edition.

Raiswell, R., Benning, L. G., Davidson, L., and Tranter, M. (2008a). Nanoparticulate bioavailable iron minerals in icebergs and glaciers. *Mineralogical Magazine*, 72(1):345–348.

Raiswell, R., Benning, L. G., Davidson, L., Tranter, M., and Tulaczyk, S. (2009). Schwertmannite in wet, acid, and oxic microenvironments beneath polar and polythermal glaciers. *Geology*, 37(5):431–434.

Raiswell, R., Benning, L. G., Tranter, M., and Tulaczyk, S. (2008b). Bioavailable iron in the Southern Ocean: the significance of the iceberg conveyor belt. *Geochemical Transactions*, 9:7.

Raiswell, R. and Canfield, D. E. (2012). The Iron Biogeochemical Cycle Past and Present. *Geochemical Perspectives*, 1(1):1–220.

Raiswell, R., Tranter, M., Benning, L. G., Siegert, M., De'ath, R., Huybrechts, P., and Payne, T. (2006). Contributions from glacially derived sediment to the global iron (oxyhydr)oxide cycle: Implications for iron delivery to the oceans. *Geochimica et Cosmochimica Acta*, 70(11):2765–2780.

Raiswell, R., Vu, H. P., Brinza, L., and Benning, L. G. (2010). The determination of labile Fe in ferrihydrite by ascorbic acid extraction: Methodology, dissolution kinetics and loss of solubility with age and de-watering. *Chemical Geology*, 278(1-2):70–79.

Raskin, L., Stromley, J. M., Rittmann, B. E., and Stahl, D. A. (1994). Group-specific 16S rRNA hybridization probes to describe natural communities of methanogens. *Applied and Environmental Microbiology*, 60(4):1232–1240.

Reitner, J., Quéric, N. V., and Arp, G. (2010). *Advances in Stromatolite Geobiology*. Lecture Notes in Earth Sciences. Springer.

Rimstidt, J. (2003). Pyrite oxidation: a state-of-the-art assessment of the reaction mechanism. *Geochimica et Cosmochimica Acta*, 67(5):873–880.

Rippin, D., Willis, I. A. N., Arnold, N., Hodson, A., Moore, J., Kohler, J., Ornsson, H. B. J., and Bjï¿œRnsson, H. (2003). Changes in geometry and subglacial drainage of Midre Lovenbreen, Svalbard, determined from digital elevation models. *Earth Surface Processes and Landforms*, 28(3):273–298.

Rivkina, E. M., Friedmann, E. I., McKay, C. P., and Gilichinsky, D. A. (2000). Metabolic activity of permafrost bacteria below the freezing point. *Applied and Environmental Microbiology*, 66(8):3230–3233.

Russell, J. B. and Cook, G. M. (1995). Energetics of bacterial growth: balance of anabolic and catabolic reactions. *Microbiological Reviews*, 59(1):48–62.

Samsonoff, W. A. and MacColl, R. (2001). Biliproteins and phycobilisomes from cyanobacteria and red algae at the extremes of habitat. *Archives of Microbiology*, 176(6):400–405.

Sattler, B., Tilg, M., Remias, D., and Psenner, R. (2012). Laser Induced Fluorescence Emission (L . I . F . E .): In Situ Non-Destructive Detection of Microbial Life on Supraglacial Environments. 14(APRIL):13353.

Schippers, A. and Jorgensen, B. B. (2001). Oxidation of pyrite and iron sulfide by manganese dioxide in marine sediments. *Geochimica et Cosmochimica Acta*, 65(6):915–922.

Semevskij, D. and Škatov, E. (1965). *Materialy po geologii picbergena. (The geology of Spitsbergen.)*. Scientific Research Institute of Arctic Geology, Leningrad.

Sharp, M., Parkes, J., Cragg, B., Fairchild, I. J., Lamb, H., and Tranter, M. (1999). Widespread bacterial populations at glacier beds and their relationship to rock weathering and carbon cycling. *Geology*, 27(2):107–110.

Shine, K. P., Derwent, R. G., Wuebbles, D. J., and Morcrette, J.-J. (1990). Radiative Forcing of Climate. *Climate Change: The IPCC Scientific Assessment. Report prepared for Intergovernmental Panel on Climate Change by Working Group I.*

Siegfried, W. R., Condy, P. R., and Laws, R. M. (2013). *Antarctic Nutrient Cycles and Food Webs*. Springer Berlin Heidelberg.

Simon, M. and Azam, F. (1989). Protein content and protein synthesis rates of planktonic marine bacteria . *Marine Ecology Progress Series*, 51:201–213.

Singer, P. C. and Stumm, W. (1970). Acidic mine drainage: the rate-determining step. *Science (New York, N.Y.)*, 167(3921):1121–3.

Skidmore, M., Anderson, S. P., Sharp, M., Foght, J., and Lanoil, B. D. (2005). Comparison of microbial community compositions of two subglacial environments reveals a possible role for microbes in chemical weathering processes. *Applied and Environmental Microbiology*, 71(11):6986–6997.

Skidmore, M., Tranter, M., Tulaczyk, S., and Lanoil, B. (2010). Hydrochemistry of ice stream beds - evaporitic or microbial effects? *Hydrological Processes*, 24(November 2008):517–523.

Skidmore, M. L., Foght, J. M., and Sharp, M. J. (2000). Microbial Life beneath a High Arctic Glacier. *Applied and Environmental Microbiology*, 66(8):3214–3220.

Skidmore, M. L. and Sharp, M. J. (1999). Drainage system behaviour of a High-Arctic polythermal glacier. *Annals of Glaciology*, 28(1):209–215.

Slemmons, K. E. H., Saros, J. E., and Simon, K. (2013). The influence of glacial meltwater on alpine aquatic ecosystems: a review. *Environmental Science. Processes and Impacts*, 15(10):1794–806.

Smith, L. a., Jim Hendry, M., Wassenaar, L. I., and Lawrence, J. (2012). Rates of microbial elemental sulfur oxidation and 18O and 34S isotopic fractionation under varied nutrient and temperature regimes. *Applied Geochemistry*, 27(1):186–196.

Sonjak, S., Frisvad, J. C., and Gunde-Cimerman, N. (2006). Penicillium mycobiota in Arctic subglacial ice. *Microbial Ecology*, 52(2):207–216.

Stam, M. C., Mason, P. R., Laverman, A. M., Pallud, C., and Cappellen, P. V. (2011). 34S/32S fractionation by sulfate-reducing microbial communities in estuarine sediments. *Geochimica et Cosmochimica Acta*, 75(14):3903–3914.

Stanish, L. F., Bagshaw, E. a., McKnight, D. M., Fountain, a. G., and Tranter, M. (2013). Environmental factors influencing diatom communities in Antarctic cryoconite holes. *Environmental Research Letters*, 8(4):045006.

Stankiewicz, B. a., Briggs, D. E. G., Michels, R., Collinson, M. E., Flannery, M. B., and Evershed, R. P. (2000). Alternative origin of aliphatic polymer in kerogen. *Geology*, 28(6):559–562.

Statham, P. J. and Hart, V. (2005). Dissolved iron in the Cretan Sea (eastern Mediterranean). *Limnology and Oceanography*, 50(4):1142–1148.

Statham, P. J., Skidmore, M., and Tranter, M. (2008). Inputs of glacially derived dissolved and colloidal iron to the coastal ocean and implications for primary productivity. *Global Biogeochemical Cycles*, 22(August):1–11.

Stibal, M., Bælum, J., Holben, W. E., Sørensen, S. R., Jensen, A., and Jacobsen, C. S. (2012a). Microbial degradation of 2,4-dichlorophenoxyacetic acid on the greenland ice sheet. *Applied and Environmental Microbiology*, 78(15):5070–5076.

Stibal, M., Hasan, F., Wadham, J. L., Sharp, M. J., and Anesio, A. M. (2012b). Prokaryotic diversity in sediments beneath two polar glaciers with contrasting organic carbon substrates. *Extremophiles*, 16(2):255–65.

Stibal, M., Sabacká, M., and Kastovská, K. (2006). Microbial communities on glacier surfaces in Svalbard: impact of physical and chemical properties

on abundance and structure of cyanobacteria and algae. *Microbial Ecology*, 52(4):644–54.

Stibal, M., Wadham, J. L., Lis, G. P., Telling, J., Pancost, R. D., Dubnick, A., Sharp, M. J., Lawson, E. C., Butler, C. E. H., Hasan, F., Tranter, M., and Anesio, A. M. (2012c). Methanogenic potential of Arctic and Antarctic subglacial environments with contrasting organic carbon sources. *Global Change Biology*, 18(11):3332–3345.

Stone, P. (1980). The Geology of South Georgia: IV. Barff Peninsula and Royal Bay Areas.

Stubbins, A., Hood, E., Raymond, P. a., Aiken, G. R., Sleighter, R. L., Hernes, P. J., Butman, D., Hatcher, P. G., Striegl, R. G., Schuster, P., Abdulla, H. a. N., Vermilyea, A. W., Scott, D. T., and Spencer, R. G. M. (2012). Anthropogenic aerosols as a source of ancient dissolved organic matter in glaciers. *Nature Geoscience*, 5(3):198–201.

Swift, D. ., Nienow, P. W., Hoey, T. B., and Mair, D. W. (2005). Seasonal evolution of runoff from Haut Glacier d'Arolla, Switzerland and implications for glacial geomorphic processes. *Journal of Hydrology*, 309(1-4):133–148.

Telling, J., Anesio, A. M., Tranter, M., Irvine-Fynn, T., Hodson, A., Butler, C., and Wadham, J. (2011). Nitrogen fixation on Arctic glaciers, Svalbard. *Journal of Geophysical Research: Biogeosciences*, 116(3):2–9.

Telling, J., Boyd, E. S., Bone, N., Jones, E. L., Tranter, M., MacFarlane, J. W., Martin, P. G., Wadham, J. L., Lamarche-Gagnon, G., Skidmore, M. L., Hamilton, T. L., Hill, E., Jackson, M., and Hodgson, D. a. (2015). Rock comminution as a source of hydrogen for subglacial ecosystems. *Nature Geoscience*, 8(11):851–855.

Thomas, A. G. and Raiswell, R. (1984). Solute acquisition in glacial melt waters. II. Argentiere (French Alps): bulk melt waters with open-system characteristics. *Journal of Glaciology*, 30(104):44–48.

Thór Marteinsson, V., Rúnarsson, Á., Stefánsson, A., Thorsteinsson, T., Jóhannesson, T., Magnússon, S. H., Reynisson, E., Einarsson, B., Wade, N., Morrison, H. G., and Gaidos, E. (2012). Microbial communities in the subglacial waters of the Vatnajökull ice cap, Iceland. *The ISME Journal*, pages 427–437.

Tichomirowa, M. and Junghans, M. (2009). Oxygen isotope evidence for sorption of molecular oxygen to pyrite surface sites and incorporation into sulfate in oxidation experiments. *Applied Geochemistry*, 24(11):2072–2092.

Tipson, R. S. (1968). Infrared Spectroscopy Of Carbohydrates: a Review of the literature. Technical report, The National Bureau of Standards, Washington D.C..

Torgersen, T. and Branco, B. (2007). Carbon and oxygen dynamics of shallow aquatic systems: Process vectors and bacterial productivity. *Journal of Geophysical Research: Biogeosciences*, 112:1–16.

Touratier, F., Legendre, L., and Vézina, A. (1999). Model of bacterial growth influenced by substrate C:N ratio and concentration. *Aquatic Microbial Ecology*, 19(2):105–118.

Tranter, M., Brown, G., Raiswell, R., Sharp, M., and Gurnell, A. (1993). A conceptual model of solute acquisition by Alpine glacial meltwaters. *Journal of Glaciology*, 39(133):573–581.

Tranter, M., Brown, G. H., Hodson, A., Gurnell, A., and Sharp, M. (1994). Variations in the nitrate concentration of glacial runoff in alpine and subpolar environments. In Jones, H. and Davies, T., editors, *Snow And Ice Covers: Interactions With The Atmosphere And Ecosystems*, pages 299–311. IAHS Publications.

Tranter, M., Brown, G. H., Hodson, A. J., and Gurnell, A. M. (1996). Hydrochemistry as an indicator of subglacial drainage system structure: A comparison of Alpine and sub-polar environments. *Hydrological Processes*, 10(4):541–556.

Tranter, M., Sharp, M. J., Lamb, H. R., Brown, G. H., Hubbard, B. P., and Willis, I. C. (2002). Geochemical weathering at the bed of Haut Glacier d'Arolla, Switzerland - a new model. *Hydrological Processes*, 993(January 2001):959–993.

Tranter, M. and Skidmore, M. (2005). Hydrological controls on microbial communities in subglacial environments. *Hydrological Processes*, 998(January):995–998.

Trevors, J. T. (1996). Sterilization and inhibition of microbial activity in soil. *Journal of Microbiological Methods*, 26(1-2):53–59.

Uroz, S., Calvaruso, C., Turpault, M.-P., and Frey-Klett, P. (2009). Mineral weathering by bacteria: ecology, actors and mechanisms. *Trends in Microbiology*, 17(8):378–87.

Vaclavkova, S., Schultz-Jensen, N., Jacobsen, O. S., Elberling, B., and Aamand, J. (2015). Nitrate-controlled anaerobic oxidation of pyrite by Thiobacillus cultures. *Geomicrobiology Journal*, 32(5):412–419.

Velicogna, I., Sutterley, T. C., and van den Broeke, M. R. (2014). Regional acceleration in ice mass loss from Greenland and Antarctica using GRACE time-variable gravity data. *Geophysical Research Letters*, 41(22):8130–8137.

Vick-majors, T. J., Michaud, A. B., and Priscu, J. C. (2013). Physiological Ecology of Bacteria in the Water Column of Subglacial Lake Whillans, Antarctica. In *Polar and Alpine Microbiology Conference*, Big Sky, Montana.

Viollier, E., Inglett, P. W., Hunter, K., Roychoudhury, N., and Van Cappellen, P. (2000). The ferrozine method revisited: Fe(II)/Fe(III) determination in natural waters. *Applied Geochemistry*, 15(6):785–790.

Vorren, T. O., Bergsager, E., Dahl-Stamnes, Ø. A., Holter, E., Johansen, B., Lie, E., and Lund, T. B. (2013). *Arctic Geology and Petroleum Potential: Proceedings of the Norwegian Petroleum Society Conference, 15-17 August 1990, Tromso, Norway*. Norwegian Petroleum Society Special Publications. Elsevier Science.

Wadham, J. L., Bottrell, S., Tranter, M., and Raiswell, R. (2004). Stable isotope evidence for microbial sulphate reduction at the bed of a polythermal high Arctic glacier. *Earth and Planetary Science Letters*, 219(3-4):341–355.

Wadham, J. L., Tranter, M., Hodson, A. J., Hodgkins, R., Bottrell, S., Cooper, R., and Raiswell, R. (2010a). Hydro-biogeochemical coupling beneath a large polythermal Arctic glacier: Implications for subice sheet biogeochemistry. *Journal of Geophysical Research*, 115:1–16.

Wadham, J. L., Tranter, M., Skidmore, M., Hodson, A. J., Priscu, J., Lyons, W. B., Sharp, M., Wynn, P., and Jackson, M. (2010b). Biogeochemical weathering under ice: Size matters. *Global Biogeochemical Cycles*, 24(3):GB3025.

Wadham, J. L., Tranter, M., Tulaczyk, S., and Sharp, M. (2008). Subglacial methanogenesis: A potential climatic amplifier ? *Global Biogeochemical Cycles*, 22(December 2007):1–16.

Welch, S. A. and Ullman, W. J. (1993). The effect of organic acids on plagioclase dissolution rates and stoichiometry. *Geochimica et Cosmochimica Acta*, 57(12):2725–2736.

Wigley, T. and Plummer, L. (1976). Mixing of carbonate waters. *Geochimica et Cosmochimica Acta*, 40:989–995.

Williamson, M. A. and Rimstidt, J. (1994). The kinetics and electrochemical rate-determining step of aqueous pyrite oxidation. *Geochimica et Cosmochimica Acta*, 58(24):5443–5454.

Wright, A., Tarney, J., Palmer, K., Moorlock, B., and Skinner, A. (1973). The geology of the Angmagssalik area, East Greenland and possible relationships with the Lewisian of Scotland. In Park, R. and Tarney, J., editors, *The early Precambrian of Scotland and related rocks of Greenland*, pages 157–177. University of Keele.

Wynn, P., Hodson, A., and Heaton, T. H. E. (2006). Chemical and isotopic switching within the subglacial environment of a high Arctic glacier. *Biogeochemistry*, 44(78):173 – 193.

Wynn, P. M., Hodson, A. J., Heaton, T. H. E., and Chenery, S. R. (2007). Nitrate production beneath a High Arctic glacier, Svalbard. *Chemical Geology*, 244(1-2):88–102.

Yallop, M. L., Anesio, A. M., Perkins, R. G., Cook, J., Telling, J., Fagan, D., MacFarlane, J., Stibal, M., Barker, G., Bellas, C., Hodson, A., Tranter, M., Wadham, J., and Roberts, N. W. (2012). Photophysiology and albedo-changing potential of the ice algal community on the surface of the Greenland ice sheet. *The ISME Journal*, 6(12):2302–2313.

Yamashita, Y., Scinto, L. J., Maie, N., and Jaffé, R. (2010). Dissolved Organic Matter Characteristics Across a Subtropical Wetland's Landscape: Application of Optical Properties in the Assessment of Environmental Dynamics. *Ecosystems*, 13(7):1006–1019.

Yde, J. C., Finster, K. W., and Ba, T. G. (2010a). Methane flux and high-affinity methanotrophic diversity along the chronosequence of a receding glacier in Greenland. *Annals of Glaciology*, 51(56):23–31.

Yde, J. C., Finster, K. W., Raiswell, R., Steffensen, J. P., Heinemeier, J., Olsen, J., Gunnlaugsson, H. P., and Nielsen, O. B. (2010b). Basal ice microbiology at the margin of the Greenland ice sheet. *Annals Of Glaciology*, 51(56):71–79.

Yde, J. C., Gillespie, M. K., Løland, R., Ruud, H., Mernild, S. H., De Villiers, S., Knudsen, N. T., and Malmros, J. K. (2014). Volume measurements of Mittivakkat Gletscher, southeast Greenland. *Journal of Glaciology*, 60(224):1199–1207.

Yde, J. C., Hodson, A. J., Solovjanova, I., Steffensen, J. P., Nørnberg, P., Heinemeier, J., and Olsen, J. (2012). Chemical and isotopic characteristics of a glacier-derived naled in front of Austre Grønfjordbreen, Svalbard. *Polar Research*, 31:1–15.